High Throughput Isolation and Analysis of Circulating Tumor Cells for Monitoring Cancer

by

Kaylee Judith Smith

A dissertation submitted in partial fulfillment
of the requirements for the degree of
Doctor of Philosophy
(Chemical Engineering)
in The University of Michigan
2021

Doctoral Committee:

Associate Professor Sunitha Nagrath, Chair
Professor Mark A. Burns
Associate Professor Kyle Cuneo
Professor Daniel F. Hayes
Associate Professor Geeta Mehta
Associate Professor Greg Thurber

Kaylee Judith Smith

kjsm@umich.edu

ORCID iD: 0000-0003-1479-6102

DEDICATION

To Pamela Satterfield and Braelyn Smith. Thank you for supporting me every step of the way.

ACKNOWLEDGMENTS

The path to earning my PhD would have been more difficult or impossible without the support of mentors, colleagues, friends, and family.

First, I would like to thank my advisor, Dr. Sunitha Nagrath. She has been supportive both on a professional and personal level over the past five years. Thank you for bringing me into your lab group and introducing me to multiple interdisciplinary teams. You have taught me the importance of collaboration in addition to engineering and science. I have enjoyed working with you.

I would like to thank committee members Dr. Mark Burns, Dr. Kyle Cuneo, Dr. Daniel Hayes, Dr. Geeta Mehta, and Dr. Greg Thurber – for being supportive and willing to answer questions throughout my time at Michigan. Your suggestions have been greatly appreciated and strengthened my work.

Collaborating with people from multiple disciplines has been a highlight of my time here. I would like to thank Dr. Kyle Cuneo, Dr. Theodore Lawrence, Dr. Theodore Welling, and Dr. David Karnak for their support on undertaking the HCC project. You were all instrumental in the design and outcome of the project. I would also like to thank Shaneta Waddy for her support in scheduling and obtaining patient samples.

Many lab groups collaborated to develop the ex-dwelling system. From the lab of Dr. Daniel Hayes, I would like to thank Dr. Costanza Paoletti, Emily Dolce, and Elizabeth Darga for their support in obtaining healthy control blood, completing CellSearch® runs, and general knowledge about clinical studies. Your knowledge about CTCs was appreciated. I would like to thank Dr. Laura Cooling for sharing her experience about aphaeretic procedures in clinic and helping me understand what was feasible. I would like to thank Dr. Douglas Thamm and Barbara Rose for their aid in conducting the canine experiments. Their contribution to my work was invaluable. Thank you to Dr. Kenn Oldham and Jason Smyth for designing a control scheme for

this system. The passion of this group to improve the lives of both humans and canines is infectious and participating in this collaboration was incredible.

I am grateful to the patients and healthy volunteers who have participated in these studies by donating blood. Without your generous donations, this work would not be possible.

I would like to thank the funding sources that have supported me throughout my PhD career: National Institute of Healthy T32 Cellular Biotechnology Training Program and Rackham Travel Grants. I have been offered many opportunities through these programs.

The resources on the University of Michigan campus have made this work possible. The Lurie Nanofabrication Facility has fantastic, supportive staff who were essential in manufacturing the devices used in this work. The Advanced Genomics Core and Bioinformatics Core were particularly helpful in obtaining and processing genetic data.

I would like to thank my lab members for their support. A special thank you to Dr. Tae Hyun (Kevin) Kim and Dr. Molly Kozminsky for their training when I started. Thank you to our lab manager, Dr. Mina Zeinali, for dealing with crises as they occurred. Thank you to the Labyrinth and DEPArray teams for their support through long nights and willingness to help with experiments: Dr. Sarah Owen, Brittany Rupp, and Harrison Ball. Thank you to the GO team for helping make and run devices: Emma Purcell and Zeqi Niu. A special thank you to Jessica Jana, my partner in research for several months, for both your help with research and unwavering positive attitude. This work was heavily supported by undergraduate researchers. Thank you to Tyler Opdycke, Samuel Meinel, Anna Kaehr, Madeline Grzesik, Courtney Coleman, Zachary Gdowski, Owen Nakatani, and Ryan Delaney for all the time you dedicated to the lab. To all Nagrath lab members, past and present, it has been a pleasure working with you.

Thank you to the department, ChEGS, and the third floor of NCRC for providing communities of support. Our research space consists of diverse research areas and individuals who are supportive both professionally and personally. Thank you to all the friends who have supported me throughout graduate school, especially Brittany Rupp, Dr. Sarah Owen, Zeqi Niu, Elizabeth Wilson, Cailin Buchanan, Alex Adams, and John Hemmerling. A special thank you to Emma Purcell for being a friend both in and out of lab. You all made this journey truly enjoyable.

Thank you to all the educators and mentors who prepared me for this journey. Dr. Shannon Servoss, thank you for instilling in me an excitement for research and supporting me every step of the way.

Finally, I would like to say thank you to my family. Dr. T. Ray Wheeler, you may have been a late addition to this process but your support and proofreading enthusiasm has been greatly appreciated. Indran Kamalanathan, I cannot thank you enough for your support of my dreams and passions throughout the last several years. Braelyn Smith, you have been my partner in crime for longer than either of us can remember and for that I am grateful. To my mother, Pamela Satterfield, thank you is not enough for without your guidance and support I would not be here today. I have always known I could count on both you and Braelyn to be there no matter what.

Table of Contents

List of Tables

List of Figures

ABSTRACT

Although tissue biopsies are an excellent diagnostic and prognostic tool, they are highly invasive and therefore are performed with cause. “Liquid biopsies” are a possible alternative to traditional tissue biopsies that are less invasive and lower risk, so they can be performed more routinely. Liquid biopsies allow for the detection and analysis of circulating biomarkers such as circulating tumor cells (CTCs). Although prognostically informative, CTCs are extremely rare with around 10 CTCs per mL of blood compared to 10^6 white blood cells in the same blood volume. Isolating and analyzing a larger number of CTCs will allow for more informative analysis to be conducted.

To isolate a larger number of CTCs, a high throughput continuous wearable system was developed. This system uses an inertial microfluidic device, the CTCKey™, in series with three herringbone graphene oxide (^{HB}GO) devices. The inertial device enriches CTCs 5-fold at 2.4 mL/min from whole blood based on cell size, then directs the CTC enriched streams to ^{HB}GO devices where CTCs are captured on the chips surface. After being processed through the system, the blood is then returned to the patient, increasing the volume of blood that can be processed from approximately 10 mL using traditional blood draws to 240 mL over a two-hour period. The CTCKey™ was able to recover 99% of MCF7s and CellSearch post CTCKey™ recovered 71% of MCF7s.

Another part of this work was to isolate CTCs from hepatocellular carcinoma patients before, during, and after radiation treatment from 29 unique patients. CTCs were enumerated based on the expression of Ck18, asialoglycoprotein receptor, and EpCAM. The differences in number of CTCs and different sub-populations of CTCs between patients and time points were compared. It was determined that an increase in CTC numbers before and during treatment was highly prognostic of disease progression ($p=0.0173$) while that same trend did not hold for changes in CTC numbers before and after treatment. RNA analysis was also performed on these patients using microarrays. A small number of genes were identified as being differentially regulated in

progressed patients when compared with stable patients. This data shows promise in predicting HCC patient outcomes, but it would be beneficial to verify the findings in a larger patient cohort.

In addition to characterizing bulk CTCs, analysis from individual CTCs at the single cell level could provide information about tumor heterogeneity that is missed in bulk analysis. The workflow used to isolate cells from HCC patient samples was modified to prepare samples for the DEPArray, a single cell isolation technology. After process modification, single CTCs were able to be isolated from samples processed using the Labyrinth then fixed using either PFA or alcohol fixation. It was demonstrated that the optimized methods yielded single cell DNA/RNA and the samples have been successfully prepared for copy number variation analysis; however, the developed approach can enable other analysis such as transcriptomic expression.

Overall, innovative microfluidic technologies developed in the thesis work provides the ability to isolate more CTCs through a high throughput wearable system which allows for large blood volumes to be processed. Downstream analysis of HCC samples showed that changes in CTCs are correlated with patient outcomes. Now that single cells can be isolated, heterogeneity between single CTCs can be determined. Collectively, these advancements in CTC isolation and analysis will lead to improved patient outcomes.

Chapter 1: Introduction

1.1 Background

The American Cancer Society predicted that 1.8 million new invasive cancer cases would be diagnosed in 2020 while over 606,000 Americans would die from some form of cancer.[1] Of those patients, approximately 90% of them will die from cancer metastasis, not the primary tumor.[2] If diagnosed early enough, the primary tumor is often treatable; whereas, it is difficult to treat cancer that has already metastasized. Consequently, early diagnosis is the key to high probability of survival. Current cancer diagnosis relies heavily on tissue biopsies which are invasive, and therefore, only performed to diagnose cancer after another test or symptom indicates the possibility of cancer. Due to the nature of cancer, symptoms often do not become apparent until the cancer has progressed to a late stage. Liquid biopsies are a promising alternative for the diagnosis and monitoring of cancer since the analysis is performed on a non-solid tissue, in this case blood. Because this analysis is performed on a peripheral blood sample, liquid biopsies are less invasive and lower risk to patients than traditional tumor biopsies which means they can be performed regularly.[3] Liquid biopsies can be taken at routine check-ups to diagnose the disease and can be used to monitor cancer progression after diagnosis if the analysis technologies are sensitive and selective enough for these applications.[4] For liquid biopsies to become a potential alternative to tissue biopsies, consistent biomarkers need to be identified and reliable methods need to be developed to isolate and analyze the desired biomarkers.[5] Possible biomarkers include ctDNA and exosomes as well as circulating tumor cells (CTCs), the focus of this study.[6]

CTCs are cancer cells that were released from a tumor into the blood stream.[7] Once released, they travel through the blood and can attach elsewhere in the body where they can potentially seed a new tumor or metastasis.[5] By isolating and studying CTCs, the metastatic potential of a specific tumor can be determined.[5,8–10] CTC populations have also been shown to be heterogeneous and, therefore, may provide a better overview of the whole tumor than tissue biopsies since tissue biopsies sample a very specific location in the tumor.[10–13] Having a better overview of the whole tumor can lead to the detection of target protein expression or rare genetic mutations that are utilized by certain treatment regimens to target cancer cells more effectively.[14,15] This information can help doctors recommend the treatment regimen to which the patient will best respond.[16] Since liquid biopsies can be performed routinely, changes in protein and gene expression and mutations can be monitored to effectively modify patients' treatments over time.

Although CTCs offer significant promise to improve diagnosis and monitoring of cancer, as well as predict patient outcomes and direct treatment decisions, they must first be isolated at a high enough throughput for this information to be obtained.[17] CTCs are extremely rare in blood with approximately 10 cells/mL compared to a million white blood cells (WBCs), and a billion red blood cells in addition to platelets and other blood components.[18] Because of the rarity of CTCs, isolation technologies need to be highly sensitive while maintaining high specificity.[4,5]

1.1.1 CTC Significance in Solid Tumors

The presence of even very low CTC numbers has been shown to be indicative of poor patient outcomes. The Mayo Clinic says that 5 or more CTCs isolated from 7.5 mL of blood by CellSearch® is correlated with shorter overall survival in patients that are marked as stable or partially responding to treatment according to traditional imaging scans.[19] Using the cutoff of 5 CTCs/ 7.5 mL of blood for poor prognosis, one study showed the number of CTCs present before

and after treatment indicated patient outcomes in metastatic breast, prostate, and colorectal cancer. Patients with fewer than 5 CTCs both before and after treatment had the longest survival time and patients who had fewer than 5 CTCs after treatment had the second longest survival time.[20] Since the completion of this study, additional studies have confirmed that increased CTC numbers are indicative of worse prognosis in many solid tumors including breast, prostate, colorectal, pancreas, lung, skin, and bile duct cancers.[21–24] Additionally, one study suggested that CTC counts may be a used as a biomarker to monitor response to radiation treatment.[25]

1.2 Circulating Tumor Cell Isolation Methods

Over the past couple of decades many CTC isolation methods have been developed from the original CTC-chip, a microfluidic technology, to CellSearch®, the only FDA approved CTC detection technology.[26,27] In addition to these technologies developed specifically for CTCs, many techniques, such as density gradients and filters, have been reoptimized to isolate CTCs.[28] CTC isolation technologies tend to isolate cells based on either their biological or physical properties.[29,30]

1.2.1 CTC Isolation Based on Biological Properties

CTCs are typically of epithelial origin, meaning the proteins that these cells express vary from the proteins found on white blood cells (WBCs).[8] Since the development of CellSearch®, the first biological property-based CTC detection technology, these distinguishing proteins have been targeted to isolate CTCs from blood with existing lab techniques such as flow cytometry.[28] Although this approach allows for CTC isolation without developing or optimizing new technologies, these techniques were designed for large cell numbers and, therefore, struggle to effectively capture rare cells such as CTCs. This challenge is additionally complicated because complex fluids such as blood further hamper rare cell isolation. To overcome the limitations of

systems designed for large cell numbers, many microfluidic devices have been developed to capture specific cell populations by targeting cell surface proteins, the first of these devices being the CTC-chip.[31] Microfluidic devices often offer the advantages of higher purity and lower cost while being able to test a wide variety of designs during the development phase.[26,32–36] Following the CTC-chip, a number of immunoaffinity based devices have been developed including the Herringbone Chip, CTC-iChip, NanoVelcro, and Graphene Oxide based microfluidic device, GO Chip, among others.[30,37–41]

Isolating CTCs based on protein expression can be achieved through either positive selection or negative depletion.[42] The most common target for positive selection is the epithelial cell adhesion molecule (EpCAM) which is expressed in most epithelial tissues but is not present on WBCs.[29] Other surface markers have also been targeted including EGFR and CD133.[43] The most common marker to deplete WBCs is CD45.[29,44] Although biological property-based isolation techniques lead to high-purity samples, these systems are typically low throughput and miss cells which do not express the specific protein being targeted.

1.2.2 CTC Isolation Based on Physical Properties

To combat the limitations of biological property-based isolation, many methods have been developed to isolate cells based on differences in their physical properties such as size, density, and deformability. For example, CTCs tend to be slightly larger (~15 μm) than WBCs (~12 μm), and CTCs tend to be less deformable.[45] Physical property based separation techniques include filters, density gradients, electrical fields, and inertial microfluidics.[46] Isolation by Size of Epithelial Tumor Cells (ISET), is one of the more common filter techniques.[47,48] Similarly, both the Parsortix® and Cluster-Chip systems trap cells based on size and deformability.[34,49] Methods

including Ficoll-Paque separate cells using density gradients, but these methods are typically developed to isolate nucleated cells, including white blood cells, instead of focusing on CTCs.[28]

Alternatively, inertial microfluidics devices separate cells based on size by utilizing the fluidic forces in straight or curved channels.[50] Straight microfluidic channels have been used to isolate CTCs by pushing them towards the center of a sheath buffer filled channel.[51] Various spiral microfluidic devices have been developed to focus CTCs into independent streamlines while serpentine channels have also been shown to effectively separate particles based on size.[52–54] These devices operate at remarkably higher flow rates than immunoaffinity based devices, allowing them to process more blood in a similar amount of time. By processing a higher blood volume, a larger number of CTCs can be recovered, enabling sensitive downstream assays to profile CTCs and identify heterogeneity between individual cells.[55] This will lead to a more thorough overview of the tumor which will improve treatment decisions.

Inertial microfluidic devices take advantage of competing wall and shear induced lift forces that occur in laminar flow to isolate particles of varying sizes.[56–59] Laminar flow is defined as systems with low channel Reynolds numbers (Equation 1). In these systems, the wall force pushes cells away from the wall of the device while a shear induced lift force pushes cells back towards the wall due to the parabolic velocity profile. These competing forces push particles to four focusing positions in square channels which condense down to two focusing positions in channels with high and low aspect ratios (height/width << or >>1).[58] Studies have been conducted to determine the combined lift force caused by the competing wall and shear induced lift forces is F_L (Equation 2), where C_L is the experimentally determined scaling factor.[60] Because focusing of particles is dependent on the parabolic velocity profile, different sized particles focus differently in the same channel due to different variations in velocity across the particle. To account for this,

the particle Reynolds number (Equation 3) is used.[59] Unlike the channel Reynolds number, the particle Reynolds number accounts for particle properties in addition the channel properties.

$$Re = \frac{\rho u L}{\mu} \tag{1}$$

$$F_L = \frac{\rho {U_m}^2 {a_p}^4}{{D_h}^2} C_L \tag{2}$$

$$Re_p = Re_c \times \left(\frac{a_p}{L}\right)^2 \tag{3}$$

Table 1-1: List of Variables in Equations

Symbol	Variable
Re	Reynolds Number
ρ	Density ($^{kg}/_{m^3}$)
u	Velocity ($^{m}/_{s}$)
L	Characteristic Channel Length (m)
μ	Dynamic Viscosity $\left(^{kg}/_{m\,s}\right)$
F_L	Lift Force
U_m	Maximum Velocity ($^{m}/_{s}$)
D_h	Smallest Channel Dimension (m)
C_L	Lift Coefficient
Re_p	Particle Reynolds Number
De	Dean Number
R_c	Radius of Curvature (m)

Adding curvature to these inertial systems introduces secondary flow driven by centrifugal forces due to the differences in velocity across the width of the channel. These centrifugal forces vary the focusing position of different sized particles such that they focus into different

streamlines. This secondary flow is called Dean flow and is characterized by the Dean number, De (Equation 4).[59,61]

$$De = Re\sqrt{\frac{L}{2R_c}} \tag{4}$$

Although inertial focusing does occur in microfluidic systems, particles in blood flown through serpentine channels do not strictly follow these patterns. Blood, like most bodily fluids, is a viscoelastic fluid instead of a Newtonian fluid for which these equations most accurately define fluid flow. Whole blood also has many particle-particle interactions largely from the red blood cells and white blood cells present in the fluid.[62] In addition, these equations have previously been shown to be mediocre predictors of focusing in serpentine channels, most likely resulting from the directional changes that occur in the system caused by the sharp curvature.[54]

1.3 Continuous CTC Isolation Methods

Because CTCs are extremely rare in blood, it is desirable to obtain more cells than can be isolated from peripheral blood draws. Collecting more blood for ex-vivo processing can be challenging. To overcome this limitation researchers are investigating using traditional apheresis techniques or developing continuous systems to isolate CTCs.[63]

1.3.1 Modified Traditional Apheresis Techniques

Diagnostic leukapheresis (DLA) has been used to pre-enrich CTCs into a smaller volume to be processed using CellSearch.[48,55,64] This method uses continuous centrifugation to collect cells with a specific target density. DLA was designed to isolate mononuclear cells but has been used to isolate CTCs since they fall within the density range targeted by the procedure. Studies that use DLA are typically limited to around 2.7 liters of blood because adverse events are associated with

higher blood process volumes.[55] Although 2.7 liters of blood is significantly more than the 10 mL of blood that can be drawn into a blood tube, the system isolates WBCs as well as CTCs, meaning further processing must be performed to isolate the CTCs. Even with these limitations, studies have shown the ability to not only isolate significantly more CTCs using DLA followed by CellSearch than can be detected with CellSearch alone, but they were also able to isolate CTCs from non-metastatic cancer patients.[55,64]

1.3.2 Gilupi Cell Collector

The Gilupi CellCollector® is approved for use in European and Chinese markets. It is an antibody coated wire that is inserted into the blood stream for half an hour. After that time the wire is removed and processed such that the CTCs can be enumerated.[65] It was determined that metastatic prostate patients with 5 or more CTCs measured by the Gilupi CellCollector® had decreased overall survival compared to patients with less than 5 CTCs.[66] Although the Gilupi CellCollector® processes a significant portion of the human blood volume, the capture efficiency is extremely low and the threshold numbers used are identical to those used by CellSearch® from a 7.5 mL sample, indicating that the Gilupi Cell Collector is effectively not collecting a larger CTC sample than is isolated using CellSearch®.[67,68]

1.3.3 Viatar: Cancer Dialysis

Viatar developed a system to remove CTCs from patient blood. The system passed blood over a filter that allowed normal blood cells to pass through it but prevented CTCs from returning to the patient. It was designed to run for three hours and was advertised as a way to remove CTCs, effectively removing the seeds of metastasis from the blood stream.[69] This company received approval for a clinical trial, but they never enrolled patients and the company no longer exists.

While the Viatar system appeared to be promising, research did not indicate that removing CTCs for three hours was an effective treatment method. CTC dissemination is likely a continuous process with small numbers of CTCs being released regularly and rapidly cleared from the body. It is known that treatments such as radiation can rapidly release large numbers of CTCs, but it is believed that these cells are largely dead or dying and unlikely to seed metastasis.[70]

1.3.4 MagWIRE Technology

Recently Stanford research team developed a magnetic wire for intravascular retrieval and enrichment (MagWIRE) to capture CTCs *in vivo*. A magnetic wire is inserted into the blood stream and anti-EpCAM coated magnetic beads are injected upstream of the wire. This allows the beads time to bond to EpCAM expressing cells in the blood stream then the magnetic beads are captured by the wire. *Ex vivo* studies found that this system captured 10% of EpCAM expressing cells in a single pass and 96% of the magnetic beads injected. In their porcine model, the MagWIRE captured up to 8% of the EpCAM cells injected.[68] The MagWIRE saw a significant increase in the CTC capture efficiency as compared to the Gilupi Cell Collector; however, the necessity of injecting magnetic particles into the patient will drastically limit its ability to be approved for use on human patients.

1.4 Hepatocellular Carcinoma

The methods discussed so far are applicable to many cancer types; however, my thesis is largely focused on Hepatocellular Carcinoma (HCC), the most common primary liver malignancy.[71] In 2019, HCC was estimated to be the fourth leading cause of cancer-related deaths globally and the incidence of HCC is rapidly increasing.[72] Historically, the primary cause of HCC was hepatitis B and C with 78% of cases being attributed to these diseases from 2001 to 2006; however, the recent increase in HCC is largely due to alcoholic steatohepatitis and nonalcoholic

fatty liver disease (NAFLD).[73,74] Current HCC diagnostic technologies include ultrasound, MRI, and CT scans, sometimes in conjunction with α-fetoprotein, the original HCC biomarker.[75,76] Although these diagnostic techniques can have up to 90% sensitivity and 90% specificity, they are less effective in obese and hepatitis patients.[71] Since hepatitis and NAFLD are primary causes of HCC and obesity is a significant attributor to NAFLD, these tests tend to have low sensitivity in this patient population.[77] This inefficiency in diagnostic techniques indicates that CTCs could make a significant impact on the diagnosis of HCC.

Currently the only "cure" to HCC is surgical resection or a liver transplant, but even these only have a two-year recurrence free rate of 9.1% and a two-year overall survival of 69.6%.[78] The presence and number of CTCs has been shown to be a good predictor of disease outcomes in other metastatic cancers so it is reasonable to conclude that CTCs can also be used to diagnose and monitor disease progression in HCC patients.[79]

1.5 Single Cell Isolation Techniques

Bulk CTCs can be advantageous over bulk tissues not only because blood draws are less invasive than tissue biopsies, but they also give a more comprehensive overview of the tumor since they can come from a variety of tumor locations. However, by analyzing cells as a bulk population, heterogeneity is still often missed because this analysis averages the results from all cells.[80] Analyzing single cells allows the heterogeneity of the tumor to be observed. Many methods have been developed to isolate single cells including fluorescence activated cell sorting (FACS), magnetic-activated cell sorting (MACS), laser capture microdissection (LCM), manual cell picking using micromanipulation, and microfluidics.[81] FACS requires a large number of starting cells making it difficult to isolate pre-enriched CTCs because there are very few cells.[82] MACS isolates cells into populations but does not provide single cells as the output.[83] LCM is used on

tissue samples so although it does isolate single cells, it is still subject to the spatial restrictions of collecting a tissue biopsy.[84] Manual cell picking is an optimal option for selecting single cells but requires highly skilled personnel, thus is not accessible to many labs and would be difficult to implement in a clinical setting.[85] Microfluidic technologies for single cell isolation are similar to those used for bulk CTC isolation and are often used in conjunction with other isolation methods such as FACS and MACS.[86]

Once single cells are isolated, downstream analysis methods can be used to analyze their DNA, RNA, and protein expression. Techniques were developed to perform all these analyses on bulk samples, but the inefficiencies of each are amplified in single cells due to the low input material. Researchers have modified the existing techniques to be suitable for single cells. For example, polymerase chain reaction (PCR) can be highly biased but multiple research groups have worked to modify the amplification process to help remove these biases.[81] This work is beneficial to both DNA and RNA sequencing since RNA is first reversed transcribed to cDNA due to DNAs increased stability over RNA. When specific mutations are of interest, digital droplet PCR can be used to detect the presence of the targeted mutations and their relative abundance compared to the wildtype variant in a single cell.[87] This method is limited by the fluorescent probes available but researchers have multiplexed assays to allow multiple mutations to be detected at once.[88]

Fluidigm and Menarini Silicon Biosystems have developed and marketed microfluidic based single cell isolation systems. The Fluidigm C1 isolates up to 96 single cells and amplifies 96 transcripts that can later be sequenced.[89] The Nagrath lab has successfully isolated and analyzed single cells using this method; however, since the machine only loads 6% of the sample and there is no control over which cells get loaded from a sample, this method will likely miss rare cell populations.[90] The DEPArray, developed by Menarini Silicon Biosystems, enables the user to

select up to 96 single cells from the loaded sample which may contain up to 6000 cells. Although not perfect since the machine loads just over 75% of the sample, this is drastic improvement for CTC selection and isolation over the Fluidigm C1 for rare cell populations. The DEPArray was designed to work with fixed tissue samples as well as incorporated into the CellSearch® procedure so the downstream assays available from the company target that particular workflow.[91] Additional workflows are needed for single cells isolated using the DEPArray from other input technologies.

Both single cell isolation and analysis techniques have improved greatly in recent years; however, all these techniques and assays could be further improved to yield more reliable and higher quality results, specifically for rare and low abundant cells. Current single cell isolation techniques have low throughput, low yield, or strict input guidelines limiting the sample types that can be processed. The assays currently used to process these single cells were primarily developed for bulk sample processing, so they are designed to process the larger amounts of material provided by hundreds of cells rather than the miniscule amount obtained from a single cell. Having low input volume amplifies the difficulties associated with the inefficiencies in these assays. To reliably isolate single CTCs from cancer patients and investigate intra-tumor heterogeneity, isolation techniques must be able to isolate single cells of interest from low purity samples and downstream assays must be able to process single cells with low input material while maintaining high quality material processing.

1.6 Scope of Thesis

This thesis is focused on developing methods to perform high throughput isolation of CTCs and the appropriate downstream analysis methods depending on the goals of the project. This work consists of three main aims: (i) develop an ex-dwelling system to continuously capture CTCs *in vivo*, (ii) isolate and analyze CTCs from HCC patients and correlate the CTC analyses with patient

outcomes, and (iii) isolate single cells using the DEPArray technology downstream of labyrinth processing to enable single cell analysis of CTCs from various cancer types.

1.6.1 Aim 1: Develop an Ex-Dwelling System to Continuously Capture CTCs in vivo

By capturing CTCs directly from whole blood and returning the remaining blood to the patient, the blood volume that can be processed is drastically increased over the amount that can be drawn into blood tubes. Traditionally, whole blood processing techniques are low throughput or require pre-processing in the form of dilution, a sheath buffer, or red blood cell depletion. Low throughput isolation methods will not increase the number of CTCs that can be isolated due to time limitation of apheresis systems and pre-processing is not applicable since the blood is to be returned to the patient. In this study, we developed a high throughput CTC isolation system that processes whole blood without the need for the pre-processing.

1.6.2 Aim 2: Isolate and Analyze CTCs from HCC Patients and Correlate the CTC Analyses with Patient Outcomes

The presence of CTCs has been shown to be a good predictor of patient outcomes in many cancer types, but CTCs have not been studied as thoroughly in HCC. In this study, we use the Labyrinth device to isolate CTCs from HCC patients and correlate the number and phenotypes of the CTCs detected with patient outcomes. Simultaneously, RNA was isolated from the bulk CTC enriched sample. Bulk RNA analysis had not been performed downstream of the Labyrinth and could be beneficial to monitor CTC RNA expression without the need for further cell isolation after the Labyrinth.

1.6.3 Aim 3: Isolate Single Cells using the DEPArray Technology Downstream of Labyrinth Processing to Enable Single Cell Analysis of CTCs from Various Cancer Types

To determine intra-tumor heterogeneity, it is beneficial to analyze CTCs individually and determine their differences. For our lab, the single cell isolation method would ideally be incorporated into our current workflow. This aim is focused on modifying both pre- and post-Labyrinth processing to enable single cell isolation from the DEPArray. Once isolated, either DNA or RNA analysis will be performed on the cells to determine copy number variation or differential gene expression depending on the aims of the specific study.

Chapter 2: Ex-dwelling, Intravenous Aphaeretic Device to Capture CTCs

2.1 Abstract

Circulating Tumor Cells (CTCs) are extremely rare cells shed from tumors into the blood stream. These cells can provide valuable information about their tumor of origin and direct treatment decisions to improve patient outcomes. Current technologies isolate CTCs from a limited blood volume and often require pre-processing that leads to CTC loss, making it difficult to isolate enough CTCs to perform in-depth tumor analysis. Many inertial microfluidic devices have been developed to isolate CTCs at high flow rates, but they typically require either blood dilution, pre-processing to remove red blood cells, or a sheath buffer rather than being able to isolate cells directly from whole blood. To decrease the need for pre-processing while increasing CTC yield, we developed an inertial device, the CTCKey™, to focus CTCs in whole blood at high throughput yielding a concentrated product stream enriched for CTCs. The CTCKey™ consists of two sections to create CTC enriched blood that can be further processed using any CTC isolation device to selectively isolate the CTCs. A thorough analysis was performed using the MCF7 breast cancer cell line spiked into bovine serum albumin (BSA) solutions of varying concentrations, as well as whole blood to characterize the focusing patterns of the CTCKey™. At the optimal flow rate of 2.4 mL/min, the CTCKey™ reduces the CTC containing blood volume by 78%; the CTCs from 1 mL of blood are now in 0.22 mL of blood. The CTCKey's™ ability to concentrate CTCs from a large original blood volume to a smaller, highly concentrated volume enables a much greater blood

volume to be interrogated by downstream isolation and characterization methods despite their low volume input limitations.

2.2 Related Publications

Smith, K.J., Jana, J.A., Kaehr, A., Purcell, E., Opdycke, O., Paoletti, C., Cooling, L., Thamm, D.H., Hayes, D.F., and Nagrath, S. Inertial Focusing of Circulating Tumor Cells in Whole Blood at High Flow Rates using the Microfluidic CTCKey™ Device for CTC Enrichment. In review.

Smyth, J., Smith, K.J., Nagrath, S., and Oldham, Kenn. Modeling, Identification, and Flow Control for a Microfluidic Device using a Peristaltic Pump. DOI: 10.23919/ACC45564.2020.9147528

Kim, T.H., Wang, Y., Oliver, C.R., Thamm, D.H., Cooling, L. Paoletti, C. Smith, K.J., Nagrath, S., and Hayes, D.F. A temporary indwelling intravascular aphaeretic system for in vivo enrichment of circulating tumor cells. DOI: 10.1038/s41467-019-09439-9

Smyth, J., Smith, K.J., Nagrath, S., and Oldham, Kenn. Modeling, Identification, and Flow Control for a Microfluidic Device using a Peristaltic Pump. Invention Disclosure.

Smith, K.J., Hayes, D.F. and Nagrath, S. Inertial Focusing of Circulating Tumor Cells in Whole Blood at High Flow Rates using the Microfluidic CTCKey™ Device for CTC Enrichment. Invention Disclosure.

2.3 Introduction

Breast cancer is the most commonly diagnosed cancer type in women with over 281,000 new cases predicted this year in the United States. It is estimated that over 44,000 people will die from the disease in the same time frame.[92] In the past 30 years the breast cancer death rate has drastically decreased, largely due to improvements in diagnostic techniques. Early diagnosis allows for the tumor to be resected before metastasis occurs, which is the primary cause of breast

cancer death. Metastasis is hypothesized to be initiated by CTCs. Multiple studies have shown CTC enumeration to be a reliable prognostic factor for progression and overall survival in breast cancer.[93,94] Using CellSearch®, the only FDA approved CTC detection technology, the Mayo Clinic demonstrated that metastatic breast cancer patients with five or more CTCs in 7.5 mL of blood had shorter overall survival than those patients with fewer than five CTCs.[19] In addition, CTCs can provide information about the heterogeneity of the tumor that is often missed by a tissue biopsy due to spatial differences in the tumor.[95] The analysis of these CTCs has been shown to be a reliable biomarker for treatment selection.[96]

Although CTCs can be isolated from a liquid biopsy and provide information about the heterogeneity of the tumor, they are rare in the blood, ~10 CTCs/ mL; therefore, it is extremely difficult to obtain enough cells to perform some of the desired assays. Many technologies have been developed to sensitively and selectively isolate CTCs.[30] These technologies have expanded the types of downstream assays to include proteomics, genomics, and transcriptomics; however, they are still limited by the volume of blood that can be drawn from a patient at any one time. The majority of studies process 1 – 5 mL of blood with very few exceeding 10 mL.[30] Studies often report data on a very small number of cells (~10), so although tumor heterogeneity can be observed, the data may not be comprehensive or statistically significant due to the low number of cells isolated.

The volume limitation can be overcome by either an indwelling capture system that never removes the blood or an intravenous ex-dwelling system that returns the blood to the patient. The only such device on the market is the Gilupi Cell Collector, an anti-EpCAM coated wire that is left in a patient vein for half an hour then enumerated.[66] The Gilupi Cell Collector is approved for use in both European and Chinese markets. It does allow for a large volume of blood to be sampled

but the capture efficiency is low such that it does not yield more cells than other CTC isolation technologies.

Recently, two other indwelling devices have been published: the MagWIRE and a black phosphorous therapeutic catheter.[68,97] The MagWIRE requires the injection of anti-EpCAM coated magnetic particles upstream of the magnetic wire used to capture the particles after they have had the opportunity to attach to cells. This wire had a capture efficiency of 56% in the lab, but this decreased to 8% in their porcine model. The researchers hypothesize this decrease in capture efficiency is due to the branching vasculature, but it also indicates the possibility for loss of magnetic particles into the blood stream which could be problematic if they are not properly filtered by the liver. The black phosphorous therapeutic catheter has a capture efficiency of 1.8% *in vitro* when cells are being circulated but it increases to 3.18% in stationary conditions. It was designed to kill CTCs *in vivo* instead of to capture CTCs for further analysis. Although the black phosphorous therapeutic catheter has the advantage of being able to kill CTCs *in vivo*, to the best of my knowledge, there is no data supporting that killing CTCs *in vivo* is more beneficial than removing them for analysis. Although both of these systems have the ability to interrogate a larger blood volume than *in vitro* devices, both are lacking in capture in efficiency.

2.3.1 Original Indwelling System Design

Previously, I co-authored *A Temporary Indwelling Intravascular Aphaeretic System for in vivo Enrichment of Circulating Tumor Cells* which isolated CTCs at a flow rate of 6 mL per hour from canines for two hours.[98] Because the system is aphaeretic, removes a blood component then returns the rest of the blood to the patient, the blood volume is limited by processing time and flow rate instead of by the amount of blood that can be drawn. This system utilized a dual-lumen catheter to allow blood to be drawn and returned at the same puncture site. Heparin was injected as close

to the draw site as possible to prevent clotting. A peristaltic pump was used to pump the blood through the CTC capture module then the blood was returned to the patient (Figure 2-1). The CTC capture module used in this system was the herringbone graphene oxide (^{HB}GO) device. This chapter will build on our previously published work by improving the indwelling system capture module to increase the flow rate while maintaining a small enough footprint that the system can remain wearable.

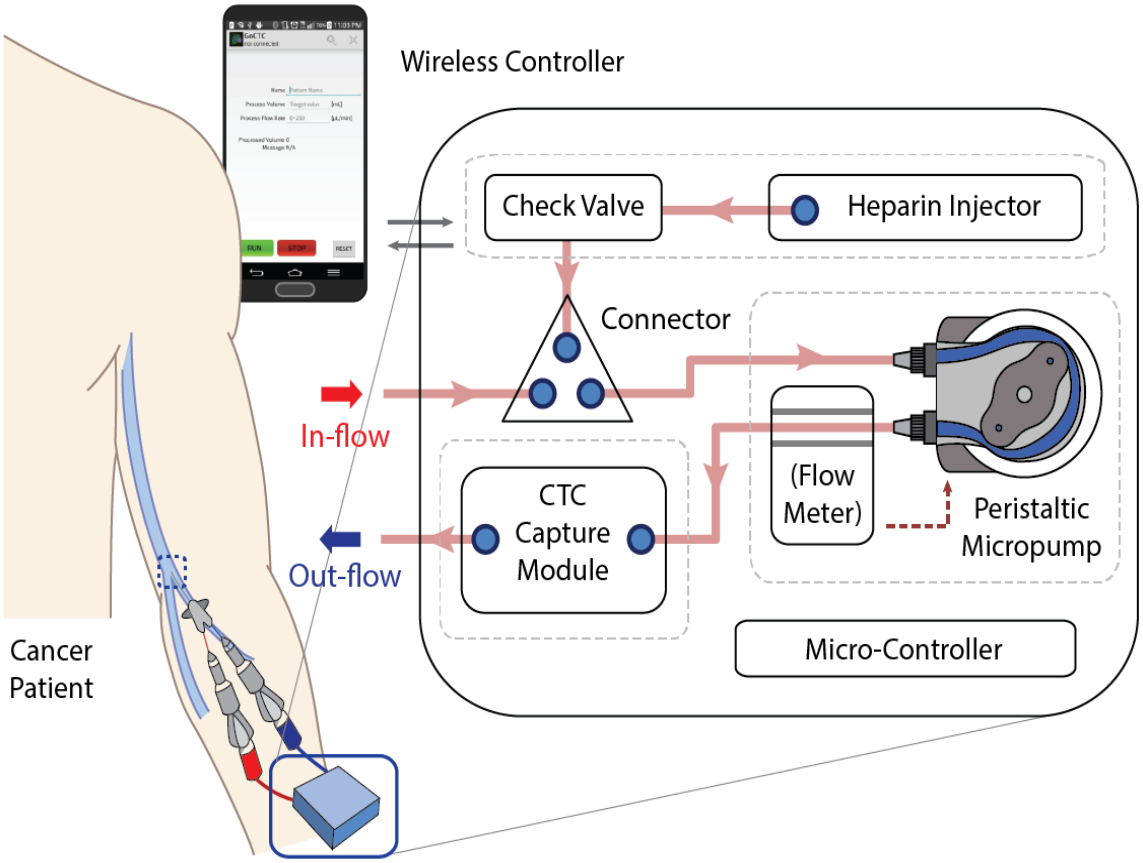

Figure 2-1: Original indwelling system design.

2.3.2 Development of a microfluidic CTCKey device for the enrichment of CTCs from whole blood at high throughput

Even though many inertial devices have been developed to isolate CTCs at high flow rates, these methods require undesirable pre-processing, dilution, and/ or the use of a sheath buffer.[35,46,99] Pre-processing adds additional steps where cell loss could occur while also increasing the processing time. Dilution and sheath buffers both increase the volume of fluid that must be processed thereby increasing the processing time, while further diluting the already low CTC concentration. Here we devise a high throughput inertial device, the CTCKey™, which focuses cells in unprocessed whole blood, forgoing the need for pre-processing that was necessary in previous devices.

2.4 Methods

2.4.1 PDMS Device Fabrication

Polydimethylsiloxane (PDMS) devices were fabricated from SU8 molds. The device design was printed onto a mylar mask. SU8 (Kayaku, USA) was spin coated onto a silicon wafer (Kayaku, USA) at an appropriate height then soft baked until no longer sticky. Depending on the device height, either SU8 2025, SU8 2050, or SU8 100 was used to make the devices. The most recent device design was made using SU8 2100 but all the early designs that were 100 µm tall used SU8 100 due to availability. After baking, the wafer was exposed to the desired design using the manufacturer provided exposure rates for each height. Post-exposure, the SU8 coated wafers were hard baked before being developed. After being fully developed, the wafers were cleaned with isopropyl alcohol, dried using nitrogen gas, and post-baked for 5 minutes at 150°C.

Before pouring PDMS onto the SU8 coated silicon wafers, the wafers were treated with silane (Sigma, USA) for two hours. PDMS was prepared with the curing agent at a 10:1 ratio and

poured on the SU8 silicon mold. The PDMS was then degassed for 1 – 2 hours until all the bubbles had dissipated. After degassing, the devices were cured overnight in a 70°C oven. Devices were then peeled from the mold and appropriately sized holes were punched for both inlet and outlets. Except when connecting larger tubing to use the peristaltic pump, all inlets and outlets were punched with 0.75 mm holes. To connect larger tubing, 1.5 mm holes were used. For inertial devices, a plasma etcher was used to bond the PDMS to the glass slide. A corona discharge was used to bond PDMS to functionalized graphene oxide.

2.4.2 Graphene Oxide (GO) Substrate Fabrication

Functionalized graphene oxide substrates were fabricated using our previously published method.[32] Briefly, a silicon wafer is coated with chrome and gold then patterned using SP 331. The unpatterned metals were etched away then the SP331 was stripped to create the desired surface area. The surface was coated with a tetrabutylammoniμm hydroxide stabilized GO monolayer and functionalized by phospholipid–polyethylene–glyco-amine (PL–PEG–NH2). N-g-maleimidobutyryloxy succinimide ester, which forms an amide with PL–PEG–NH2, is used as a linker to attach neutravidin. Because of the strong biotin-neutravidin bond that forms, any biotinylated antibody can be attached to the chip surface. For this study anti-EpCAM is used since only cell lines are being captured, but additional antibodies have been used for other studies in the lab.

2.4.3 Cell Culture and Preparation

All cell lines were obtained from ATCC and cultured at 37°C and 5% CO2 in Dulbecco's Modified Eagle Medium (Invitrogen, USA) with 10% Fetal Bovine Serum (Sigma, USA) and 1% Antibiotic-Antimycotic (Invitrogen, USA) added. For cell maintenance media was changed every 2 – 3 days and cells were passaged when they reached 60 – 80% confluency. For experimentation,

cells were seeded into cell culture dishes 3 – 5 days before experimentation. Cells were passaged at 70 – 80% confluency using TrypLE then tracker dyed using Cell Tracker Green CMFDA Dye (Invitrogen, USA). Cells were live during experimentation and used immediately.

2.4.4 Human Subjects

Whole blood from healthy volunteers was obtained as part of Institutional Review Board approved protocols (HUM00070190 and HUM00037943). All subjects were consented by the study team prior to the scheduled blood draw in accordance with standard procedures for clinical research at the University of Michigan Comprehensive Cancer Center (UMCCC). Blood was drawn into 10 mL CellSave Tubes (Menarini Silicon Biosystems, USA) and used with 96 hours.

2.4.5 Canine Subjects

The experiments using canines were conducted under Colorado State University IACUC protocol 16-6490A. All canines were fully immune intact and were monitored for seven days following experiments to ensure no adverse effects occurred.

2.4.6 Device and Buffer Preparation

Before running samples through the device, it was prepped using a 1% (w/v) pluronic (Sigma, USA) solution that was allowed to sit for a minimum of 10 minutes after being run through the device using a Harvard Apparatus Syringe Pump at 100 µL/min. After preparation, the samples were loaded into a syringe and run through the device using the same pump.

Bovine serum albumin (BSA) solutions were prepped by dissolving BSA (Sigma, USA) into PBS. The solution was stored in the fridge until ready to be used.

2.4.7 Flow Pattern Characterization

Flow images were taken on a Nikon Eclipse LV100 Upright microscope equipped with an X-Cite Series 120Q fluorescent light box. A Harvard Apparatus Syringe Pump was used to maintain continuous flow. Flow was allowed to stabilize for a minimum of one minute, before data collection began. Multiple images were taken at the outlets during device optimization and at the locations shown in Figure 2-6 b for the CTCKey™ for each buffer solution and flow rate.

2.4.8 Image Acquisition and Analysis

Images were analyzed using the Nikon Analysis Software. Lines were drawn across the device channel in the Nikon Analysis Software and the LUTs were exported. The LUT data was imported into MatLab where the Peaks function was used to determine the peak height and width at half-prominence.

2.5 Results

2.5.1 Inertial Focusing in Whole blood

In order to develop a whole blood inertial focusing device, flow patterns in inertial devices needed to be explored. I initially tested the Labyrinth device available in lab to demonstrate the feasibility of this method. In the Labyrinth device, cancer cell lines focus to two streamlines. Because the Labyrinth device has a series of tight curves in the center then more relaxed curves on the outside, it was a good model for how cancer cells focused in whole blood in 100 μm wide devices (Figure 2-2). In this device, cells focused to a single stream at the beginning and remained in a single tight stream in the center where the radius of curvature remains small. As the cells traveled towards the outside of the device, two focusing positions developed.

Based on the Labyrinth device results and observations made in literature, I tested a series of devices that varied in width from 50 μm to 1000 μm, had heights of 50 μm or 100 μm, varied

in radii of curvature from 6.22 x 10^5 to 6.25 x 10^6, and varied in length from 5290 µm to 3.7 x 10^5 µm. The devices consisted of multiple switchbacks because early experiments demonstrated that maintaining tight curvature was crucial to maintain focusing. Figure 2-3 shows some of the device designs tested.

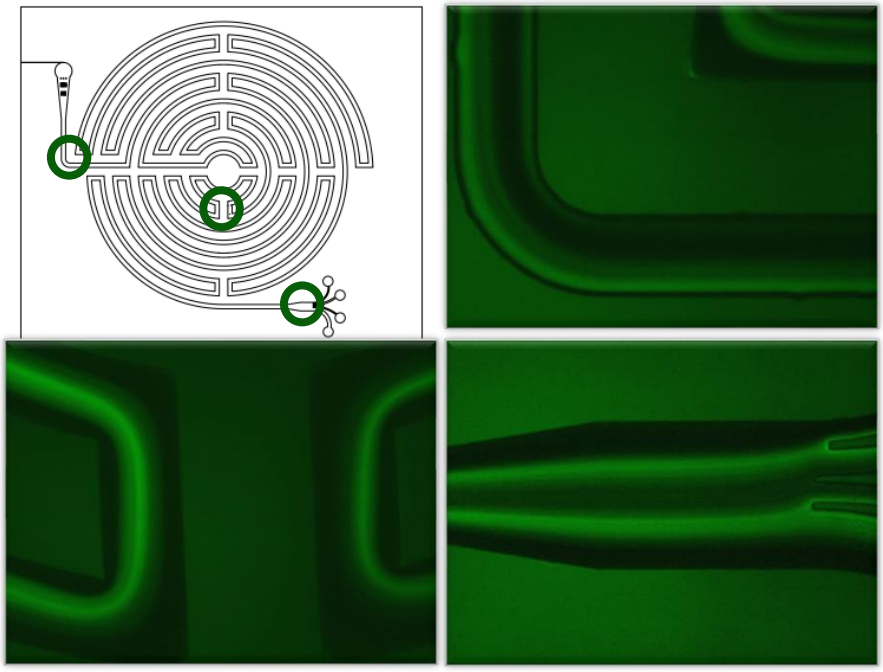

Figure 2-2: Focusing of Hep3B cells in the Labyrinth device.

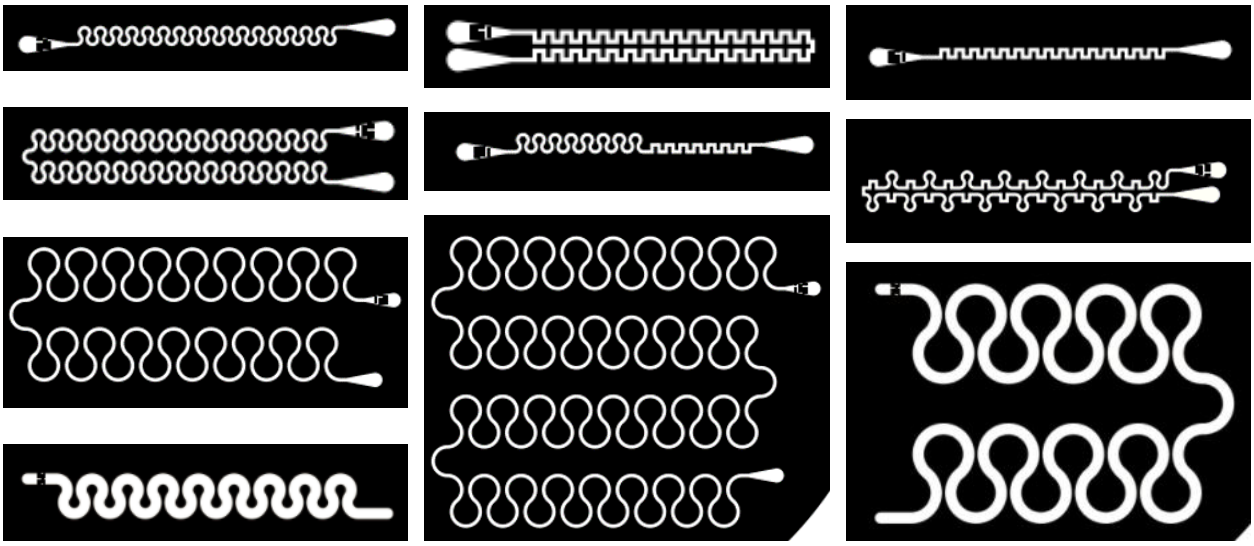

Figure 2-3: Examples of whole blood inertial devices tested.

In these experiments, it was observed that in wider (400 and 500 μm) channels multiple cancer cell line focusing streams formed while in the skinnier channels (100 and 200 μm) a single focusing stream formed under most conditions. No focusing occurred in the widest channels (1000 μm). White blood cells (WBCs) typically focused to the same position as CTCs in the skinnier channels and did not focus in the wider channels. Figure 2-4 shows an example of focusing in one of the device designs at different widths. Images are shown for the smaller channels while LUT intensity graphs are shown for the wider channels to enable the non-focusing of WBCs to be observed in these channels.

The data collected from these experiments was analyzed by comparing the non-dimensional numbers typically used to characterize inertial focusing: Reynold's Number, Particle Reynold's Number, and Dean's Number. For rigid spheres in a Newtonian fluid, particles focus when the Particle Reynold's Number is above 1 and the Reynold's Number is below approximately 150.[59] However, our comparison confirmed that the largest factor predicting focusing was cell type (Figure 2-5) indicating that the models used for rigid spheres in Newtonian fluids are

inadequate for cells in blood. In these graphs CTCs are marked with circles while WBCs are marked with square outlines. The colors of the markings represent the focusing observed: blue – good focusing, orange – some focusing, and gray – no focusing. We believe the difference in focusing between cancer cell lines and WBCs is due to their different sizes but differences in other properties such as deformability may also contribute. Unfortunately, the comparison of these non-dimensional numbers did not yield any more in-depth insight than the observation that cell type was the largest predictor of focusing.

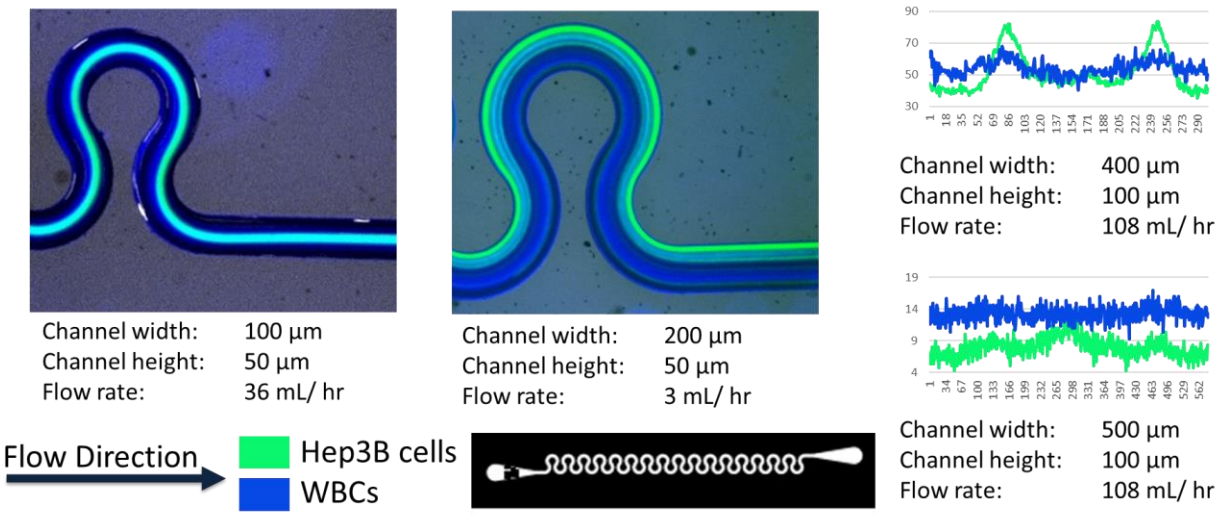

Figure 2-4: Example of focusing at different widths of one device design.

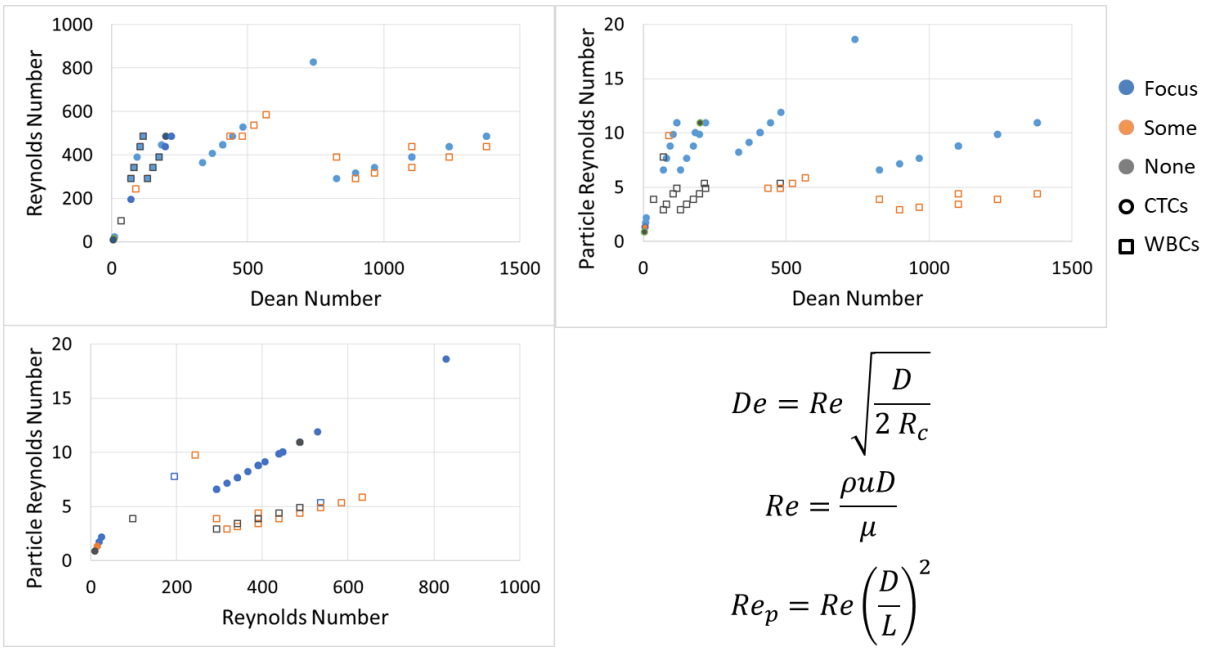

Figure 2-5: Comparison of inertial focusing in whole blood using non-dimensional numbers.

2.5.2 CTCKey™

Based on the focusing in whole blood results, an inertial focusing device was designed to focus CTCs at high flow rates in whole blood. Because focusing into single tight streamlines was observed in smaller channels but the desired flow rate was higher than these channels could withstand, a dual-stage device was developed. The first stage enriches CTCs into the two outer channels without focusing WBCs while the second stage focuses CTCs and WBCs to the center. The initial design results were used to further optimize the inertial device to achieve the desired result of having CTC enriched blood to be run directly through the ^{HB}GO device.

2.5.2.1 CTCKey™ Design

The goal of this study was to enrich CTCs at the fastest reliable flow rate without the need for pre-processing steps. Briefly, the CTCKey™ is a multi-section microfluidic device made using a PDMS top bonded to a glass slide, allowing for easy fabrication, high flow rates, and easy

imaging. The CTCKey™ was designed to operate with whole blood at flow rates up to 2,800 µL/min. Beyond this flow rate the PDMS to glass bond begins to fail when blood is flowed through the device at around 3,000 µL/min due to the high pressure accumulated in the microfluidic channels owing to the high viscosity of the blood.

We designed the CTCKey™ device to have dual sections to increase the focusing of cells using inertial forces (Figure 2-6 a). The initial section of the device focuses the CTCs towards the outer wall (Figure 2-6 ai). The subsequent second stage of the device consists of narrower channels that quickly focus the cells into the middle of the channel (Figure 2-6 aii). Having this two-stage focusing enables multifold enrichment of CTCs directly from whole blood. Both sections of the device have a height of 100 µm. The first section of the device is 400 µm wide and consists of 61 alternating corners, creating a zig-zag pattern. Upon entering the second section, the flow from the first section is split into three streams as it enters three channels in parallel: the top, middle, and bottom channels. Each of the three channels in the second section of the device are 200 µm wide with radii of curvature of 200 µm at the inner wall and 400 µm at the outer wall. The middle channel is split a second time to further reduce the pressure in the device. The top and bottom channels do not have this second split to keep the footprint of the device small (Figure 2-6 b). At the optimal flow rate, the first section (Figure 2-6 a, blue) of the CTCKey™ enriches CTCs by focusing them into two streamlines closer to the outer wall of the channel (Figure 2-6 i). In the second section (Figure 2-6 a, red), CTCs focus to the center of the channel (Figure 2-6 ii).

The focusing of cells while also splitting the fluid into multiple streams in the second section leads to concentrated CTCs in the collected portions from the top and bottom channels of the second section. As the first section of the device is split into three streams, approximately 50% of the fluid goes to the middle and 25% goes to each of the outer streams for a 50% volume

reduction of the CTC containing fluid. In the second section outlets, approximately 65% of the fluid volume is lost to the two outer streams while the remaining 35% of the fluid is enriched with CTCs and collected from the center of the top and bottom outlets. This results in an approximately 82.5% volume reduction of the CTC containing fluid. Overall, the CTCKey™ device reaches a previously unobtained 5-fold CTC enrichment from whole blood at a flow rate of 2.4 mL/min. By using the CTCKey™ to pre-enrich the CTCs, larger volumes of blood can be processed rapidly which leads to more CTCs for robust downstream analysis. For example, a typical CellSearch run processes 7.5 mL,[27] but pre-enrichment with the CTCKey™ would allow for interrogation of the equivalent of 43 mL of undiluted blood in its 7.5 mL sample which is over a 5-fold increase.

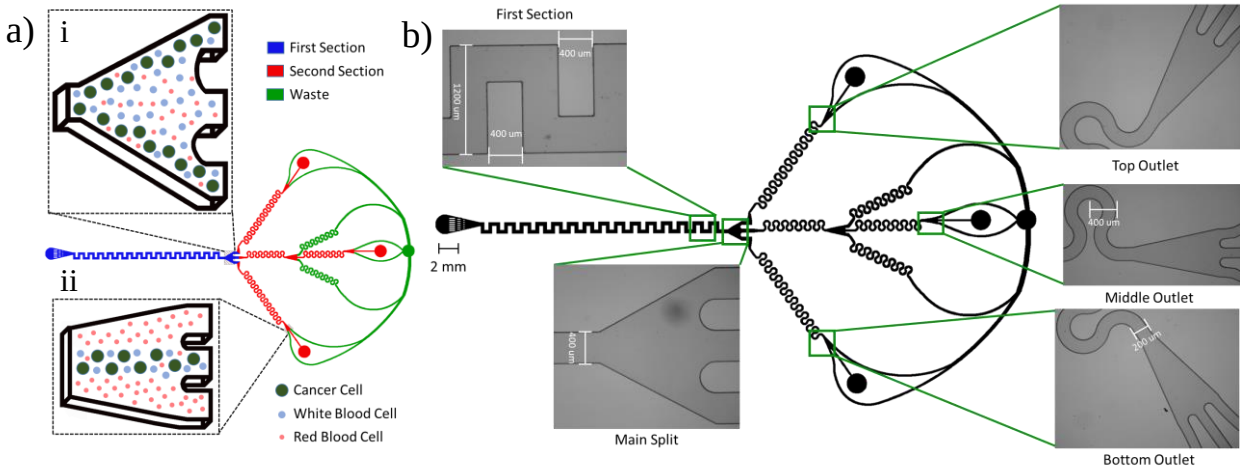

Figure 2-6: CTCKey™ Device. a) Schematic of the device and the expected focusing positions of the cells found in blood as they move through the device at a flow rate of 2.4 mL/min. The first section, represented in blue, focuses larger cells to the outer walls. The second section, represented in red, consists of two longer outer channels and four smaller inner channels. In the second section, CTCs focus to the middle of the channel. The channels shown in green are waste and are predicted to never have CTCs when focusing occurs. b) Fabricated device engineering design with dimensions. The inset images show the channel structure at selected locations of interests, where cell focusing data is presented. The first channel is a 400 µm wide square channel with right corners, while the second channel is a 200 µm wide serpentine curved channel.

2.5.2.2 Characterization of CTCKey™ using Buffer Solutions

Although there was a substantial increase in CTC concentration using the CTCKey™ device with PBS, it is critical to understand the effects of protein presence on cell focusing. To do

this, pre-fluoresced cell lines were spiked into PBS with three concentrations of bovine serum albumin (BSA), PBS (No BSA), 3.5 g/dL BSA, and 7 g/dL BSA solutions, and then flowed through the device where focusing was observed using an inverted fluorescent microscope. These BSA solution concentrations were selected because 7 g/dL is the typical protein concentration found in blood.[100] All experiments were performed using live MCF7 breast cancer cells spiked into the corresponding BSA solution. All three solutions were tested at flow rates from 200 µL/min to 3600 µL/min to observe the effects of flow rate, Reynolds Number, and Dean's Number on focusing. BSA solutions were flowed at a variety of flow rates to allow for comparison of these solutions with that of blood based on similar Reynold's Number and Dean's Number in addition to the comparison at the same flow rate.

2.5.2.3 Focusing of MCF7 Cancer Cells in PBS (No BSA)

Figure 2-7 presents the cell focusing patterns of MCF7 cells in the No BSA condition, this represents cells in pure PBS and acts as the baseline for comparisons. Images of the first section (Figure 2-6 b) at selected flow rates are shown in Figure 2-7 a. Figure 2-7 b shows a series of ridge plots of the LUTs across the first section of the device along the line displayed on the image. Each flow rate is a horizontal line in the graph, with the peaks representing the locations of cells within the channel. The larger the peak, the higher the fluorescence at that location and hence more cells. The higher and narrower the peak, the better the focusing. The table right of the graph lists the flow rate of each graph along with the Reynold's Number for the first section and Particle Reynold's Number for WBCs and CTCs based on the estimate of 10 µm diameter particles for WBCs and 15 µm diameter particles for CTCs. This analysis was performed at two locations on the device: the first section and the bottom channel. The first section of the device indicates the

initial focusing within the device. The analysis at the bottom outlet demonstrates the focusing within the final product stream of the channel.

In the first section of the device, two focusing streams form towards the outer walls up to a flow rate of 800 µL/min. Between 800 and 1,200 µL/min, the focusing shifts from two outer streams to a single stream close to the center of the channel. As the flow rate is increased above 1,600 µL/min, focusing decreases until it becomes non-existent and instead mixing is observed.

Similar to Figure 2-7 a and b, the same analysis is shown for the bottom outlet of the device in Figure 2-7 c and d. The flow rates listed in Figure 2-7 d correspond to the flow rates in Figure 2-7 b. The first section of the device splits the flow into three streams. The three channels off the first section behave similarly but the bottom channel and outlet are discussed here. The flow rates listed for the bottom outlet are approximations based on the COMSOL® model of the device (Figure 2-8). For focusing to be observed in the bottom outlet, MCF7 cells must have focused to the outer wall or the bottom outlet does not have any cells in it to focus. For example, at 1,600 µL/min, MCF7 cells focus to the center of the device so no cells are present at 379 µL/min in the bottom channel. Figure 2-7 d includes the Dean's Number at 300 µm radii of curvature which corresponds to the center line of the device.

In the bottom channel of the device, MCF7 cells focus into one streamline that shifts from the outer wall towards the inner wall with increasing flow rate. The focusing peak becomes narrower and more distinct until around 142 µL/min after which it begins to widen. Even though the peak shifts across the channel at the center of the curve, the MCF7 cells remain directed towards the center outlet as shown in Figure 2-7 c.

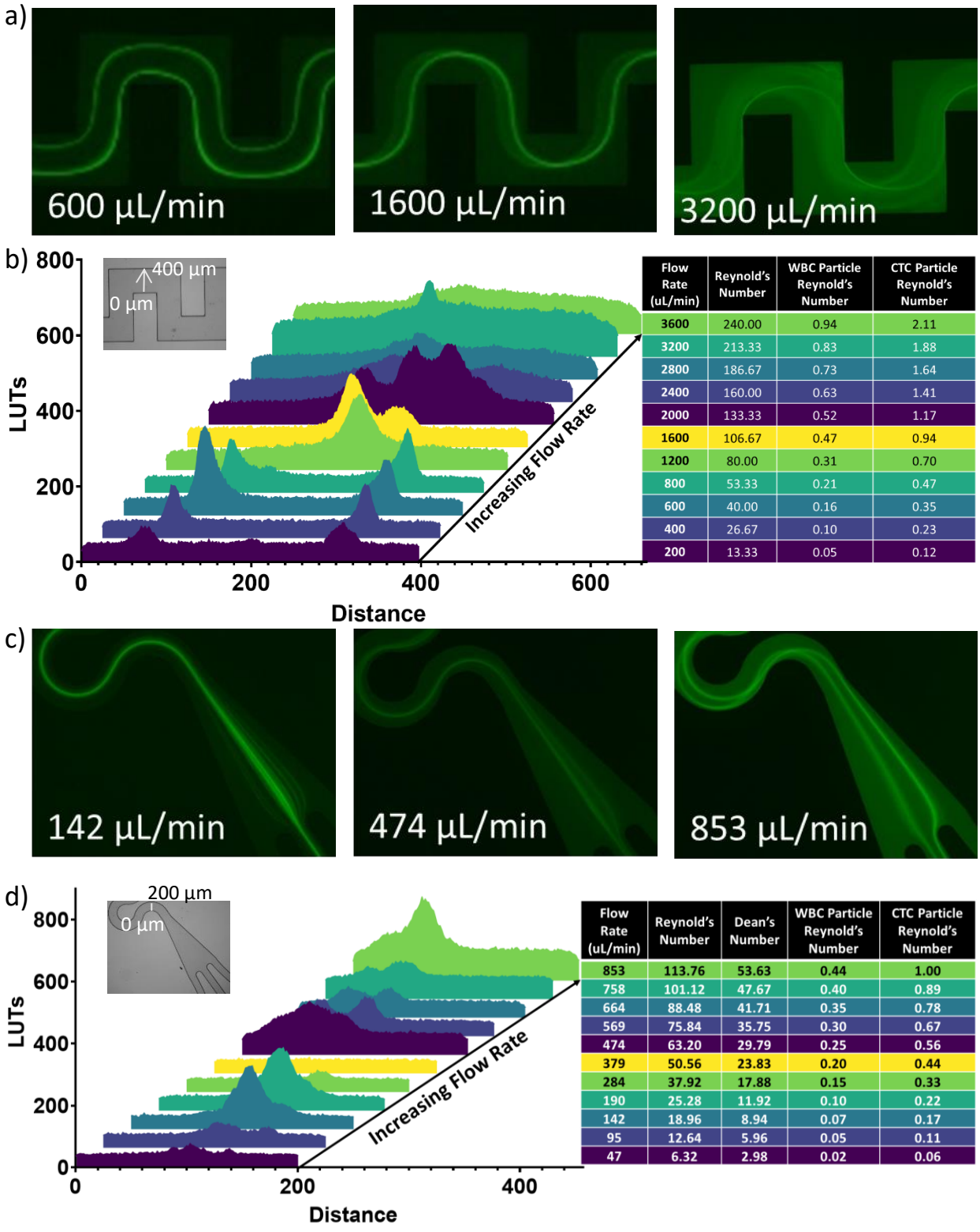

Flow Rate (uL/min)	Reynold's Number	WBC Particle Reynold's Number	CTC Particle Reynold's Number
3600	240.00	0.94	2.11
3200	213.33	0.83	1.88
2800	186.67	0.73	1.64
2400	160.00	0.63	1.41
2000	133.33	0.52	1.17
1600	106.67	0.47	0.94
1200	80.00	0.31	0.70
800	53.33	0.21	0.47
600	40.00	0.16	0.35
400	26.67	0.10	0.23
200	13.33	0.05	0.12

Flow Rate (uL/min)	Reynold's Number	Dean's Number	WBC Particle Reynold's Number	CTC Particle Reynold's Number
853	113.76	53.63	0.44	1.00
758	101.12	47.67	0.40	0.89
664	88.48	41.71	0.35	0.78
569	75.84	35.75	0.30	0.67
474	63.20	29.79	0.25	0.56
379	50.56	23.83	0.20	0.44
284	37.92	17.88	0.15	0.33
190	25.28	11.92	0.10	0.22
142	18.96	8.94	0.07	0.17
95	12.64	5.96	0.05	0.11
47	6.32	2.98	0.02	0.06

Figure 2-7: Focusing of Cells in PBS. a) Images of pre-fluoresced MCF7 cells in the first section of the device at specified flow rates. b) Fluorescent intensity graphs at various flow rates across the shown position in the first section of the device. c) Images of pre-fluoresced MCF7 cells in the bottom outlet of the device at specified flow rates. d) Fluorescent intensity graphs at various flow rates across the shown position in the bottom section of the device.

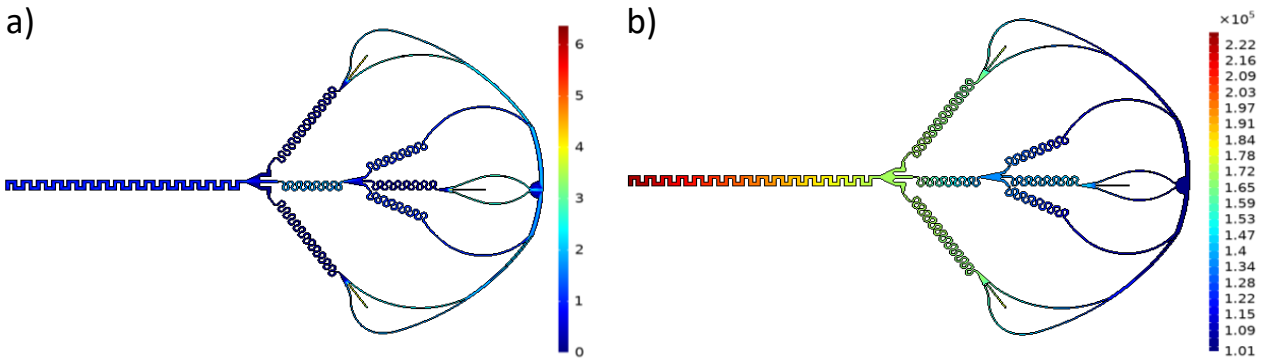

Figure 2-8: COMSOL® Model of the CTCKey™ with an inlet flow rate of 2400 µL/min. a) Velocity profile of blood through the CTCKey™. b) Pressure in the CTCKey™ with blood.

2.5.2.4 Focusing of MCF7 Cancer Cells in 3.5 g/dL BSA Solution

Similar to Figure 2-7, Figure 2-9 shows the focusing of MCF7 cells in a 3.5 g/dL BSA solution. This concentration is the halfway point between no protein and a typical protein concentration of whole blood. At flow rates below 800 µL/min, MCF7 cells focus toward the two outer walls. As the flow rate is increased, focusing is lost then reforms near the center of the channel at 1,600 µL/min. At 2,000 µL/min, the focusing starts to decrease until mixing occurs.

In the bottom outlet of the device, the focusing patterns are similar to those observed in the No BSA condition. Focusing occurs in the center of the channel until 190 µL/min. At 569 µL/min, focusing has shifted towards the inner wall and continues to do so as flow rate is increased. Even as the focusing shifts toward the inner wall, MCF7 cells are still directed toward the center outlet.

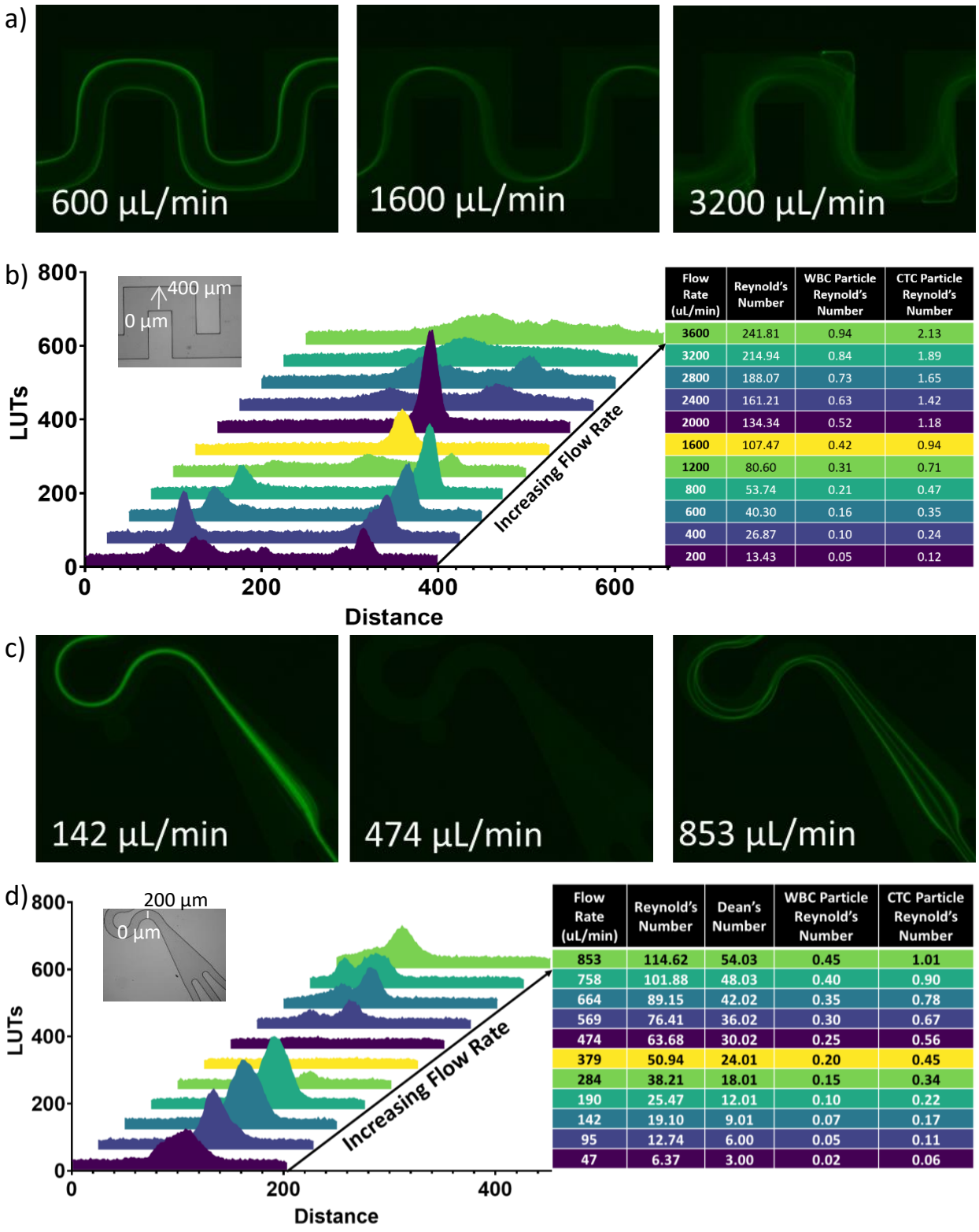

Flow Rate (uL/min)	Reynold's Number	WBC Particle Reynold's Number	CTC Particle Reynold's Number
3600	241.81	0.94	2.13
3200	214.94	0.84	1.89
2800	188.07	0.73	1.65
2400	161.21	0.63	1.42
2000	134.34	0.52	1.18
1600	107.47	0.42	0.94
1200	80.60	0.31	0.71
800	53.74	0.21	0.47
600	40.30	0.16	0.35
400	26.87	0.10	0.24
200	13.43	0.05	0.12

Flow Rate (uL/min)	Reynold's Number	Dean's Number	WBC Particle Reynold's Number	CTC Particle Reynold's Number
853	114.62	54.03	0.45	1.01
758	101.88	48.03	0.40	0.90
664	89.15	42.02	0.35	0.78
569	76.41	36.02	0.30	0.67
474	63.68	30.02	0.25	0.56
379	50.94	24.01	0.20	0.45
284	38.21	18.01	0.15	0.34
190	25.47	12.01	0.10	0.22
142	19.10	9.01	0.07	0.17
95	12.74	6.00	0.05	0.11
47	6.37	3.00	0.02	0.06

Figure 2-9: Focusing of Cells in 3.5% BSA. a) Images of pre-fluoresced MCF7 cells in the first section of the device at specified flow rates. b) Fluorescent intensity graphs at various flow rates across the shown position in the first section of the device. c) Images of pre-fluoresced MCF7 cells in the bottom outlet of the device at specified flow rates. d) Fluorescent intensity graphs at various flow rates across the shown position in the bottom section of the device.

2.5.2.5 Focusing of MCF7 Cancer Cells in 7 g/dL BSA Solution

Focusing in a 7 g/dL BSA solution, which approximates the total protein concentration in whole blood, is shown in Figure 2-10. This analysis mirrors what was performed for the No BSA and 3.5 g/dL BSA solutions shown in Figure 2-7 and 2-9. MCF7 cells do not focus in 7 g/dL BSA at 200 µL/min but do focus to two streamlines towards the outer walls between 400 µL/min and 1,200 µL/min. By 2,000 µL/min, MCF7 cells are focused into a single stream near the center of the channel. Above 2,400 µL/min, this focusing decreases until mixing occurs.

Focusing of MCF7 cells in the bottom outlet is similar to that observed in No BSA and 3.5 g/dL BSA solutions. MCF7 cells focus to a single streamline that becomes more distinct as flow rate is increased to 190 µL/min. Above 474 µL/min, the focusing of MCF7 cells becomes less distinct. As flow rate is increased, the focused streamline slowly shifts from the inner wall toward the outer wall but continues to be directed to the center outlet.

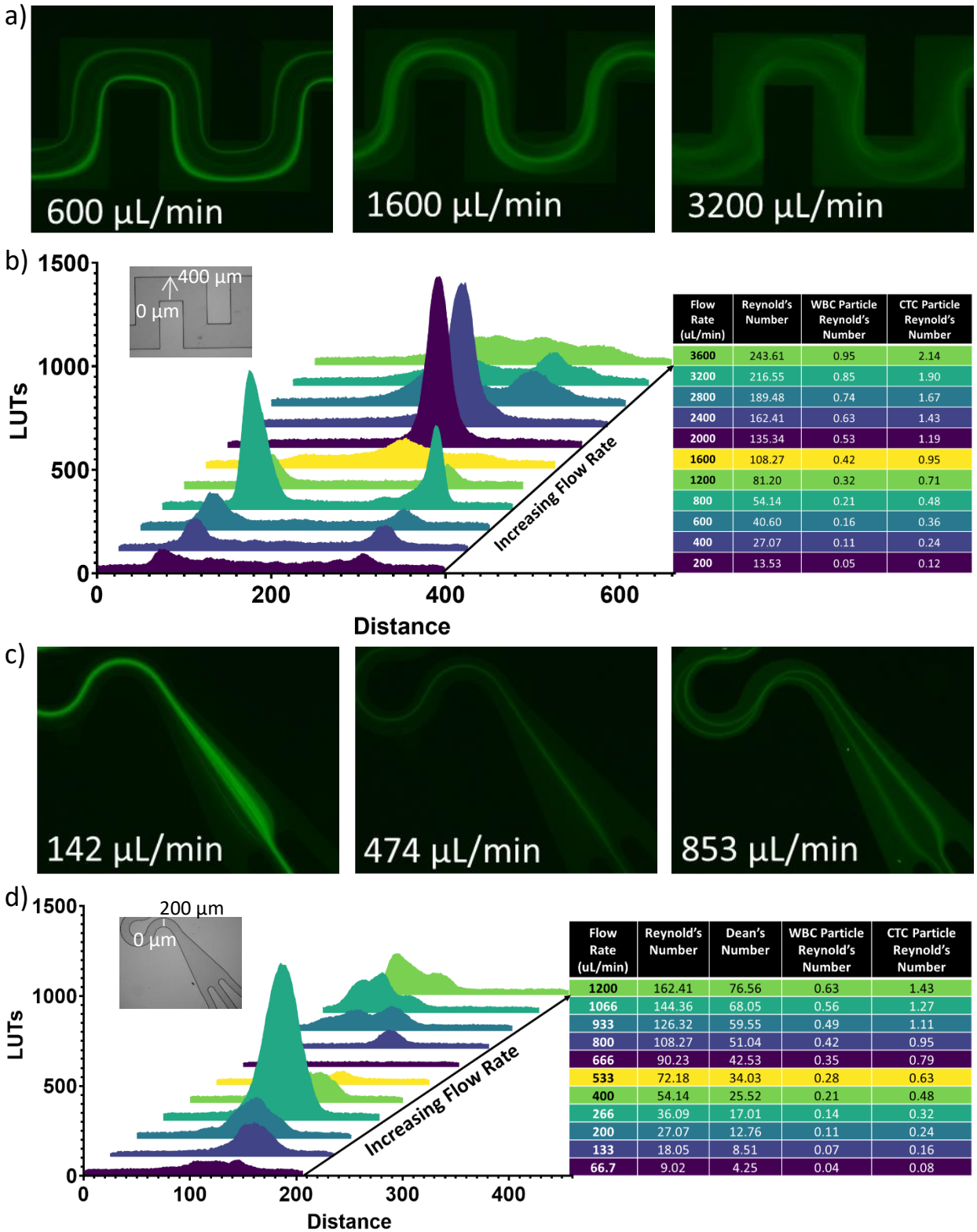

Flow Rate (uL/min)	Reynold's Number	WBC Particle Reynold's Number	CTC Particle Reynold's Number
3600	243.61	0.95	2.14
3200	216.55	0.85	1.90
2800	189.48	0.74	1.67
2400	162.41	0.63	1.43
2000	135.34	0.53	1.19
1600	108.27	0.42	0.95
1200	81.20	0.32	0.71
800	54.14	0.21	0.48
600	40.60	0.16	0.36
400	27.07	0.11	0.24
200	13.53	0.05	0.12

Flow Rate (uL/min)	Reynold's Number	Dean's Number	WBC Particle Reynold's Number	CTC Particle Reynold's Number
1200	162.41	76.56	0.63	1.43
1066	144.36	68.05	0.56	1.27
933	126.32	59.55	0.49	1.11
800	108.27	51.04	0.42	0.95
666	90.23	42.53	0.35	0.79
533	72.18	34.03	0.28	0.63
400	54.14	25.52	0.21	0.48
266	36.09	17.01	0.14	0.32
200	27.07	12.76	0.11	0.24
133	18.05	8.51	0.07	0.16
66.7	9.02	4.25	0.04	0.08

Figure 2-10: Focusing of Cells in 7% BSA. a) Images of pre-fluoresced MCF7 cells in the first section of the device at specified flow rates. b) Fluorescent intensity graphs at various flow rates across the shown position in the first section of the device. c) Images of pre-fluoresced MCF7 cells in the bottom outlet of the device at specified flow rates. d) Fluorescent intensity graphs at various flow rates across the shown position in the bottom section of the device.

2.5.2.6 Focusing of MCF7 Cancer Cells in Whole Blood Samples

To test the focusing of cells in whole blood, MCF7 cells were spiked into whole blood and flown through the CTCKey™ device at various flow rates. Focusing of MCF7 cells at the main split, the split from the first section to the second section, is shown in Figure 2-11 a. The flow rate is listed above the image and the Reynold's number below each image. At 800 µL/min, MCF7 cells are pushed away from the walls but distinct focusing is not observed. As the flow rate increases, the focusing splits into two streamlines as the flow rate approaches 2,000 µL/min. The streamlines continue to become more distinct and shift slightly further out with increasing flow rate. Due to pressure limitations of the PDMS to glass bond, flow rates were only tested up to 2,600 µL/min. In the second section of the device, MCF7 cells continue to focus to the center as was seen in Figure 2-7, 2-9, and 2-10.

The CTCKey™ device was designed to operate with whole blood at 2,400 µL/min (Figure 2-11 b). At this flow rate, the MCF7 cells focus to the outer two walls in the first section and the center of the channel in the second section. Distinct streamlines are observed in both sections of the device indicating that focusing occurs. The focusing wavers toward the middle channel of the first section if the flow rate is decreased to 2,000 µL/min but remains in the outer two channels with small fluctuations in flow rate. To confirm the focusing patterns correlated with cell enrichment even at low numbers of target cells, MCF7 cells were spiked at low concentrations into whole blood and processed through the CTCKey™ device at select flow rates. The output from the top, bottom, middle and waste were collected and MCF7 cells were enumerated (Figure 2-11 c). At 800 µL/min, 45% of cells went to the top and bottom outlets while 34% of cells went to the middle outlet. As the flow rate is increased to 2000 µL/min, the cells shift towards the outside with 86% of cells going to the top and bottom outlets. When the flow rate is further increased to 2400

µL/min, the cells going to the top and bottom outlets decreases slightly to 75%. These numbers correspond to the observed streamlines.

When operated at 2,400 µL/min, the flow rate out of the collected portion of the bottom outlet is approximately 200 µL/min which lies within our target range of 100 µL/min – 300 µL/min. This target range was selected because it is the typical inlet flow rate range for other CTC isolation devices. With the CTC enriched blood at this flow rate, it can be directly processed using an established CTC isolation technology. To further investigate the compatibility of the CTCKey device with a standard CTC isolation technology, pre-enriched MCF7 cells from the CTCKey™ were isolated using the CellSearch® technology. MCF7 cells were spiked into whole blood at low concertation (~100 cells/mL) and then processed through the CTCKey™ and the collected product was run on the CellSearch® system using the typical protocol. The percentage of cells recovered were compared to that of standard CellSearch® processing without enrichment (Figure 2-11 d). Although, there is a slight decrease in cell recoveries (85 vs 71%), when processed with the CTCKey™, more cells would still be detected using the CTCKey™ as a pre-enrichment technology due to the increase in blood volume that can be processed overall.

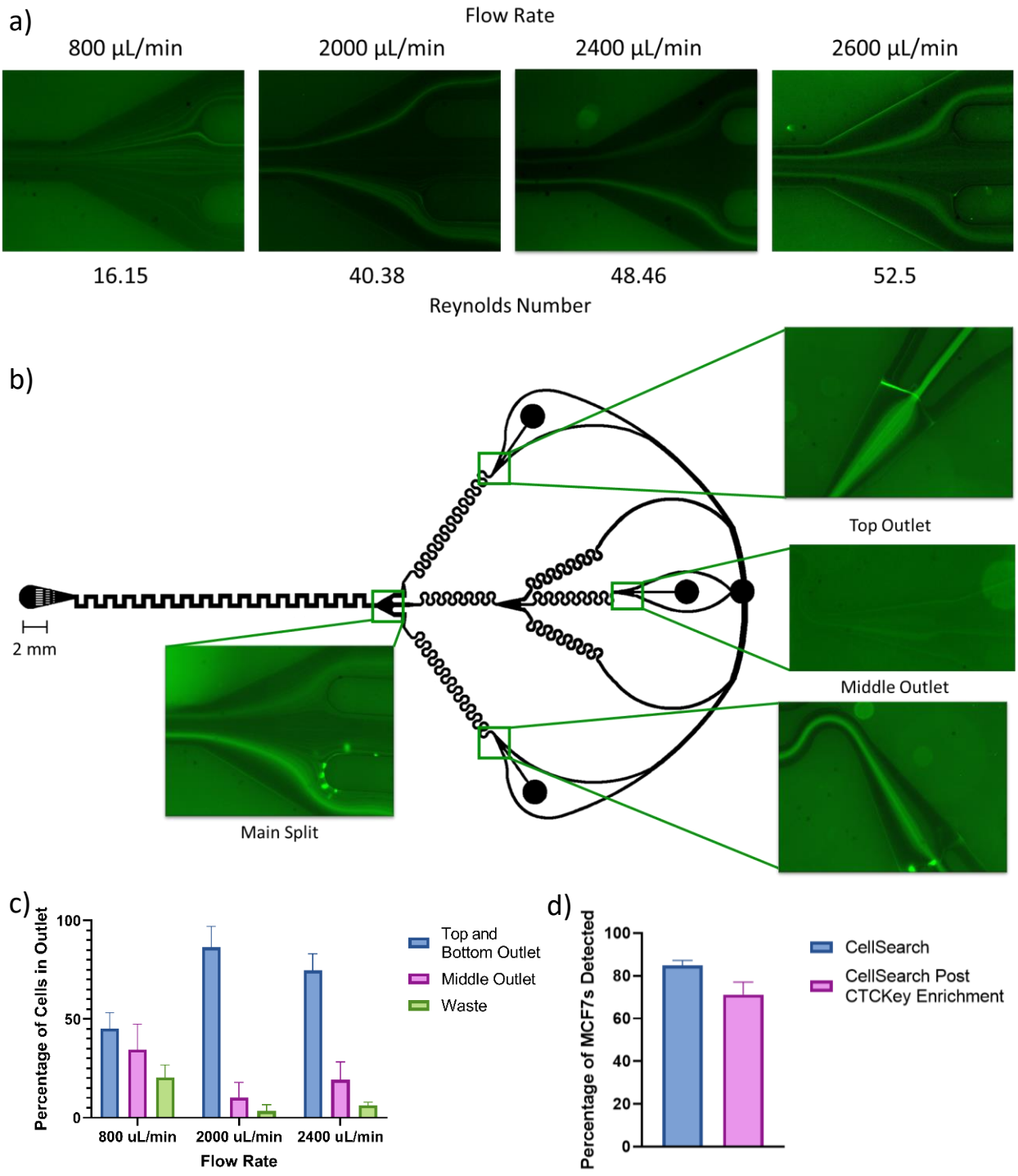

Figure 2-11: Focusing of Cells in Whole Blood. a) Images of pre-fluoresced MCF7 cells focusing in whole blood shown at the main split in the device with increasing flow rate. The Reynold's Numbers in the first section of the device at the specified flow rate is listed below each image. b) Images of pre-fluoresced MCF7 cells focusing in whole blood through the CTCKey™ at 2400 uL/min. c) Quantification of cell recoveries from the CTCKey™ device at various flow rates. Percentage of cells recovered by the CTCKey™ device from samples with ~100 MCF7 cells spiked into whole blood and processed through CTCKey™ device at various flow rates. Percentage of cells collected in top and bottom outlet are shown together (blue) while the middle outlet (pink) and waste are shown individually (green). d) Percentage of MCF7 cells detected by CellSearch® with and without pre-enrichment by the CTCKey™.

2.5.2.7 Comparison between CTC Focusing in Buffer and Whole Blood

Inertial focusing is influenced by a variety of factors including velocity, density, viscosity, aspect ratio, and particle size. Although MCF7 cells tend to focus toward the center outlet in the second section of the device, the focusing patterns still differ. Figure 2-12 a shows images of the bottom outlet at an inlet flow rate of 2400 µL/min which corresponds to a flow rate of 800 µL/min in the bottom outlet. At this flow rate, MCF7 cells focus to two streams that both get directed towards the center outlet in the No BSA and 3.5 g/dL BSA solutions while in the 7 g/dL solution and in whole blood a single focusing stream is observed.

The various factors that affect focusing were simultaneously compared by graphing Reynold's Number vs Dean's Number for samples from all three BSA solutions in Figure 2-12 b. This graph demonstrates that in the second section of the device focusing of a single tight streamline occurs as long as both the Reynold's Number and Dean's Number are low enough. The Reynold's and Dean's Number for the whole blood image shown in Figure 2-12 a is also marked on this graph. At this flow rate, MCF7 cells form a single wide peak at the bottom outlet even though the Reynold's Number and Dean's Number are low enough for a tight single peak to form based on the BSA solution data. This difference in observation is likely due to the high number of particle interactions that occur in whole blood. These particle interactions may prevent the MCF7 cells from forming as tight of a streamline due to steric hinderance in the solution.

Although looking at Reynold's and Dean's Number is useful, it does not allow focusing comparison for the first section of the device since Dean's Number is undefined around corners. The fluorescent intensities were graphed using the find Peaks function in MatLab to better compare the focusing patterns for each solution. This function smooths out the curve and provides information about the peaks (Figure 2-12 g). The peak intensity, location, and width at half-

prominence can be exported. Figure 2-12 c shows the MatLab graphs at the specified flow rates for the first section of the device. Figure 2-12 d graphs the locations and width at half-prominence for each condition allowing for comparisons to be made. The peak height represents the number of cells that are found in each peak while the width at half-prominence is a good indicator of how focused the cells are in each peak. A smaller width at half-prominence demonstrates that the cells form a tight streamline for that peak.

At 800 µL/min all three BSA solutions produce two peaks with the right peak having slightly more cells in the 3.5 g/dL BSA solution while the left peak has more cells in the 7 g/dL BSA solution. It is unclear why this shift in focusing occurs. To validate the shift, the same batch of cells was used at increasing BSA solution on the same day for the graphs shown and each graph is the average of three separate images. At 2000 µL/min, MCF7 cells do not focus in the No BSA solution, have some focusing in the 3.5 g/dL BSA solution, but form a single tight streamline in the 7 g/dL BSA solution. Similarly at 2400 µL/min, the cells form a single tight streamline in the 7 g/dL BSA solution; however, they do not focus in the 3.5 g/dL solution but form two streamlines in the No BSA solution. The fluid properties that define Reynold's Number and Dean's Number vary slightly between these three solutions but not enough to account for the drastic change in focusing that occurs between the fluids, indicating that other factors effect inertial focusing of MCF7 cells more than has been accounted for previously. One possibility is that the varying protein concentrations effect cell properties such that the deformability varies enough between these solutions to drastically change the focusing patterns.

The same program was used to compare the focusing in the second section of the device. The graph results from this comparison are shown in Figure 2-12 e and f. Unlike in the first section, single peaks form in roughly the same position for all three BSA solutions. At 800 µL/min, MCF7

cells focus extremely well to the outer two outlets so there are not cells in the middle to be focused in the 3.5 g/dL solution. Similarly, the variations in peak height between the different fluids is due to the number of cells that get directed to that particular outlet from the first section. Based on the peak widths at half-prominence, focusing becomes more distinct with increasing flow rate. If flow rate continues to increase, focusing begins to be lost as the peak becomes wider (Figure 2-7, 2-9, and 2-10). To confirm the streamline data was representative of target cell focusing even when present at low concentrations, low cell numbers of MCF7s and A549s were spiked into 7 g/dL BSA solution, processed through the CTCKey™ device at various flow rates. MCF7 cells collected in all the outlets were enumerated (Figure 2-12 h, 2-13). At 800 µL/min the majority of cells went to the top and bottom outlets while at 2000 µL/min the cells went to the middle outlet both of which correspond to the observed streamlines. At 2400 µL/min, MCF7s focused to the center while A549s appear to have defocused. Since A549s are slightly smaller in size than MCF7s, it makes sense that these cells have already begun to de-focus since this is observed at the next highest flow rate tested for MCF7s. The focusing of MCF7 cells was also imaged in brightfield using a high speed camera to visualize the focusing of individual cells (Figure 2-14).

Previous work has indicated that focusing occurs when the particle Reynold's number is greater than one; however, in the CTCKey™, focusing often occurs even if the particle Reynold's number is significantly less than one. This same phenomenon has been observed in other serpentine channels indicating that this criteria is not applicable to all systems.[54]

Although Reynold's number and Dean's number are often used to quantify flow in inertial systems, this study demonstrates that they are not sufficient for all systems. In the second section of the device where Dean's number is defined, cell focusing is similar for all three BSA solutions; however, in the first section of the device this does not hold indicating there are more factors that

help define focusing when right corners are present. The increased protein concentration could lead to changes in particle properties as well as other fluid properties often neglected in inertial microfluidics such as fluid elasticity and rheology.[62] Future studies should compare the focusing of polystyrene beads to that of cells to distinguish changes in focusing patterns due to particle properties from those that are caused by differences in fluid properties. Fluid properties should be additionally altered using techniques such as adding glycerol to the solution to further decipher how each property effects the focusing of CTCs in whole blood.

It was not surprising that the focusing predictions do not hold in whole blood due to the large number of particle interactions, but the inaccuracy of the predictions in the BSA solutions indicates the need for more sophisticated focusing equations that account for more fluid and particle properties.

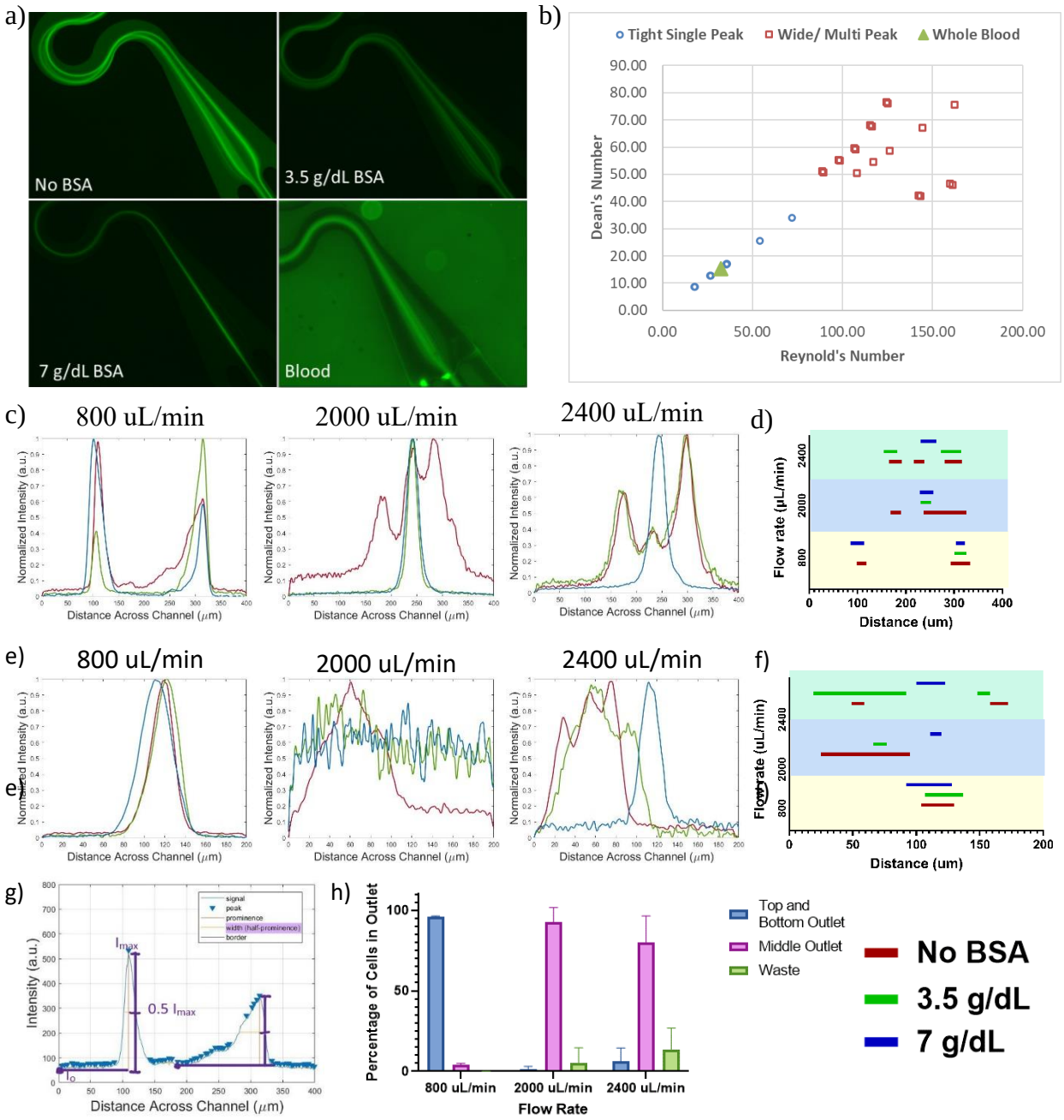

Figure 2-12: Focusing Comparison of MCF7 Cells in a Variety of Fluids. a) Images of bottom outlet at the optimal flow rate of 2400 µL/min inlet flow rate. b) Reynold's vs. Dean's Number Graphs. c) Peak height and width of normalized fluorescent intensity graphs from t first section of the device. d) Peak width at half-prominence comparison between BSA solutions in the first section of the device at selected flow rates. The distance is the distance across the channel along the line shown in figures 2-7, 2-9, and 2-10 and the width at half-prominence is marked for each condition. e) Peak height and width of normalized fluorescent intensity graphs from the bottom outlet of the device. f) Peak width at half-prominence comparison between BSA solutions in the bottom outlet of the device at selected flow rates. The distance is the distance across the channel along the line shown in figures 2-7, 2-9, and 2-10 and the width at half-prominence is marked for each condition. g) Graph marking peak and width at half-prominence definitions. h) Quantification of cell recoveries from the CTCKey™ device at various flow rates. Percentage of cells recovered by the CTCKey™ device from samples with ~1000 MCF7 cells per mL spiked into 7g/dL BSA and processed through the CTCKey™ device at various flow rates. Percentage of cells collected in top and bottom outlet are shown together (blue) while the middle outlet (pink) and waste are shown individually (green).

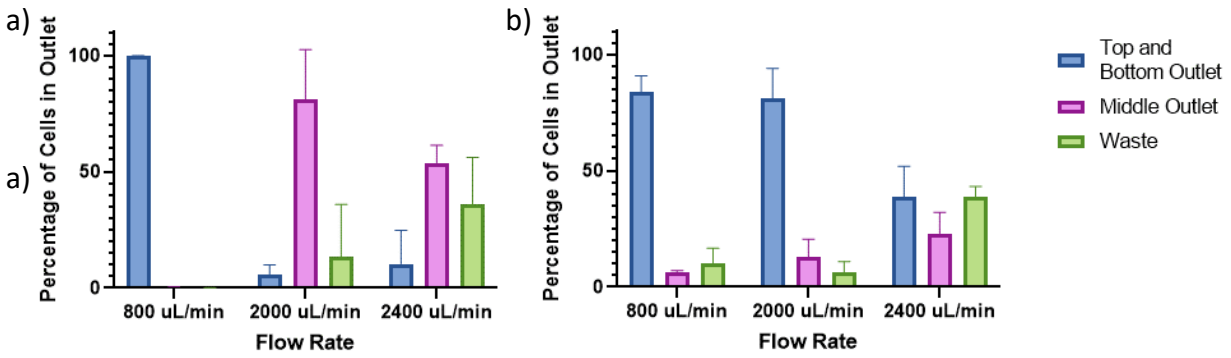

Figure 2-13: Small Cell Numbers Spiked into 7 g/dL BSA. Quantification of cell recoveries from the CTCKey™ device at various flow rates. Percentage of cells recovered by the CTCKey™ device from samples with a) ~1000 A549 cells and b) ~300 WBCs per mL spiked into 7 g/dL BSA.

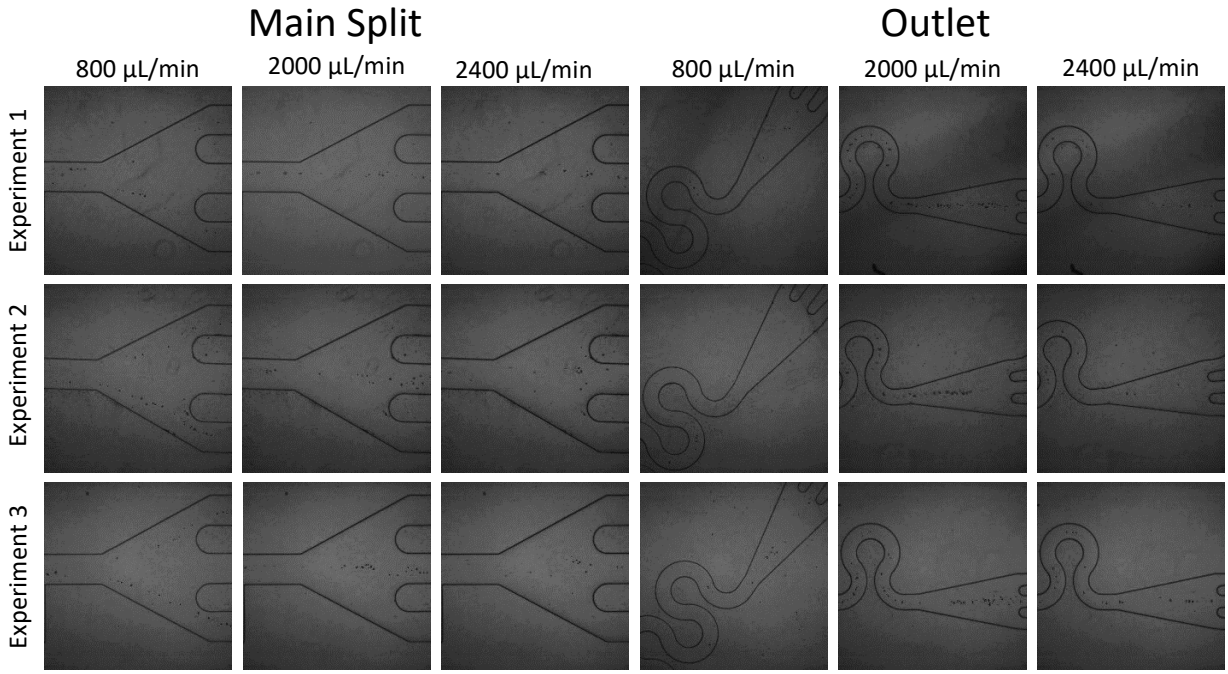

Figure 2-14: Images taken with a high-speed camera of MCF7 cells focusing in 7 g/dL BSA. Each row represents images from an individual repeat experiment. Videos from experiment two at 2000 µL/min are attached as supplementary files.

2.5.3 Herringbone Graphene Oxide (^{HB}GO) Device

The ^{HB}GO device was used as the capture module in the first version of the indwelling CTC capture system.[98] This device is a combination device between the functionalized GO (^{FC}GO) chip

and the herringbone device.[32,33] The GO chemistry enables highly specific, highly sensitive capture of target cells while the herringbone structure increases cell-surface interactions.

Before this device was tested in vivo, viability studies were performed using MCF7 cells (Figure 2-15 a). As expected, based on the predicted forces present on the cells, cell viability remained high even at the high flow rates tested. This allowed us to move forward with testing the ^{HB}GO as the capture module in the indwelling system.

In addition to cell viability, capture efficiency is also important. MCF7 cells were processed through the chip at a variety of flow rates and the capture efficiency was compared to that of the ^{FC}GO chip (Figure 2-15 b). The herringbone pattern forces cells towards the functionalized bottom surface allowing high capture efficiency to be maintained even at higher flow rates.

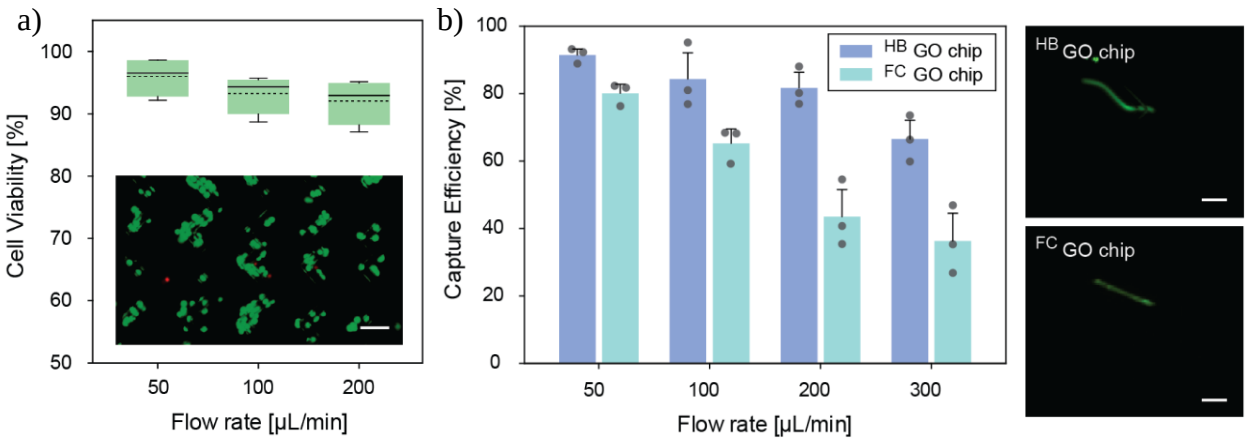

Figure 2-15: MCF7 Cells in the ^{HB}GO device. a) Cell viability of MCF7 cells in the ^{HB}GO device. b) Capture efficiency of MCF7 cells in the ^{HB}GO and ^{FC}GO devices with images of cell flow patterns in both device.

In order to use this device in conjunction with the CTCKey™, slight modifications were made. The original ^{HB}GO device had four individual chambers to prevent chamber bonding and aid in directing streamlines; however, the increased pressure of the combined system caused this thin bonding area to rupture so the ^{HB}GO was modified to be a single chamber. Because the corona

discharge bonding is not as strong as bonding performed by the plasma etcher, the high pressure of the system sometimes caused the bonding between the PDMS and silicon wafer to fail. To prevent critical failure even if the pressure fluctuated, holders were re-purposed from another project then redesigned to better fit the specific needs of this system. These holders screw down at the corners, helping to maintain the bonding while blood is being processed. After processing, the holders are removed to analyze the captured cells.

2.5.4 Integrated Ex-Dwelling System

For the ex-dwelling system, the CTCKey™ is used to pre-enrich CTCs into streamlines that are directed towards three modified ^{HB}GO devices (Figure 2-16). At the optimal flow rate of 2400 µL/ min, the CTCs are sent to the outer two ^{HB}GO devices but at lower flow rates CTCs primarily go to the middle ^{HB}GO device. To better monitor cell focusing, all three ^{HB}GO devices were functionalized with anti-EpCAM to capture CTCs for this initial round of experiments. This allowed us to test capture efficiencies even when the flow rate was not what was predicted.

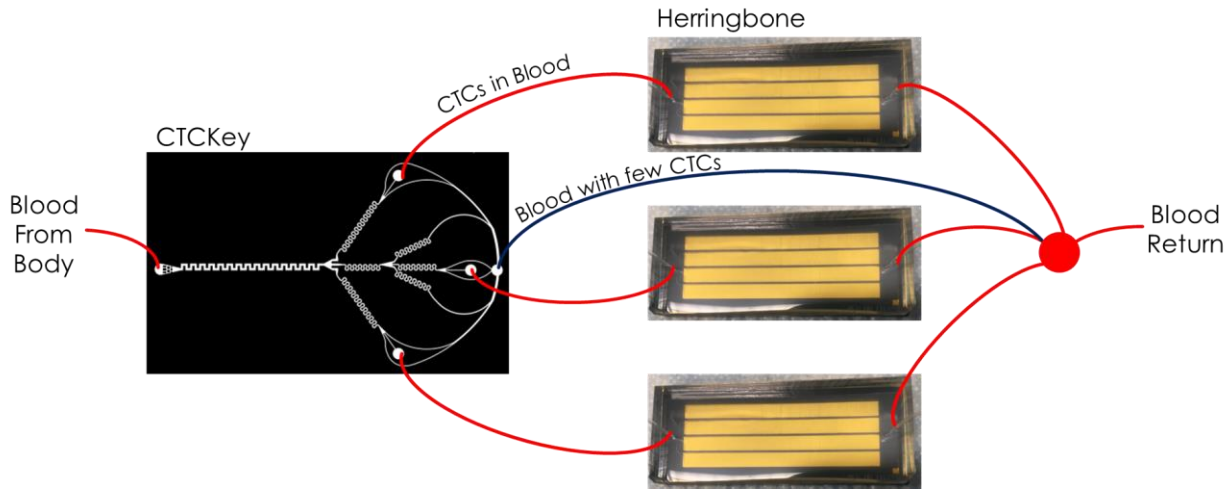

Figure 2-16: Integrated ex-dwelling device schematic.

The combined device was attached to other components to create a complete integrated system (Figure 2-17). Similar to the first version of the indwelling catheter, the system consists of a dual-lumen catheter, a peristaltic pump, and a CTC capture module. The CTC capture module includes the CTCKey™, three ^{HB}GO devices, and a combining device. The combining device is a simple PDMS device that combines the outlet streams from all three ^{HB}GO devices and the waste stream from the CTCKey™ to one stream to be returned to the patient. The heparin injector is not used for *in vitro* testing but the yellow arrow indicates where it is attached to the system for canine experiments.

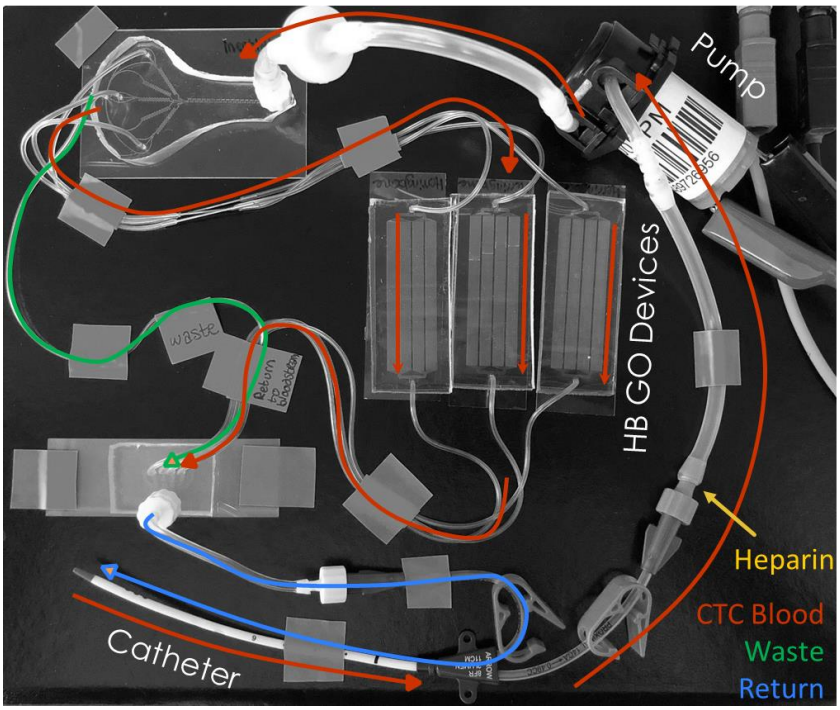

Figure 2-17: Complete system for lab testing

This system was optimized by making changes over time (Figure 2-18). The graph indicates what changes were made between each experiment. Most changes were tested independently off-system to determine how each change effects flow.

Each change was made because it was either necessary to make the system wearable or was predicted to improve the system. We switched to the 6V pump because it is a wearable size and the original pump was not. The tubing size was increased to reduce pressure on the system but we realized after the fact that changing the tubing size drastically decreased our capture efficiency The larger tubing did not seal as well which allowed micro bubbles to enter the ^{HB}GO devices. The bubbles changed the ^{HB}GO devices to function closer to the ^{FC}GO devices by getting trapped in the upper chambers, essentially removing the herringbone pattern. The backflow preventer helped the pump maintain a consistent flow rate and decreased critical failure of devices due to sudden changes in pressure. We switched from EDTA to CellSave tubes for blood collection because this allowed for a more direct comparison to the previous ^{HB}GO control devices as well as enabled experimental flexibility since blood can be stored in CellSave tubes for 72 hours and blood from multiple people can be combined due to the preservative in CellSave tubes. Adapters were added to devices to allow individual devices to be disconnected from the system and replaced in the case of clotting or clogging. Then, the catheter and combining device were added to make the system as close to the in vivo system as possible. After experiment 6, we switched to new MCF7 cells to ensure the cell line had not mutated over time and changed the middle channel in the second section to split later. The device was optimized to avoid losing cells on the chance the system was operating at a lower flow rate than predicted. Before moving into canines, we started functionalizing with EpCAM overnight and switched to a new batch of EpCAM because we had used all of the previous batch. The lab used to perform the antibody attachment overnight but had changed the procedure to better accommodate collecting patient samples. Since all of these experiments are planned and prepped for at least one day ahead of time, we went back to

functionalizing the devices with EpCAM overnight which had been shown to have slightly higher capture efficiency and decreases preparation time on the day of the experiment.

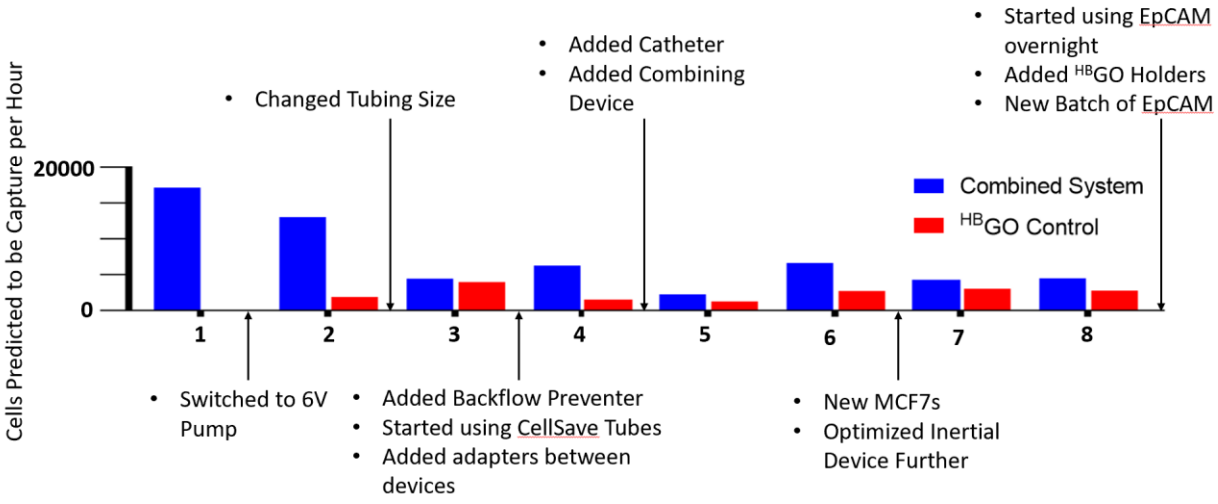

Figure 2-18: Cells predicted to be captured by the ex-dwelling system over time. The timeline along with the modifications are presented against the cells captured subsequent those changes.

Even after changing tubing sizes and seeing a drastic decrease in the cells predicted to be captured per hour by the ex-dwelling system, the cells predicted to be captured per hour for the system remained higher than for the control. Based on control experiments (not shown), we saw increased recovery once changing tubing sizes and expect our recovery for future experiments was closer to that seen in experiment number 2.

2.5.5 Canine Experiments

After optimizing the system *in vitro*, *in vivo* experiments were performed on canines similar to the ones performed with the previous system.[98] Twenty million red fluorescent protein (RFP) labeled MCF7 cells were injected into the canine then blood was drawn for controls and the HBGO devices were changed at pre-specified time points (Figure 2-19). Based on previous data about how quickly the canines immune system clears the MCF7 cells from the body, the time points were front loaded. At the 90-minute time point, the HBGO devices were changed but no

blood was drawn for a control. This was planned to ensure the devices were not unknowingly clotted or clogged. The *ex vivo* blood sampling for controls and the *in vivo* capture were performed on the same canine at the same time.

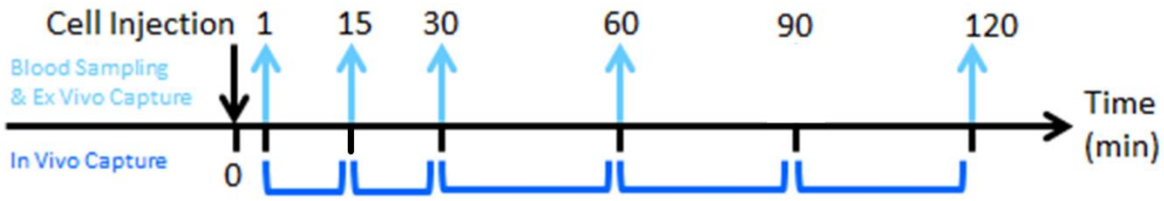

Figure 2-19: Canine experimental plan

The ex-dwelling intravenous aphaeretic system was able to capture significantly more MCF7 cells than the *ex vivo* controls at all time points (Figure 2-20). These data indicate that the *in vivo* system will be able to isolate more CTCs than can be collected from *ex vivo* blood draws. The percent increase in MCF7 cells captured is above 300% for all time points (Table 2-1). Although the increased blood volume processed drastically increases the number of CTCs that can be captured, we were also interested in the MCF7 cells captured per mL of blood processed (Table 2-2). In this experiment, the number of MCF7 cells captured per mL of blood processed was similar for both the *in vivo* and *ex vivo* systems, which is contradictory to what was observed with the original indwelling system where more MCF7 cells were captured per mL by the indwelling system than the controls. Capture efficiency is likely higher if cells are not drawn into tubes first because cells lose surface protein expression when they are removed from the body. On the other hand capture efficiency decreases with increasing flow rate. In the previous system the flow rates of the control ^{HB}GO devices and the intravenous devices were matched while for these experiments, our controls were run at the same flow rate as the previous system to enable comparison of the two systems. Based on these results we can conclude that the number of MCF7

cells captured per mL of blood was lower in the new system but the overall number of MCF7 cells captured was higher due to the increase in flow rate of the new system.

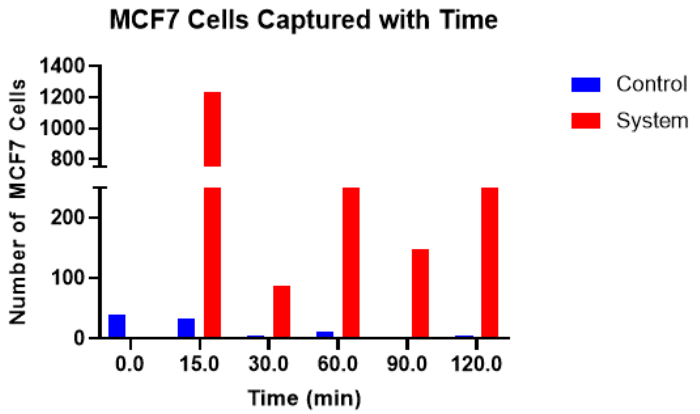

Figure 2-20: MCF7 cells captured from the canine over time on both the in vivo system and the ex vivo controls.

Table 2-1: MCF7 cells captured by the in vivo and ex vivo ^{HB}GO devices.

Time	Control	System	% Increase
0	39		
15	33	1229	3314%
30	4	86	365%
60	11	220	2833%
90		147	418%
120	5	386	7620%

Table 2-2: MCF7 cells captured per mL of blood processed by the in vivo and ex vivo ^{HB}GO devices.

Cells/ mL		
Time	Control	Systems
0	39	
15	33	40.967
30	4	2.867
60	11	3.667
90		2.45
120	5	6.433

2.5.6 Canines with Endogenous Tumors

All of the previous canine experiments were performed by injecting MCF7 cells into the canine meaning that the anti-EpCAM used needed to target human EpCAM. Our current anti-EpCAM is highly specific to target human EpCAM and is not cross reactive with canine EpCAM. To effectively capture endogenous canine CTCs, an antibody that targets canine anti-EpCAM needs to be identified and biotinylated.

To identify an appropriate antibody, multiple anti-EpCAM antibodies were purchased and tested on cell lines (Figure 2-21). MCF7s were used as a positive control and MDA-MB-231s were used as a negative control. Both of these are human breast cancer cell lines but MCF7s have high EpCAM expression while MDA-MB-231s have low EpCAM expression. MDCK is a canine cell line that is known to express EpCAM. From these results it appears the Abcam antibody is the strongest contender for capturing canine cells. The next step is to biotinylate the antibody and test capture of canine cells on a ^{HB}GO device. It is possible the biotinylation process will affect the binding so if capture does not occur, the Invitrogen antibody will be tested in a similar manner.

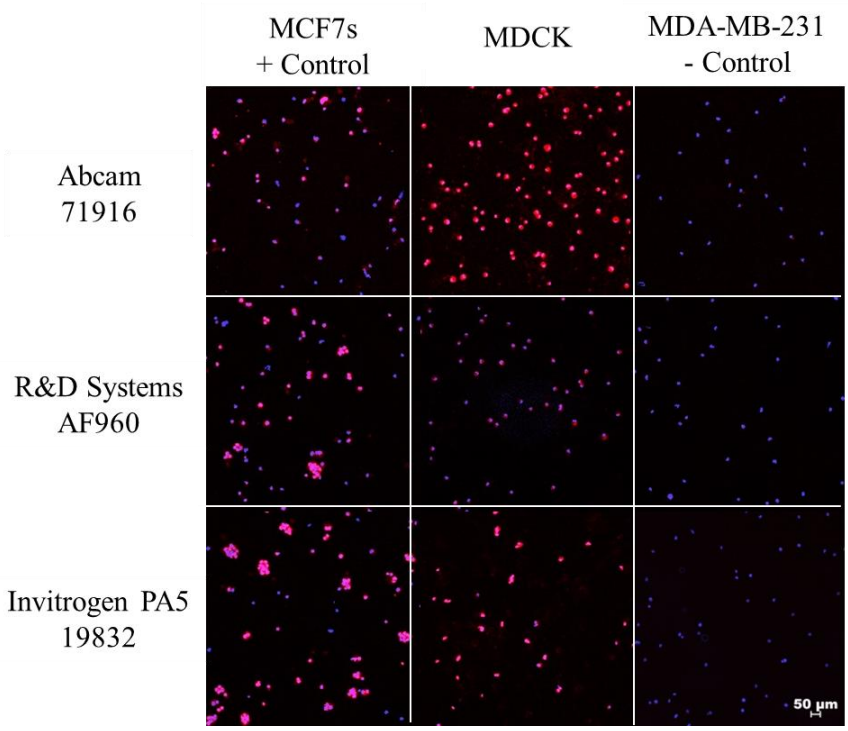

Figure 2-21: EpCAM staining on cell lines

2.6 Discussion

Developing a high throughput ex-dwelling intravenous system will enable an increase in the number of CTCs captured. Previous devices have focused particles in microfluidic channels but none had targeted the focusing of cells in whole blood which introduces several additional factors that affect the focusing pattern: particle interactions, shear thinning, elastic forces, and particle deformability.[45,62] With that goal, I developed and optimized a device to do something unprecedented: inertially focus cells in whole blood. Based on literature, I designed and tested a variety of devices. Experimental results quickly demonstrated that serpentine channels were the most promising for this application. I then tested a variety of serpentine style inertial devices which were eventually optimized into the CTCKey™.

The CTCKey™ presented here is able to focus cells in whole blood at a high flow rate, 2.4 mL/min. The dual stage strategy allows a high percentage of cells to be focused while also drastically reducing the volume of CTC containing fluid. Using the CTCKey™, the blood volume that can be processed by other CTC isolation technologies can be increased 5-fold.

The focusing patterns that occur in three different BSA solutions were compared to those in whole blood to better distinguish the changes that occur due to the particle interactions present in blood. Despite their differences, the focusing patterns of all three BSA solutions are more similar than when compared to the focusing that occurs in whole blood. From this we conclude that the particle interactions are important to changes in focusing even though they are not the sole contributor to differences in focusing between whole blood and No BSA solution.

The dramatic differences in focusing between the three BSA solutions demonstrates the importance of protein concentration and particle properties on cell focusing in addition to the particle interactions that occur in whole blood. Further studies need to be conducted to better characterize fluid flow and focusing in whole blood. These studies will need to determine how the different forces interact with each other in this complex fluid by looking at both changing fluid properties as well as the changing particle properties that are a factor when working with cells. Although the focusing pattern of this device cannot be predicted using inertial forces alone, this study demonstrates that cells can be focused in whole blood despite the particle interactions and viscoelastic forces that are present.

The ability to focus cells from whole blood directly without any dilutions can enable enrichment of CTCs *in vivo*, which should open new opportunities for continuous blood monitoring.[98] Additionally, the CTCKey™ device can concentrate the CTCs from whole blood in a label free fashion, which then can be further purified using other low throughput but highly

specific methods. To this affect we have demonstrated that the CTCKey™ enriched blood can be further processed using the FDA approved CellSearch® system, hence enabling processing higher volumes of blood (up to 5 fold) than a typical 7.5mL run using CellSearch®. However, we do recognize that further minor optimizations may be needed when CTCKey™ enrichment is used in conjunction with other CTC isolation methods, as the number of WBCS and RBCs concentrations will be slightly altered through the CTCKey™ enrichment process. The 5-fold enrichment of CTCs from 10 mL of blood in just over 4 minutes using the CTCKey™ device enables the processing of large blood volumes.

The CTCKey™ was designed such that the CTC enriched streams could be directed towards another CTC isolation device, in this case ^{HB}GO devices. Together these devices made the combined device which was tested in the lab to show capture efficiency. The capture efficiency for this system varied between experiments. We believe this is likely due to two main factors: varying numbers of cellular interactions and pump efficiency. Individuals have varying hematocrits which is a measure of the red blood cells present in a patient's blood. Since red blood cells are significantly more abundant than white blood cells and CTCs, it is likely this change is a contributing factor in how well CTCs focused. In order to make the system wearable, a small pump was used, but in the lab experiments it was observed that the pump motors began to burn out, and therefore, the flow rate decreased with time. To overcome these differences we developed a control system that adjusts the pump output based on pressure in the system.[101] This control system allows us to maintain a more constant flow rate and is also programmed to shut off the pump if pressure increases or decreases outside of a specified range. In addition we are testing a new pump that is biocompatible and designed for higher flow rates. Together the new pump and the existing control

system should allow for more stable flow rates which will increase CTC capture efficiency in the future.

Because our system is designed to process a higher blood volume as opposed to having a high capture efficiency, it was initially difficult to compare our system to other available technologies. To enable these comparisons, we determined an interrogation efficiency for various devices (Table 2-3). Interrogation efficiency is defined as capture efficiency multiplied by the blood fraction processed. All interrogation efficiencies were calculated based on the average human blood volume of 5.5 liters. The combined system has a 5-fold increase in interrogation efficiency over the original ^{HB}GO system which had a 10-fold increase in interrogation efficiency over the ^{FC}GO Chip.

Table 2-3: Interrogation efficiency of various CTC capture systems

	Capture Efficiency	Blood Fraction Processed	Interrogation Efficiency
Gilupi Cell Collector	0.0016 %	0.606 (95 mL/min for 30 min)	0.00097%
^{FC}GO Chip	95 %	2.13e-4 (1 mL)	0.0202 %
^{HB}GO System	80 %	0.00255 (2 hr at 6 mL/ hr)	0.204 %
Combined System	30 %	0.0511 (2 hr at 2 mL/min)	1.02 %

Canine experiments demonstrated the effectiveness of our ex-dwelling system to isolate CTCs *in vivo*. Once the travel restrictions put in place due to the coronavirus pandemic are lifted, we will re-run the canine experiments to better determine their significance. In the meantime, the system is being improved to run at a more consistent flow rate as well as capture endogenous canine cells.

Ideally the system will have a more consistent and higher flow rate, be made to be more user friendly such that it can be operated by clinical staff and be able to capture endogenous canine cancer cells. To improve the flow rate consistency, we are testing new pumps that are biocompatible. Once a pump is chosen, we will design our own motor and carriage to decrease the pump footprint. In order to operate at the higher flow rate of 2400 µL per minute and above as a diagnostic test, we need to use separate draw and return sites (Figure 2-22). Since this is how aphaeretic procedures are typically performed, we do not predict any issues with implementing this change. Currently, we have five different devices attached together with tubing in addition to a pump which is optimal for lab testing due to the easy maneuverability of each piece; however, it is much more complicated than clinical staff would prefer. To make the system easier for clinical operation, we would like to design a single cartridge that contains all the non-reusable components. This cartridge will snap onto the pump motor for easy operation then be removed for analysis after the test.

Figure 2-22: Ex-dwelling system connected using two ports instead of a dual lumen catheter.

The ex-dwelling intravenous aphaeretic system discussed here has distinct advantages over existing technologies. The CTCKey™ device can concentrate the CTCs from whole blood in a label free fashion, which then are directed to highly specific ^{HB}GO devices. The 5-fold enrichment of CTCs by the CTCKey™ allows for higher blood volumes to be processed by the ^{HB}GO devices. The CTCKey™ drastically increases the blood volume that can be processed while maintaining the ability to perform meaningful clinical assays such as molecular characterization on the isolated CTCs. This increase in sample size will lead to both better prognosis and improve targeted therapy selection for patients.

Chapter 3: Circulating Tumor Cells as a Biomarker to Predict Patient Outcomes in Hepatocellular Carcinoma

3.1 Abstract

Hepatocellular carcinoma (HCC) has one of the lowest survival rates of all cancer types partially due to the inability to personalize treatment plans to each patient. As more targeted therapies are introduced for other cancer types, there becomes an increased possibility that they could also be used in HCC patient populations to improve patient outcomes if the appropriate tumor monitoring techniques exist. A promising method to monitor tumors is through isolating and characterizing circulating tumor cells (CTCs), or tumor cells that have been shed from the primary tumor that circulate in the blood stream. In this study, we used the Labyrinth microfluidic device to isolate CTCs from HCC patients' peripheral blood at three timepoints during chemoradiation treatment: before radiation treatment, post round 1 of radiation treatment, and after the completion of radiation treatment. CTCs were then characterized using immunostaining for protein expression and microarray analysis for transcriptome profiling. A total of 63 samples were analyzed from 29 unique patients and had an average of 104 ± 206 CTCs/ mL of blood. The post round 1 radiation treatment samples had the largest difference in CTCs/ mL between patients who progressed (176 ± 229) compared to patients with stable disease (71 ± 126). The collected data was correlated with patient outcomes. Moving forward, this method of CTC analysis can hopefully be used to stratify patients into two groups: patients who are responding well to radiation treatment and patients who could benefit from additional or alternative treatment methods.

3.2 Related Publications

Smith, K.J., Jana, J., Meinel, S., Gdowski, Z., Smith, S., Purcell, E., Nui, Z., Lawrence, T., Cuneo, K., and Nagrath, S. Circulating tumor cells as a biomarker to predict patient outcomes in hepatocellular carcinoma. In preparation.

Wan, S., Kim, T.H., Smith, K.J., Delaney, R., Park, G., Guo, H., Lin, E., Plegue, T., Kuo, N., Steffes, J., Leu, C., Simeone, D., Raximulava, N., Parikh, N., Nagrath, S., and Welling, T.H. New Labyrinth Microfluidic Device Detects Circulating Tumor Cells Expressing Cancer Stem Cell Marker and Circulating Tumor Microemboli in Hepatocellular Carcinoma. doi:10.1038/s41598-019-54960-y

3.3 Introduction

Hepatocellular carcinoma (HCC) was the sixth most common cancer and fourth leading cause of cancer related deaths globally in 2018.[102] Incidence of HCC in the United States has more than tripled over the last four decades and is expected to continue to rise at a similar pace.[76] Historically, chronic hepatitis b (HBV) and C (HBC) accounted for the majority of HCC cases but the development of the HBV vaccine in 1982 and following distribution has drastically reduced its presence.[102] In first world countries, the presence of HCV has been decreased by improving needle sterility and the development of an antiviral treatment that cures the disease.[103] Alternatively, the recent increase in the incidence of HCC can be attributed to alcoholic steatohepatitis and nonalcoholic fatty liver disease (NAFLD) which is strongly associated with obesity, diabetes, and metabolic syndrome.[74] HCC only has a 5-year survival rate of 15%, and for the two-thirds of patients diagnosed in advanced stages has a median survival of less than a year.[75,104] Improving disease monitoring methods can increase survival rates, especially as more targeted therapies are approved for use in HCC.

Currently, HCC is diagnosed in the early stages through imaging, ultrasound, CT, or MRI, sometimes in conjunction with alpha-fetoprotein (AFP) levels, the traditional HCC biomarker. Imaging techniques often miss small lesions in addition to the fact that blood-based tests are typically easier, cheaper, and faster to perform. AFP is an unreliable biomarker for HCC because it is actually elevated due to liver inflammation, meaning many people with HCC risk factors have elevated AFP levels even without having developed the disease. In addition, AFP can be elevated by other diseases such as intrahepatic cholangiocarcinoma.[75,76] An alternative biomarker is circulating tumor cells (CTCs). CTCs are cells shed from the tumor into the bloodstream and are believed to seed metastasis.[9] The number of CTCs present in blood has been shown to be a good predictor of disease outcome in multiple cancer types.[79] Since 15% of HCC patients develop extrahepatic metastasis and 50% experience recurrence, it is hypothesized CTCs will be a good predictor of disease outcome for these patients.[104]

CTCs offer a promising biomarker for HCC, but their isolation remains challenging due to their rarity in blood. According to previous studies there are around 10 CTCs per mL of blood.[8] For comparison, there are 10^6 white blood cells, 10^9 red blood cells, and numerous other blood components in the same volume.[18] Over the past couple of decades many CTC isolation methods have been developed, but the only FDA approved method to identify CTCs is CellSearch®, a semiautomated device that detects and counts CTCs using anti-EpCAM to isolated CTCs then identifies the appropriate cells through immunofluorescent staining.[27] One CellSearch® based study found that CTC positive HCC patients had significantly shorter overall survival than patients without CTCs detected.[105] However, since CellSearch® selectively isolates EpCAM positive cells and only 35% of HCC tumors express EpCAM, this study, along with other EpCAM based

isolation methods, likely miss a large number of HCC CTCs.[106] To prevent missing EpCAM negative CTCs, ligand free enrichment methods may be used.

Many label free isolation techniques have been used to isolate CTCs. Most of these techniques rely on filtration or density gradients to isolate cells.[30] Since CTCs tend to be slightly larger than other blood components, techniques have been developed to isolate CTCs based on this size difference.[29] One such method is through the use of inertial microfluidic devices such as the Labyrinth.[107] These devices take advantage of the differences in cell properties to create streamlines of different cell types.[59] Previous studies from the Nagrath lab have demonstrated the Labyrinths ability to isolate CTCs from breast, pancreatic, and lung cancers in addition to HCC.[35,90,108,109]

This study was designed to build on our previous HCC study performed using the Labyrinth technology which demonstrated CTCs could be detected in over 85% of HCC patients.[109] This study also utilizes the Labyrinth device to isolate CTCS but we combine enumeration data with RNA analysis to better characterize the CTCs. CTCs were enumerated using anti-Ck18 and anti-asia glycoprotein (ASGPR), both of which are known to be present in liver cells but not WBCs.[110,111] Vimentin and EpCAM were both marked as well because they have previously been associated with poor clinical outcomes in HCC patients.[112,113] To perform a comprehensive RNA analysis, microarrays were used to explore highly variable tumor and liver associated markers. Together this data was used to correlate data collected from CTCs with patient outcomes.

3.4 Methods

3.4.1 Cell Culture and Preparation

Cell lines were cultured following ATCC protocols for the specific cell type. All cells were grown in 5% CO_2 at 37°C. Media was changed every two to three days and cells were passaged regularly dependent on confluency. For experiments, cells were collected between 60 and 80% confluency and passaged using trypsin. Cells were then spiked in PBS or blood as appropriate.

3.4.2 Device Fabrication

Labyrinth devices were fabricated using the same standard lithography process published previously.[35] SU8 was spin coated on a silicon wafer at the desired height of 100 – 110 um then exposed to the Labyrinth pattern. Polydimethylsiloxane (PDMS) was mixed at a 10 to 1 ratio, poured over the Labyrinth pattern, degassed, and baked at 65°C. The PDMS Labyrinth was then removed from the wafer and the inlets and outlets were punched before the Labyrinth was bonded to a glass slide using a plasma etcher. Ten-inch tubing was attached in the punch holes to make the inlet and all four outlets.

3.4.3 Human Subjects

Human subjects were enrolled in HUM00098022 or HUM004133653, both of which were approved by the Institutional Review Board at the University of Michigan. Informed consent was obtained, and all protocols were followed as set forth by the IRB. HCC patients scheduled to be treated with radiation therapy were enrolled in this study. Samples were collected before the start of radiation (visit 1), post round 1 radiation treatment (visit 2), and post the completion of radiation treatment (visit 3).

3.4.4 Sample Processing

Ten milliliters of blood was drawn by Michigan Medicine then picked up by the Nagrath lab. Immediately upon arrival in lab, RBC depletion was started using Ficoll-Paque or dextran. The samples were spun at 400 g and 20°C for 20 minutes. The top two layers (plasma and cell) were collected and diluted to five times the original blood volume with PBS.

3.4.4.1 Labyrinth

Each sample was run through the Labyrinth at 2000 µL/min. Outlet 2 was collected then run through the Labyrinth a second time. During the second run through, the first 1 mL of outflow was discarded. After the first 1 mL of processing, outlet 2 was collected. The sample was split in half for cell enumeration and RNA analysis.

3.4.4.2 Enumeration

After collection, each sample was processed using a Cytospin to obtain cells on glass slides. The sample volume was loaded such that each slide contained the equivalent of 1 mL of starting blood volume. For enumeration, immunofluorescence staining was used. Slides were permeabilized with 0.2% Triton-x for 3 minutes then blocked using 10% goat serum for half an hour. Primary antibodies were added to the slide and incubated overnight. The next day, the slides were washed with PBS then incubated with secondary antibodies for 45 minutes. Prolong Gold Antifade Mountant with 4′, 6-diamidino-2-phenylindole (DAPI) (Thermo Scientific, Massachusetts) was used to stain cell nuclei and preserve the staining for imaging.

3.4.4.3 RNA

RNA was immediately extracted from each sample using the Norgen RNA purification kit. Samples were stored at -80°C until all the desired samples had been collected. Samples were submitted to the Thermo Fisher Scientific for microarray analysis. Thermo Fisher provided the

raw data. Hierarchial clustering and PCA plots were generated using the Transcriptome Analysis Console (TAC) Software version 4.0 (ThermoFisher Scientific, USA).[114] Specific genetic data was obtained using BiocManager packages in R.[115] All samples passed both the Hybridization Controls Threshold and the Positive vs. Negative AUC Threshold performed by both TAC and the R program.

3.4.5 Image Acquisition and Analysis

Cells were imaged using a Nikon Ti2-E microscope (Nikon, USA) at 30x magnification. DAPI, FITC, Cy3, and Cy5 channels were all set to 15% light intensity with exposure time of 100 ms. Cy7 was set to 15% light intensity with an exposure time of 500 ms. Images were analyzed from ROI data collected using the NIS-elements analysis software. Cells were identified by lab personal based on the cell nuclei staining, DAPI. FITC, Cy3, and Cy5 positivity was determined based on a percentage of the maximum fluorescence found on the slide, 40%, 25%, and 25% respectively. Cy7 positivity was determined based on if the cells was more than 20% percent above the minimum intensity measured on the slide.

3.5 Results

The Labyrinth and procedure were previously modified to isolate CTCs from HCC patients.[109] This study showed optimal separation of HCC cell lines from WBCs at 2000 µL/min while maintaining a cell viability over 90%. The cell isolation remained the same for low cell numbers spiked into PBS. Using this same procedure, CTCs were successfully isolated from this patient cohort. In this study, data was analyzed from 5 patients who completed the study and 25 more patients who had a subset of samples (Table 3-1). The time between sample collection was not set but the baseline was drawn before the start of radiation treatment, the second visit was drawn at the post round 1 radiation follow-up appointment, and the post radiation follow-up was

collected following the completion of radiation (Figure 3-1). Some patients only received one round of radiation so both their visit 2 and visit 3 samples were taken after radiation had been completed. The differences in time between each draw could lead to variations in the data that were unrelated to differences in disease state.

Table 3-1: HCC Patients Enrolled in Study

				Enumeration Data			RNA Data		
Patient ID	Gender	Age	Stage	V1	V2	V3	V1	V2	V3
1	M	68	T1	X	X	X	X	X	X
2	M	59	T1	X	X	X	X	X	X
3	M	85	T3a	X	X	X	X	X	X
4	M	68	T1	X	X	X	X	X	X
5	F	51	T3b	X	X	X	X	X	X
6	F	74	T1	X	X	X	X	X	X
7	M	89	T1	X	X	X	X		X
8	M	57	T2	X	X	X	X		
9	F	72	T1	X	X	X		X	X
10	M	68	T3b	X	X	X			
11	M	59	T3a	X	X	X			
12	M	67	T3b	X	X	X			
13	M	64	T2	X	X		X	X	X
14	M	59	T3a	X	X		X	X	
15	M	72	T3a	X	X		X	X	
16	M	60	T2	X	X		X		
17	M	74	T3	X	X		X		
18	F	68	T2	X	X		X		
19	M	53	T1	X	X				
20	F	78	T1	X	X				
21	M	82	T1	X					
22	M	65	T3a		X	X	X	X	X
23	M	58	T2				X		
24	F	64	T1				X		
25	M	63	T2				X		
26	M	70	T2				X		
27	M	64	T2				X		
28	M	69	T1				X		
29	M	57	T3b				X		

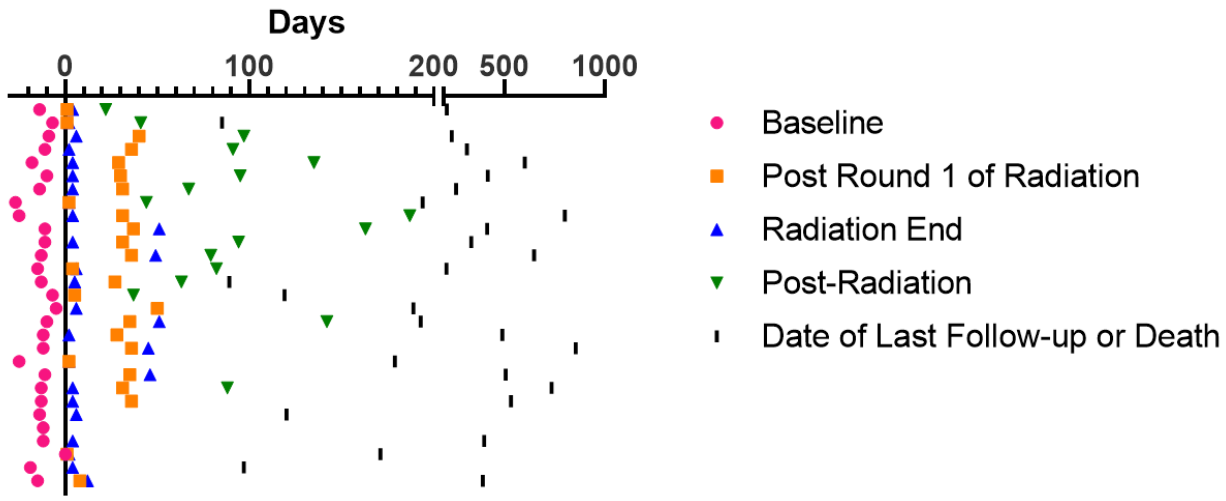

Figure 3-1: Timeline of visits and radiation treatment for each patient where radiation start is marked as time zero.

3.5.1 Enumeration Antibody Selection

CTCs were enumerated using immunofluorescence staining for CD45, Ck18/ASGPR, Vimentin, and EpCAM. A cell was classified as a CTC if it was negative for CD45 and positive for either Ck18/ASGPR or EpCAM. An example CTC and WBC from a patient are shown in Figure 3-2. Slides were analyzed for all patients. The CTCs per mL for each sample is shown using a heat map (Figure 3-3). Figure 3-4 contains summarized data by visit. The five samples with greater than 1000 CTCs/mL were excluded the summarized analysis since they drastically increased the means. Figure 3-4 a shows the change in CTC between visits for patients with stable disease while Figure 3-4 b is the same comparison for patients with reported progression or death. Since increased CTC numbers are typically correlated with worse prognosis, it was predicted that the patient cohort with reported progression would see higher CTC numbers than the patients without reported progression; however, the consolidated data at visit 1 and visit 3 was similar for both patient groups. Patients who progressed did in general have higher CTC counts at visit 2 than patients who did not progress.

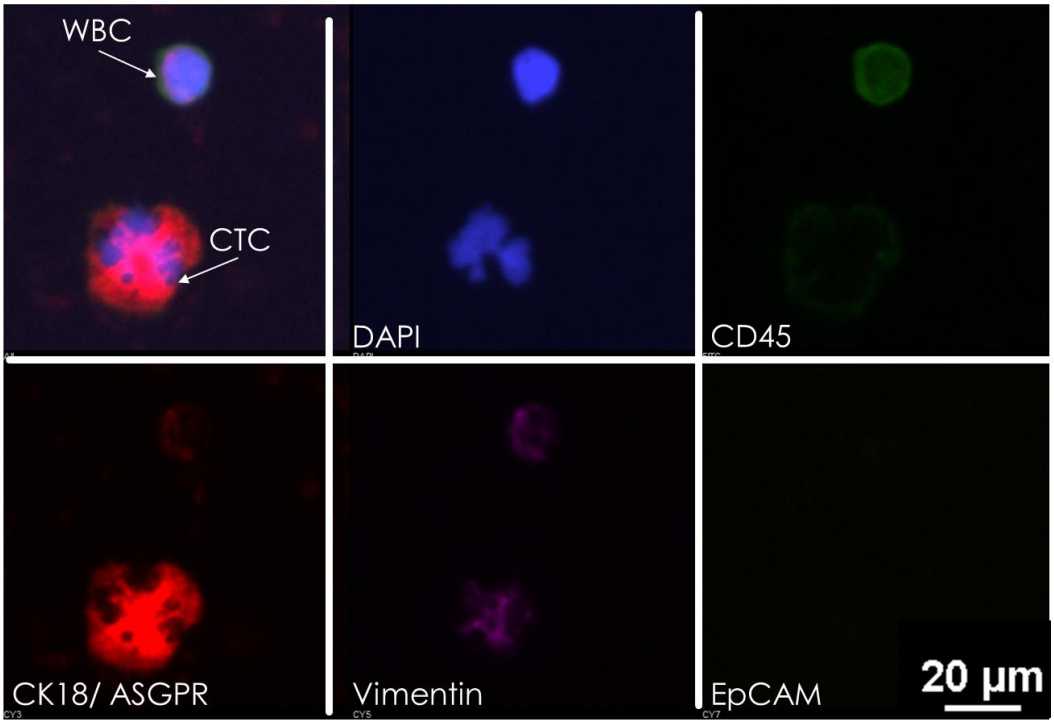

Figure 3-2: Example of immunofluorescently stained WBC and CTC from a patient sample.

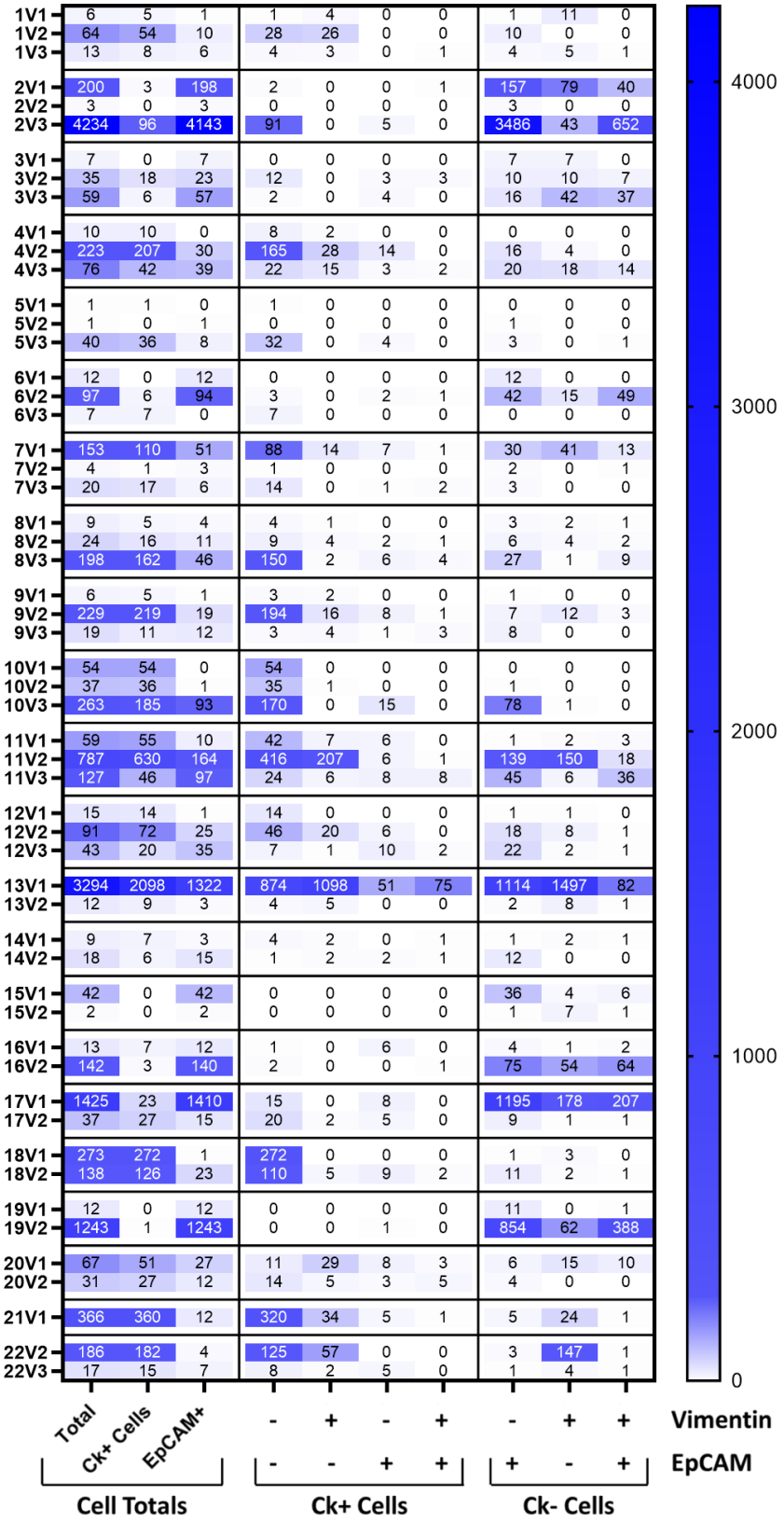

Figure 3-3: Cell counts per mL for each sample.

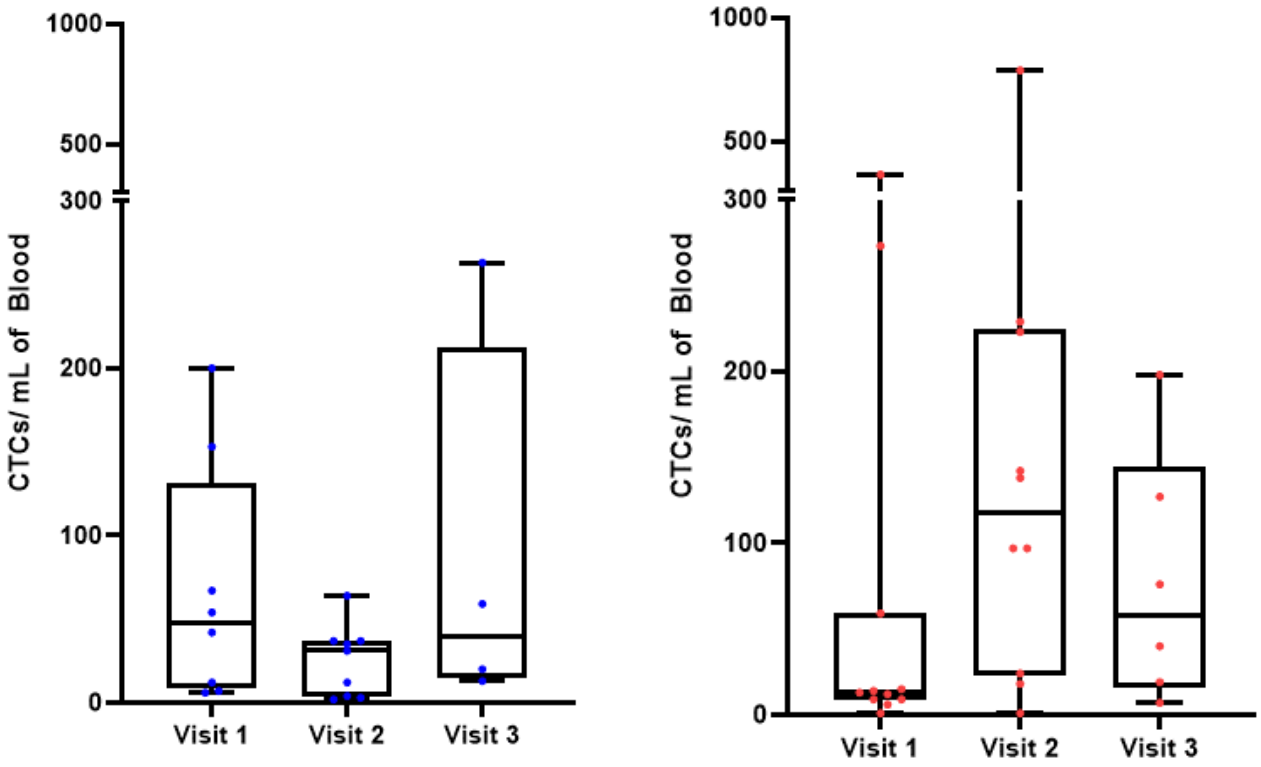

Figure 3-4: CTCs/ mL by patient outcome and visit. a) CTCs per mL of blood at each visit for patients with progression free survival. b) CTCs per mL of blood at each visit who had reported progression or death.

Because this study was designed to correlate CTC data with patient outcomes, the change in CTCs between visits was graphed for each patient. Figure 3-5 shows the change in cell numbers for individual patients between visits. With a couple exceptions, patients with reported progression had increases in CTC counts, Ck+ cells, and EpCAM+ cells between the baseline and during radiation time points (Figure 3-5 a-c). Kaplan-Meier curves indicate that an increase or decrease in total CTCs between these two timepoints is significant even in this small patient cohort (Figure 3-6 a). The patient with no change between the two time points was included in the decrease category. Using the same analysis, an increase in EpCAM+ cells between these two time points has the potential to be significant either with a larger patient cohort or longer follow-up times in the patients with an observed decrease in EpCAM+ cells (Figure 3-6 c). An increase in cytokeratin positive cells also has the potential to be significant in a larger patient cohort but the correlation

does not appear to be as strong as it is in an increase of total CTCs or EpCAM+ cells (Figure 3-6 b). This aligns with the literature that reports EpCAM expression in HCC is linked to worse prognosis. It is also possible that an increase in vimentin positive CTCs could be significant in a larger patient cohort, but in this data, one patient with a decrease in vimentin positive CTCs progressed after 89 days (Figure 3-6 d). Of note, an increase in any of these cell populations between baseline and the post-round 1 radiation visit has a stronger correlation to patient outcomes than disease stage (Figure 3-6 e). This same trend was not apparent when comparing an increase in these cell populations between the baseline and post-radiation visits (Figure 3-5 d,e).

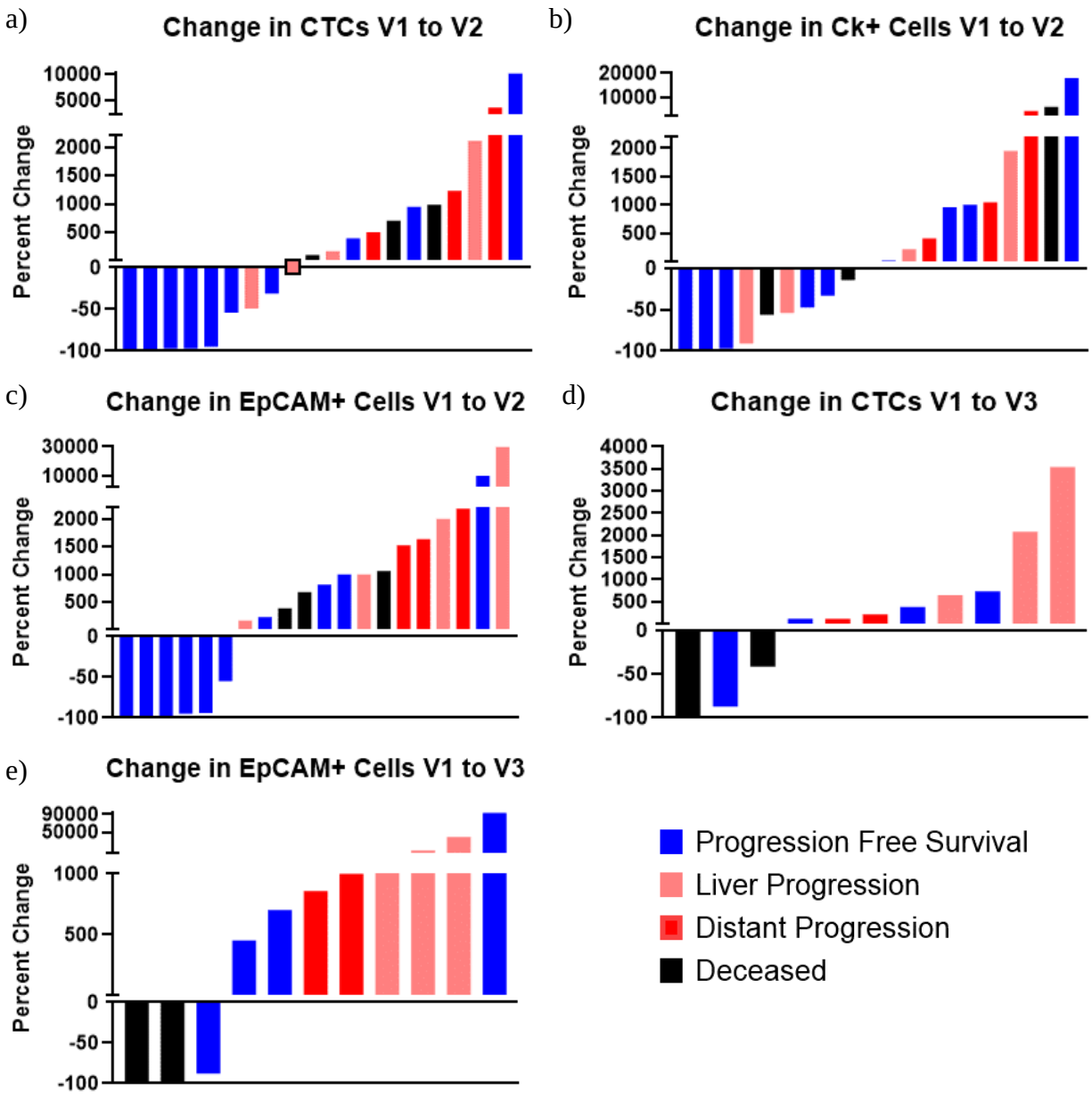

Figure 3-5: CTC changes between visits for individual patients ordered by percentage increase in the cell type being graphed. a) Change in total CTCs between before radiation treatment and post round 1 radiation visits. b) Change in Ck+ Cells between before radiation treatment and post round 1 radiation visits. c) Change in EpCAM+ cells between before radiation treatment and post round 1 radiation visits. d) Change in total CTCs between before radiation treatment and post the completion of radiation visits. e) Change in EpCAM+ cells between before radiation treatment and post the completion of radiation visits.

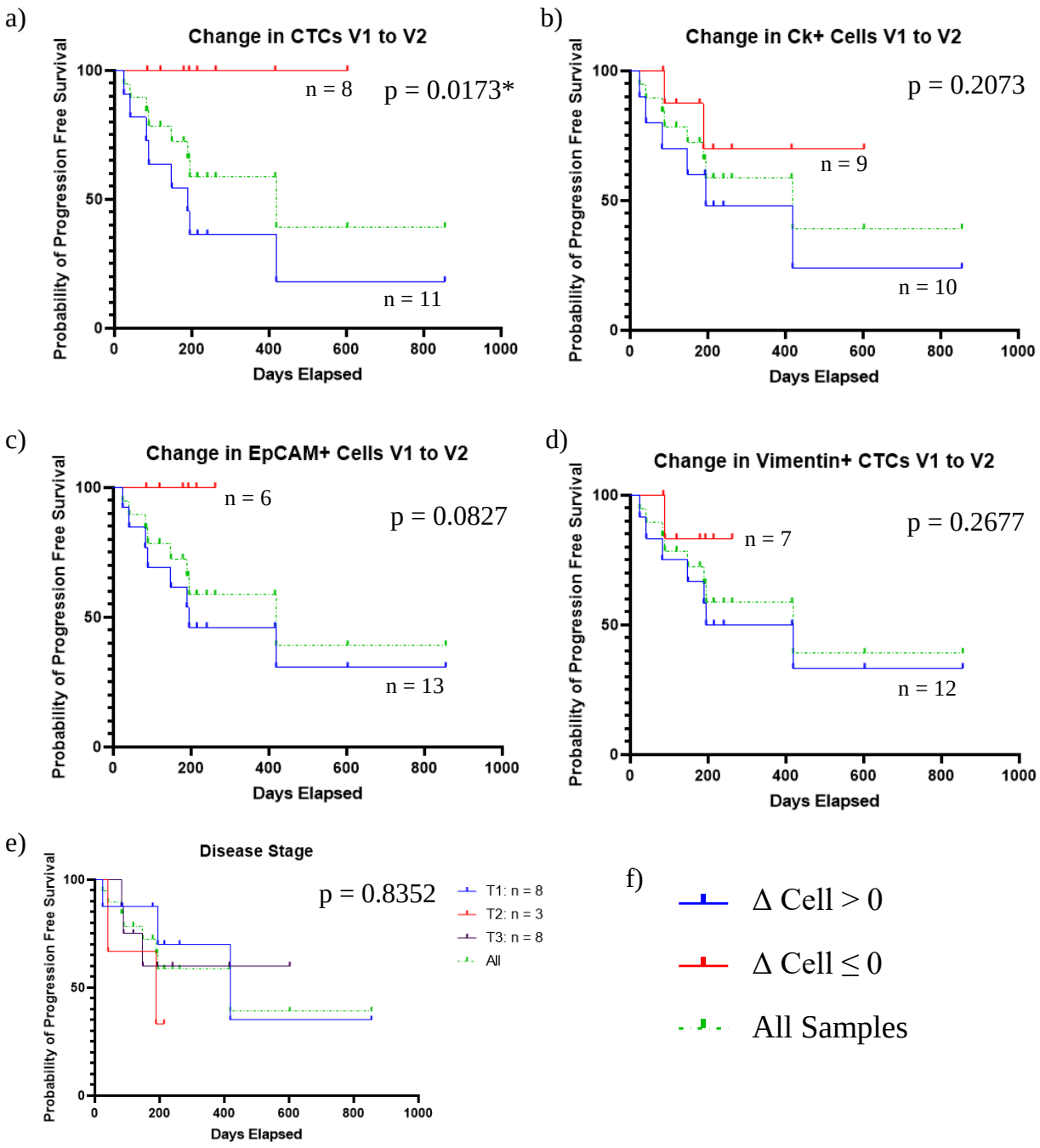

Figure 3-6: Kaplain-Meier Survival Curves of HCC Patients based on Change in Number of CTCs. a) Comparison of total CTCs between baseline and after round 1 of radiation visits. b) Comparison of EpCAM+ cells between baseline and after round 1 of radiation visits. c) Comparison of EpCAM+ cells between baseline and after round 1 of radiation visits. d) Comparison of Vimentin+ CTCs between baseline and after round 1 of radiation visits. e) Comparison of patients by disease stage. f) Legend for graphs a – d.

3.5.2 RNA Expression Analysis

In addition to analyzing the CTCs by enumerating select marker expression, RNA analysis was performed using microarrays. When patients were grouped by patient outcomes, progression free survival, liver progression, distant progression, and deceased, the non-biased hierarchical clustering of visit 1 (Figure 3-7 a) showed potential as a useful tool to predict progression. Strangely patients with progression free survival and who passed away grouped together while patients with liver or distant progression formed the second group. This could indicate the patients passed away for reasons unrelated to HCC or that the gene expression differences observed are specific to the spread of cancer and not necessarily specific to advanced disease state that already exists. Although the non-hierarchical clustering groups patients by progression, no specific genes were found to be significant when comparing baseline samples based on patient outcomes. The non-biased hierarchical clustering for during radiation treatment did not cluster in the same way (Figure 3-7 b).

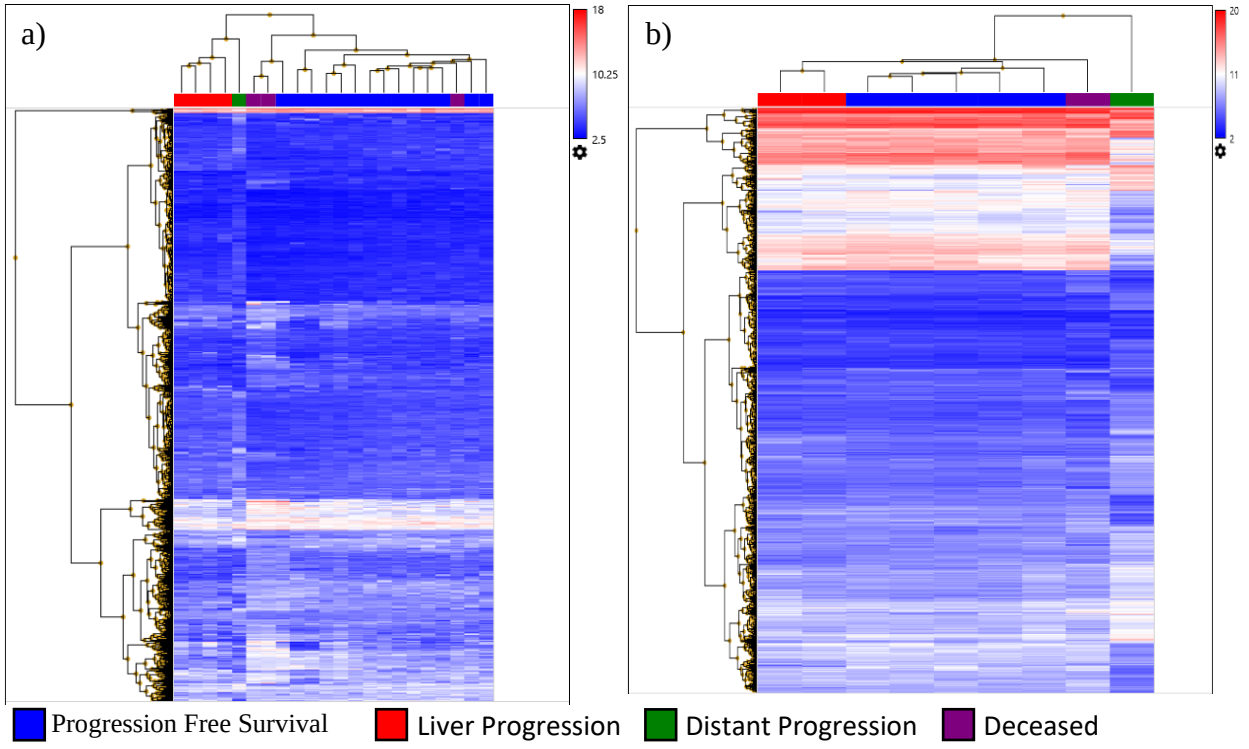

Figure 3-7: RNA microarray analysis results for HCC patients. a) Non-biased hierarchical clustering of gene expression data at baseline. b) Non-biased hierarchical clustering of gene expression data post round 1 of radiation treatment.

Analysis was run to compare data between visits as well as between patient outcomes. This analysis was performed with and without pairing samples. The unpaired sample analysis found Contactin Associated Protein-Like 3 Pseudogene 2 (CNTNAP3P2) was upregulated in samples from patients who had reported distant progression when compared to patients with stable disease (Figure 3-8 a). Myotubularin Related Protein 3 (MTMR3) was upregulated in patients with any type of progression (local, liver, distant, or deceased) in visit 2 samples (Figure 3-8 b). Little is known about CNTNAP3P2 and currently no pathway data is available.[116] MTMR3 is associated with autophagy and has been shown to be upregulated in patients with breast cancer.[117] It promotes proliferation and has been associated with metastasis.[118] Of note, the patient in the stable progression group with highly expressed CNTNAP3P2 has only been followed for 193 days currently whereas the patients in the distant progression group have been followed for 736 and 800

days. This indicates that completing the follow-up for these patients could lead to higher significance or more significant genes.

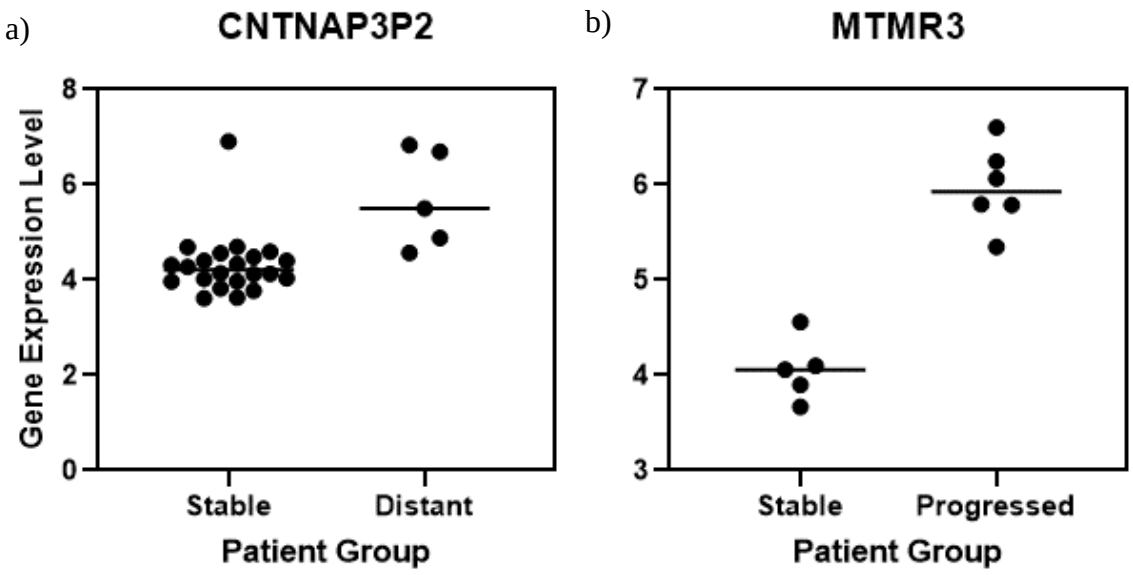

Figure 3-8: Gene Expression Level in a) all stable patient samples and distant progression samples and b) Visit 2 samples from stable patients and patients with any type of progression.

The paired analyses included fewer patients since this analysis only includes patients who had both the time points being compared. The only comparison that yielded significantly expressed genes was the paired analysis of visit 1 to visit 3 of stable patients compared to patients who passed away. There was one downregulated gene in the patient who passed away and 101 upregulated genes. Although these results indicate significance, because there is only one patient who passed away in this patient group, these results are unreliable and need to be confirmed with the addition of more patients.

3.6 Discussion

Even with the development of vaccines and treatments for hepatitis, the primary cause of HCC, the incidence of the disease continues to rise.[74] Treatment methods have improved; however, the five-year survival rate remains low.[76] By developing a method to better predict patient

outcomes for patients who receive the standard treatment regime, treatment plans could be modified to further increase progression free survival. Over the last several years, CTCs have been studied as a potential biomarker in HCC. Many of these studies target EpCAM to isolate CTCs; however, EpCAM is not expressed in healthy adult liver and is only expressed by a small portion of HCC tumors. Furthermore, even tumors that do express EpCAM do not have universal EpCAM expression meaning many CTCs would be missed in these patients as well. Although EpCAM is not universally expressed by HCC, it has been shown to be a highly prognostic marker indicating that its presence could be beneficial information.

In this study we isolated CTCs using the Labyrinth, a ligand free isolation technology, then analyzed CTCs for both protein and RNA expression to better predict patient outcomes from a peripheral blood draw. Using peripheral blood allows the analysis to be performed at multiple time points throughout treatment, enabling the changes between visits to be measured. Patients were split into two groups for analysis: those with progression free survival and those without progression free survival. It was found that the consolidated CTC enumeration data from the two groups was not significant but looking at changes for individual patients between visits has the potential to be informative. An increase in EpCAM expressing CTCs between the baseline and during radiation visits was shown to be particularly interesting. This agrees with the existing data supporting that EpCAM expressing HCC tumors are correlated with worse prognosis.

To complement the protein expression analysis, we also performed RNA analysis using microarrays on the bulk sample. Unlike the protein data, the data from a single time point, baseline, appeared to be indicative in this analysis based on non-hierarchial clustering; however, no individual genes were found to be significant. When looking at overall changes between samples in the various patient groups, three genes were found to be significantly expressed. Due to the low

patient number and that the paired analysis did not find significantly expressed genes, I believe more patient data are needed to conclude the true significance of these genes.

Here we have demonstrated the ability to isolate and analyze CTCs from HCC patients using the Labyrinth device. Based on our downstream analysis, both CTC enumeration and RNA analysis have potential prognostic value. By developing a follow-up study with more patients and stricter guidelines around blood draw timing, the significance of these differences could be confirmed. This blood-based test could be used to better direct treatment decisions to improve patient outcomes.

Chapter 4: Single Cell Isolation using the DEPArray

4.1 Abstract

Circulating tumor cells give a more comprehensive view of the tumor than a tissue biopsy due to their spatial heterogeneity; however, when cells are analyzed in bulk the results are essentially averaged for the cell population. This means that even though spatial heterogeneity is accounted for, individual cell heterogeneity is not observed, so rare phenotypes and mutations may still be missed. In this chapter I optimize our CTC isolation protocol for use with the DEPArray, a single cell isolation technology. Protocols are developed for both DNA and RNA isolation. For DNA isolation, fixed cells are used with the intention of performing copy number variation analysis on the isolated samples. It would also be beneficial to determine differences in RNA expression between cells. RNA extraction from cells off the DEPArray is achieved by modifying the protocol to be used with alcohol fixed cells. In both cases, cell isolation protocols were optimized for the desired downstream application to be performed in future patient cohorts.

4.2 Related Publications

Smith, K.J.*, Rupp, B.*, Owen, S., Ball, H., Gunchick, V. Sahai, V. & Nagrath, S. Copy number variation analysis of single circulating tumor cells and matched white blood cells from the pancreatic cancer patients isolated using the Labyrinth device in conjunction with the DEPArray. In preparation.

Ball, H., Smith, K.J., Rupp, B., Reddy, R., Ramnath, N., & Nagrath, S. RNA expression analysis of single circulating tumor cells and tumor cell clusters from stage III non-small cell lunger cancer patients. In progress.

4.3 Introduction

Circulating tumor cells (CTCs) have been shown to provide insight into tumor heterogeneity because they are less spatially biased than tissue samples. Many studies have used immunofluorescence staining to examine protein expression of individual CTCs. While this approach has provided beneficial information, immunofluorescence staining is limited to four different markers, in addition to the nuclear stain, by the different wavelengths that can be detected without overlap.[119,120] This has led many researchers to move into looking at various omics from the collected samples.[12,121] The appropriate assays can be performed on the bulk CTC sample; however, bulk sample analysis essentially averages the cells together which limits our understanding of tumor heterogeneity and increases the risk of rare events being missed.[122] By comparing single CTCs, the tumor environment can be more thoroughly understood, and subpopulations of cells can be identified.[123] Single cell analysis could allow tumor changes to be detected earlier and will enable the detection of cellular heterogeneity as well as rare mutations.[80,124,125] Detecting these differences early will inform treatment decisions and improve patient outcomes.

Performing certain omics analysis on single CTCs is of interest to the medical community due to its promise to increase understanding of the disease and in turn improve patient outcomes. Isolating single cells such that desired data are preserved and can then be analyzed is extremely difficult. Previously, our lab had used the Fluidigm C1 system to separate single cells into individual wells and perform RNA analysis on the cells.[35] While this system provided cDNA synthesized from RNA for analysis when cells were isolated, the Fluidigm C1 is a random sampling system that isolates cells into 96 wells meaning it is not possible to select cells of interest. Due to the rarity of CTCs even after label free enrichment, many samples had no cells of interest

captured in the 96 available wells. To overcome the limited number of wells, this study used the DEPArray™ which captures cells in di-electrophoretic cages and images them. The cells of interest can then be selected and routed into tubes or well-plates as desired (Figure 4-1[6]). The DEPArray™ was designed to be used with fixed samples primarily FFPE tissues and more recently protocols have been developed to integrate the DEPArray into the CellSearch® workflow.[91,126] Other groups have used various methods to enrich CTCs for isolation on the DEPArray such as FACS, AutoMACS®, and ScreenCell®.[127–129] This set the precedence to use the DEPArray to isolate single CTCs, but we still had to optimize our sample preparation method to meet the input criteria of the DEPArray™.

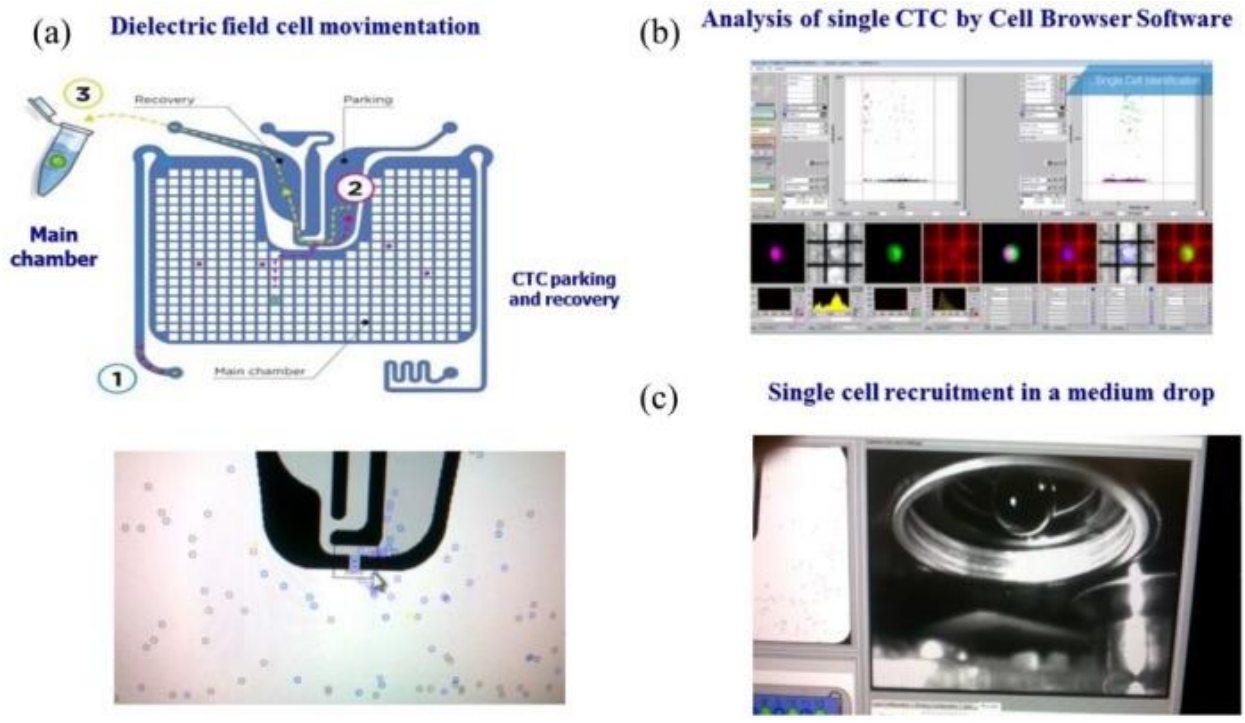

Figure 4-1: DEPArray Processing.[6] a) Loading sample into the cartridge and diagram of cells being routed to parking. b) Image of software used to select cells based on their fluorescence images. c) Image of a single cell being dropped into a tube.

This portion of my research is focused on the method to isolate single cells for further analysis in three cancer types: pancreatic, ductal carcinoma in situ (DCIS), and non-small cell lung cancer (NSCLC). Due to differences in the diseases, standard treatments, and collaborators interest, each project has slightly different goals with varying outputs. In pancreatic cancer, we are interested in performing copy number variation (CNV) analysis which is performed on DNA meaning the cells can be PFA fixed before processing is complete. Conversely, in both DCIS and NSCLC, RNA expression analysis is desired. This chapter explains the method development to isolate single cells for these studies.

4.4 Methods

This project is designed to incorporate the DEPArray into our current Labyrinth processing protocol. The general protocol is to draw blood and process it using the Labyrinth protocol. The samples are then suspension stained before being loaded on the DEPArray. Post DEPArray either RNA or DNA is extracted, prepped, and sequenced.

4.4.1 Labyrinth Processing

Patient samples were processed using the Labyrinth device discussed in chapter 3. Briefly blood was collected then the red blood cells were removed using density separation. The CTC containing layer was diluted to five times the original blood volume then flowed through the Labyrinth at either 2000 or 2500 µL/min depending on the cancer type. The CTC containing outlet (outlet 2) was collected and run through the Labyrinth a second time to further deplete the WBCs.

4.4.2 PDMS Substrate Functionalization for Cell Capture

Similar to the graphene oxide capture device discussed in chapter 2, PDMS can be functionalized with antibodies to capture cells. The surface is coated with silane then GMBS is

used to attach neutravidin. This allows any biotinylated antibody to be attached to capture cells. In this study we used anti-CD45 to further deplete WBCs from our sample.

4.4.3 Cell Culture and Preparation

Cell culture was performed as described in chapter 2 except all cell lines were grown in the media recommended by ATCC.

4.4.4 Human Subjects

Human subject protocols were followed as described in chapters 2 and 3.

4.4.5 Device and Buffer Preparation

Device and buffers were prepared in the same way described in chapter 2.

4.4.6 Suspension Staining

The samples were stained for fluorescent markers using a standard protocol. All samples were blocked using 1% BSA then incubated with primary antibodies: anti-EpCAM, anti-CD133, anti-EGFR, and anti-CD45. After the incubation, the mixture was diluted, centrifuged, and removed leaving the cell pellet. PFA fixed samples were permeabilized and incubated with pan-Ck and secondary antibodies while non-PFA fixed samples were just incubated with the appropriate secondary antibodies. The samples were Hoechsted before being centrifuged and resuspended in PBS.

4.4.7 DEPArray

For samples to be run on the DEPArray™ they must be resuspended in the appropriate media. The samples were centrifuged at 300 g for live samples or 400 g for PFA fixed samples for 10 minutes then the supernatant removed and replaced with the appropriate buffer. This was repeated to ensure complete replacement of the buffer.

The buffer to be loaded onto the DEPArray™ cartridge had to be desiccated to remove all air bubbles. Buffer was pipetted into 1.5 mL Eppendorf tubes were sealed with parafilm before being placed in the desiccator for a minimum of 15 minutes.

After preparation, the buffer and sample were loaded onto the DEPArray™ following the manufactures instruction for cartridge loading. The machine then scans the samples and the user selects cells to be isolated using the machine. The DEPArray manipulates the dielectrophoretic cages to route the cells off the machine into 0.2 mL qPCR tubes. Once collected, the volume was reduced using two centrifuge runs and stored for further analysis.

4.4.8 Whole Genome Amplification and Associated Quality Control

Whole genome amplification (WGA) was performed using the Menarini Silicon Biosystems' *Ampli1* whole genome amplification kit (USA) following the manufacturer's protocol. The cells were lysed then the DNA digested, annealed, and ligated before PCR was performed. Following PCR the samples can be QC'd and prepared for lowpass by library preparation.

To perform the QC, 1 ul of the 50ul WGA final product and control gDNA was taken and quality control (QC) was performed using the Menarini Silicon Biosystems' *Ampli1* QC kit following the manufacturer's protocol. As part of the QC, PCR is done to amplify four different genomic targets which are then seen on a gel to confirm WGA was performed correctly. A 3% agarose gel was made by combining 25ml of 1x Tris-acetate-EDTA (TAE) buffer (Lonza, USA), 2.5ul of SYBR Safe DNA gel stain (Invitrogen, USA), and 0.75g of UltraPure Agarose powder (Invitrogen, USA) in a beaker, swirling and letting the solution sit for 5 minutes. The solution was heated in a microwave in 30 seconds intervals and swirled between run times until the agarose powder was dissolved, approximately 1 minute. After allowing the solution to cool for 2 minutes,

the gel was poured into a mold and set for 45 minutes before being placed gel in a gel box and covered with TAE buffer.

To load the gel, 10 µL of sample and 2 µL of Gel Loading Dye Purple (6x) no SDS (New England Biolabs, USA), were mixed and 5 µL of the sample solution was pipetted into each lane. For the ladder, 2 µL of Tris-EDTA (TE) buffer (Corning, USA), 1 µL of gel loading dye and 1 µL of DNA ladder (New England BioLabs, USA) were combined then 3 µL of ladder solution was pipetted into the lane. Gels were run at 120V and 3A for 30 minutes and imaged using FluroChem M imaging system (Protein Simple, USA).

4.4.9 RNA Extraction and Library Preparation

Three library preparation kits were tested to determine their ability to isolate RNA from alcohol fixed cells: SMART-Seq® Single Cell PLUS Kit (Takara Bio, USA), NEBNext® Single Cell/Low Input RNA Library Prep Kit for Illumina® (New England Biolabs, USA), QIAseq FX Single Cell RNA Library Kit (Qiagen, USA). The manufacturers protocol was followed for each kit. In general, cells are lysed and the RNA is synthesized to cDNA. cDNA is then amplified and purified. All samples were purified using SPRI® beads. Beads were added to the sample, mixed, and then allowed to incubate at room temperature for five minutes. The samples were then placed in the appropriate magnetic strip to separate the beads and the supernatant was discarded. Samples were washed twice with ethanol before being allowed to dry. cDNA was eluted from the beads, washed, reattached to the beads, washed with ethanol and allowed to dry a second time to improve purity. After drying, the cDNA was eluted from the beads using 1x TE Buffer. After purification, the presence of cDNA is validated before preparing and amplifying the libraries for sequencing.

4.4.9.1 SMART-Seq® Single Cell PLUS Kit

Samples were lysed in a gentle lysis buffer before being suspended in the reaction buffer with 3' SMART-Seq CDS Primer II A. The samples were then incubated at 72°C before being cooled on ice and adding the RT mastermix. The cells were incubated at 42°C for 3 hours before being heated to 70°C then cooled to 4°C. To amplify cDNA, PCR master mix was added to each tube and placed on a thermo cycler programmed with 20 cycles.

4.4.9.2 NEBNext® Single Cell/Low Input RNA Library Prep Kit for Illumina®

Cells were suspended in lysis buffer and incubated at room temperature for 5 minutes then the RT primer mix was added and incubated for 5 minutes at 70°C to anneal the sample. RT mix was then added to the sample and incubated 42°C for 90 minutes before being heated to 70°C then cooled to 4°C. cDNA amplification mix was added to the sample and placed on a thermo cycler programmed to run 20 cycles.

4.4.9.3 QIAseq FX Single Cell RNA Library Kit

Lysis buffer was added to the cells and incubated at 24°C for 5 minutes before being heated to 95°C and cooled. gDNA Wipeout Buffer was then added to the samples at 42°C for 10 minutes. Quantiscript RT mix was added to the samples and incubated at 42°C for 1 hour then heated to 95°C to stop the reaction. After cooling, the samples were ligated at 24°C for 30 minutes. The mixture was once again heated to 95°C to stop the reaction then cooled back to 4°C. REPLI-g SensiPhi amplification mix was added to the sample and incubated at 30° for 2 hours then heated to 65°C before being cooled.

4.4.10 Polymerase Chain Reaction (PCR)

qPCR was performed on samples to determine the presence of cDNA after amplification and check for the relative abundance of known transcripts. TaqMan® Fast Advanced Master Mix

(ThermoFisher Scientific, USA) and the associated protocol was used. The appropriate assays were mixed with the master mix and loaded into wells with 2 µL of samples. Forty cycles were run on a QuantStudie 5 Real-Time PCR and the data was exported then graphed.

4.4.11 University of Michigan Advanced Genomics Core

Much of the RNA and DNA QC and all of the sequencing was performed by the University of Michigan Advanced Genomics Core. For RNA, the core provided both bioanalyzer and electrophoresis results. For DNA, the core provided DNA Screen Tape results and performed the library prep.

4.5 Results

4.5.1 Upstream Sample Processing Modifications

For the first round of testing, we loaded samples directly from the Labyrinth onto the DEPArray™. This had worked as promised by the manufacturers when we spiked cells into PBS, but when the samples were isolated from blood, the machine had difficulties routing our cells into collections tubes. From looking at the bright field images, we determined the issue was debris in the sample, but we did not observe debris when we checked the samples before loading. Further investigation led us to conclude the debris was platelets that were not removed at any stage in our process. Since this is an issue in other blood assays, procedures to remove platelets are readily available online. Before adding a step to our process, it first had to be tested to minimize cell loss. For Ficoll samples, we stopped collecting the top cell-free plasma layer and instead now just collect the second layer which contains the cells. Dextran samples only have two layers so for those samples we added a 10 minute, 120 g centrifuge spin which pellets the cells but does not pellet platelets. The effectiveness of the platelet removal was confirmed when we put samples on the DEPArray™ and the debris was no longer present.

The DEPArray can handle up to 9000 cells for isolation of rare cells, but it is recommended that no more than 6000 cells are loaded as too many cells can interfere with the machines ability to route the desired cells into collection tubes. Most samples were under this 6000 cell threshold; however, the DCIS samples were obtained from a starting blood volume of 10 – 15 mL. To decrease the cell numbers to below the 6000 cell threshold, we added a WBC depletion chip that captures cells using biotinylated anti-CD45, anti-CD11b, and anti-CD15. This chip functions similarly to the GO chip except silane is used to attach the GMBS directly to the PDMS and glass surfaces. By not having a graphene oxide substrate, we lose specificity, but since this chip is targeting WBCs instead of rare CTCs, that is not an issue. The chips were stained and scanned to ensure we did not lose CTCs during this step.

4.5.2 Single Cell Sorting of Fixed Samples for DNA Based Analysis

In pancreatic cancer, we were interested in copy number variation (CNV) meaning the samples could be PFA fixed. These samples were run through the Labyrinth with the additional platelet removal spin then fixed before suspension staining to be loaded on the DEPArray. The samples were stored at four degrees after fixation.

Cells were identified on the machine as CTCs or WBCs. CTCs were defined as cells negative for CD45 and positive for pan-Ck and/or the EpCAM, CD133, and EGFR cocktail while WBCs were defined as cells positive for CD45 (Figure 4-2). Cells were collected into individual tubes and processed using the Menarini Silicon Biosystems Ampli1™ WGA (whole genome amplification) kit which was analyzed using their Ampli1™ WGA QC Kit. This allowed us to quantify for the first time if cells were retrieved from the DEPArray and survived volume reduction.

Figure 4-3 shows one of the WGA QC gels. One band indicates a cell is present but the DNA quality is too low to obtain sequencing results while four bands indicates high quality DNA. Although two or three bands is not ideal, the DNA from these cells is high enough quality to obtain CNV results. In the first round of experiments, only cell line cells were high enough quality to move forward in the sequencing process. We further improved both the up and down stream techniques, primarily by decreasing centrifuge spin speeds, to obtain cells of high enough quality for sequencing. The cells collected to date are shown in Table 4-1. There are matched CTCs and WBCs from three patients, WBCs from an additional three patients, and CTCs from two other patients. These cells have been submitted to the sequencing core for CNV analysis.

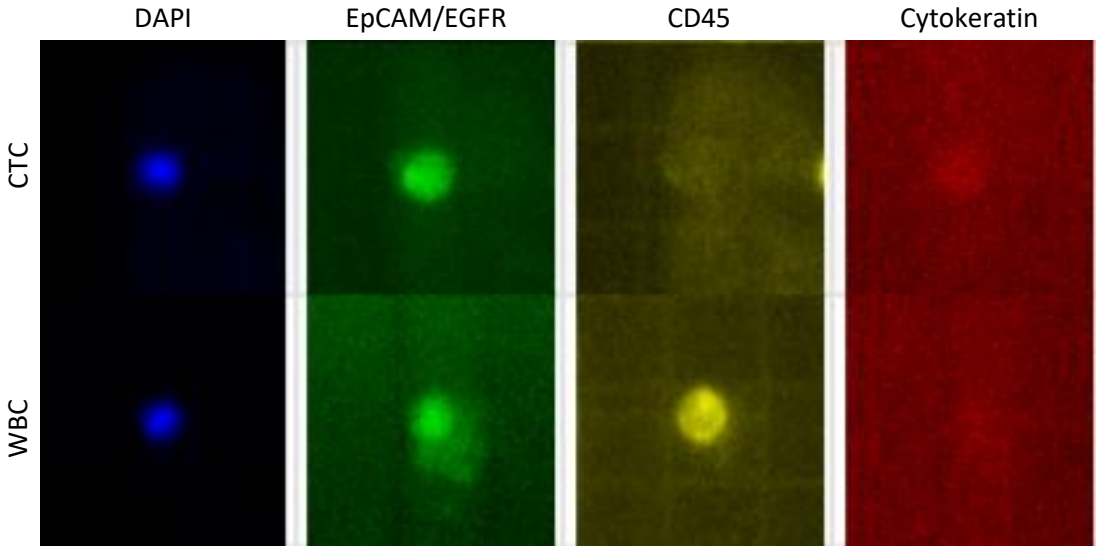

Figure 4-2: Example images of cells on the DEPArray.

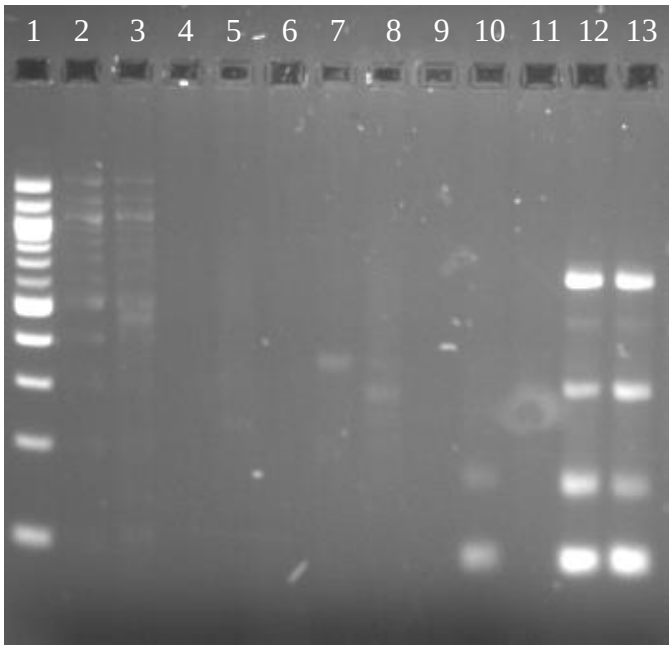

Figure 4-3: Gel from WGA QC. Lane 1: DNA Ladder, Lanes 2 – 4: Patient 1 CTCs, Lanes 5 – 6: Patient 1 WBCs, Lane 7: Patient 2 CTC, Lane 8 – 9: Patient 2 WBCs, Lane 10 – 13: Capan 2 Cells, Lane 14: Patient 3 CTC. Each lane contains a single cell.

Table 4-1: Pancreatic Cells with Usable WGA QC Results

QC Band Number	Cell Type		
	Cell Line	CTC	WBC
4	3	1	2
3	7	4	1
2	5	3	8

4.5.3 Single Cell Sorting of Live Cells for RNA Based Analysis

Traditionally, RNA extraction is performed on live cells. RNA is degraded by PFA making it difficult to get accurate results from these samples. Both the DCIS and NSCLC projects wanted to perform RNA expression analysis on single cells to determine heterogeneity within a patient's tumor which required the samples to be processed live through the RNA extraction step. From blood draw to loading the DEPArray takes approximately six hours for experienced researchers then the DEPArray itself takes another two hours to load and identify cells meaning the cells have been out of the body for at least eight hours when it is time for the DEPArray to route the cells.

Although we were able to obtain cell line cells this way, the cell membranes of patient cells would disintegrate when the machine manipulated the dielectrophoretic forces to route the cells into collection tubes. We tested several different protocol modifications but ultimately decided to investigate fixative methods that preserve RNA.

4.5.4 Alcohol Fixation as an Alternative to Live Cell Isolation for RNA Based Analysis

To obtain RNA from fixed cells, alternative fixation methods had to be used. One option was to use CellSave® Tubes; however, the preservative used in these tubes interferes with our RBC removal procedures. Another group published that methanol fixation preserved RNA, allowing RNA sequencing data to be obtained.[130] This was a promising finding for these studies, but many hurdles still remained.

The DEPArray has two programs: one for PFA fixed cells and one for live cells. The PFA fixed protocol processes cells at 4°C but is much harsher and uses SB115, a proprietary buffer. The live cell protocol allows us to use our own buffer and is much gentler, but the processing temperature is 37°C. The lower temperature used in the fixed cell protocol better preserves RNA but the routing conditions made it difficult to retrieve the cells and the effects of the SB115 were unclear. We tested the effects of SB115 by incubating alcohol fixed cells in the buffer for four hours then performing RNA extraction and comparing the results to live cells not incubated in the buffer. The buffer appeared to not affect the RNA analysis results. Similarly, we incubated methanol fixed cells at 37°C and determined this led to degraded RNA. Based on these results, we decided to proceed with the DEPArray PFA fixed cell program. By working with our Menarini Silicon Biosystems technical representatives, we were able to modify some of the DEPArray run settings to work with alcohol fixed cells.

Knowing that we could obtain cells from the DEPArray, the next step was to determine the RNA quality of alcohol fixed cells and establish a protocol. To do this we compared both methanol and ethanol fixed cells to live cells using qPCR then three common single cell RNA library preparation kits: NEBNext® Ultra™ II RNA Library Prep, SMART-Seq® Single Cell Kit, and QIAseq Stranded Total RNA Library Kit. Initial bulk cell qPCR experiments indicated methanol and ethanol fixed cells had similar results and trended with live cells. Ethanol fixed cells had CT values marginally closer to the live cell values as shown in Figure 4-4, but neither fixation method was definitively better, so the single cell RNA sequencing protocols were tested with both ethanol and methanol fixed cells.

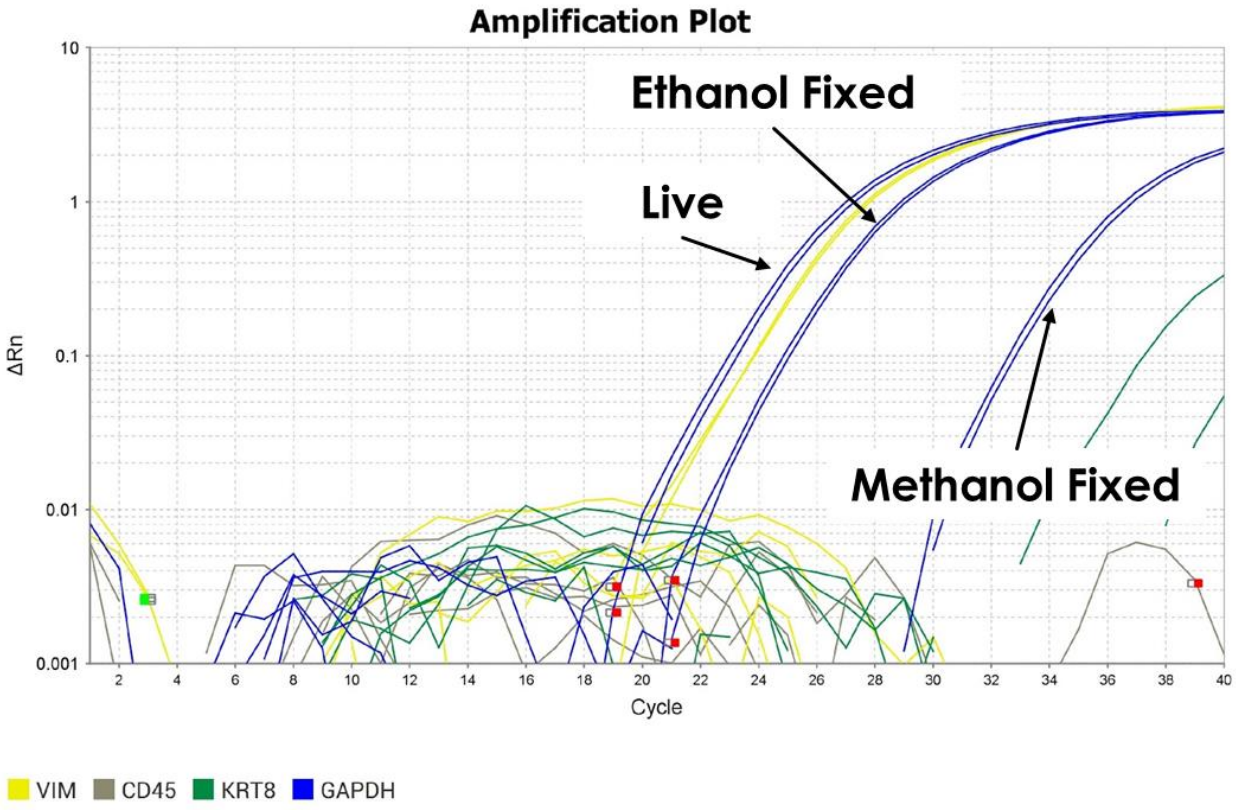

Figure 4-4: qPCR data for fixed cells from bulk samples.

To test the library prep on alcohol fixed cells, small cell numbers were spiked into wells and counted under the microscope to obtain 10 – 20 cells per sample. These small cell number samples were processed using the QIAseq kit and the QC analysis was performed, shown in Figure 4-5. One of the methanol samples had an extremely low concentration, but this is likely user error. None of the samples had bands in the expected molecular weight range which we hypothesis is due to the low cell number. A representative bioanalyzer plot is also shown. The library prep kit is designed to output fragments of 300 – 450 base pairs. Since all the bioanalyzer data graphs looked similar we believe this is likely error in our technique and not due to the alcohol fixation.

Kit	Sample	Concentration (nM)	Average Size (bp)
QIAseq	Live-1	72.0	863
	Live-2	16.6	1,034
	Methanol-1	0.6	375*
	Methanol-2	29.4	875
	Ethanol-1	37.0	918
	Ethanol-2	33.4	906

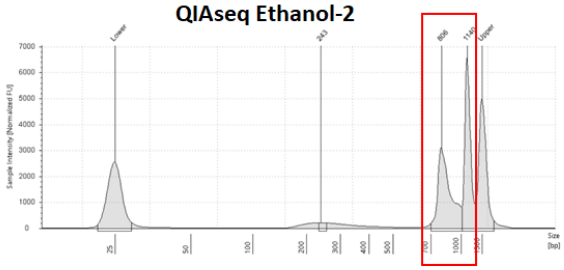

*Expected BP range: 300-450
*Expected yield: 20 nM

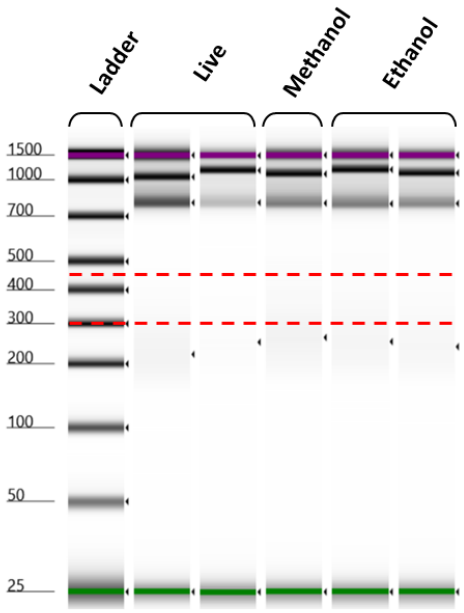

Figure 4-5:Single cell RNA extraction data for low cell numbers using the QIAseq kit. a) Table of sample concentration and average base pair length. b) Electrophoresis gel of samples. c) Example bioanalyzer graph.

4.6 Discussion

Single cell analysis holds great promise in providing disease insights; however, single cell isolation can be difficult to achieve. This challenge is enhanced when trying to isolate specific rare cells from a large population. In this study we used the DEPArray to isolate single cells from our

CTC enriched cell population. Isolation was made possible by adapting the procedure both before and after the Labyrinth to be optimized for the DEPArray and subsequent analysis.

After isolation, we were able to extract, purify, and amplify DNA from 8 pancreatic cancer patients. These samples have been submitted for sequencing to obtain CNV data. This data will then be compared to patient outcomes to determine what role CNV of various genes plays in patient outcomes. In addition to comparing CNV data between patients, we will also compare CTCs to WBCs from individual patients. The change that occurs between diseased and healthy cells may be more informative than sequencing differences between patients.

For both DCIS and NSCLC, RNA analysis of single CTCs was desired. Although it would be preferred to isolate and extract the RNA from live cells, that was not feasible using the Labyrinth and DEPArray. Instead, we optimized the DEPArray protocol for use with alcohol fixed cells while simultaneously optimizing RNA extraction and library prep for sequencing from alcohol fixed cells. Current results demonstrate this procedure provides purified RNA from single cells; however, we need to confirm the RNA quality through sequencing. Based on the results shown here, we have begun collecting and processing patient samples for single cell RNA analysis. Similar to the CNV analysis, we will collect both CTCs and WBCs from each patient which will enable us to not only compare patients but also compare the cancer cells to WBCs.

Chapter 5: Conclusion

5.1 Research Summary

CTCs have the ability to offer insight into cancer tumors that is currently unavailable using other methods. CTCs are isolated from liquid biopsies instead of traditional highly invasive tissue biopsies. Unlike tissue biopsies, liquid biopsies can be performed repeatedly and as part of routine monitoring of patients both before and after diagnosis. Although CTCs offer great promise to better predict patient outcomes and improve cancer treatment, enough cells must be isolated and the analysis must be sophisticated enough to provide data that is clinically useful. This work addresses both of these issues.

In order to isolate more CTCs we developed then improved upon an indwelling system. The initial design of this system demonstrated the feasibility to isolate CTCs directly from blood and return it to the patient, but it was limited to 12 mL of blood in a two hour period due to the limited flow rate allowed for capture. For the second generation of the ex-dwelling system, I added an inertial device designed to process whole blood. It was previously thought that the particle concentration of whole blood was too high for focusing to occur. My work demonstrates that this was an incorrect assumption due to the fact that CTCs are enough larger than red blood cells to allow focusing to occur. By studying the focusing of cancer cell lines in whole blood, I was able to develop the CTCKey™, an inertial device that adequately focuses cells for use in the ex-dwelling system. To better distinguish how the various parameters affect focusing, cells were observed in 7 g/ dL BSA. These results indicated that the protein concentration of blood affects focusing but the particle interactions that occur in blood are also important.

After development of the CTCKey™, the other system components were then updated to be compatible with the higher flow rates the inertial device enabled. Once optimized the system was tested on a canine. This experiment demonstrated the ability of the ex-dwelling system to drastically increase the number of CTCs that can be isolated from a patient. By isolating more CTCs, various downstream analyses can be performed which will be informative to patient treatment and outcome. This data will be useful in determining patient outcomes and directing treatment decisions.

Chapter three of my thesis is focused on correlating CTC data to patient outcomes in a cohort of HCC patients. Both CTC enumeration and RNA data was obtained from patients before, during, and after their radiation treatment. This data was analyzed in conjunction with patient outcomes. I found that an increase in CTCs during treatment highly correlates with poor patient prognosis. Notably, an increase in CTCs and each of the three CTC subtypes investigated during treatment is more highly correlated to poor patient outcomes than disease stage alone. Based on this finding, analyzing patient blood for the presence of CTCs could be extremely beneficial to predicting patient outcomes and eventually directing treatment decisions. In this study I also showed that RNA could be extracted from samples isolated using the Labyrinth. The results indicated that there were some differences in gene expression but very little difference between patients grouped by progression and time point. Between stable patients and patients with distant progression, the CNTNAP3P2 gene was found to be upregulated while MTMR3 was upregulated after the first round of radiation in patients with progression as compared to stable patients. Conversely, patients grouped by patient ID had a larger number of significant differently expressed genes between patients but not between time points or progression. Although these data are

inconclusive, it still indicates that monitoring changes in transcriptomic expression has the potential to inform treatment decisions.

The final portion of my thesis is focused on isolating single cells for various downstream analyses. Single cells allow intratumor heterogeneity to be observed as well as the detection of rare events that may be missed in bulk samples. Our research team wanted to add a single cell isolation technology to our current protocol, so I modified both our current Labyrinth processing protocol and the DEPArray processing protocols to be compatible with each other. The Labyrinth pre-processing had to be changed to remove platelets before using the Labyrinth since it was not possible to remove platelets later. Suspension staining was optimized for both fixed and live cells. The DEPArray settings were optimized to work with our rare cell population as well as with alcohol fixation instead of PFA fixation. This allowed us to get cells off the machine and perform our desired downstream analysis. The PFA fixed samples underwent whole genome amplification then the Advanced Genomics Core library prepped the samples. After the appropriate quality control (QC) experiments are performed, all samples that passed were sequenced by the core. Cells were alcohol fixed with the intention of performing RNA analysis to obtain gene expression data. Currently, none of the samples have been sequenced; however, qPCR data indicated that gene expression data could be obtained from alcohol fixed cells. Low cell number samples were processed using the single cell RNA extraction and library preparation kits then QC'd by the advanced genomics core. The QC results indicated that the desired samples had a high enough quality to be sequenced successfully. Now that a method has been developed, patient samples will be collected and processed using the updated protocol. The ability to obtain data from single cells will enhance the information used to inform treatment decisions.

All of the research presented here is aimed at improving cancer patient diagnosis and treatment by providing data that complements current clinical assays. By looking at CTCs, the data can be obtained from a liquid biopsy instead of a traditional tumor biopsy. Liquid biopsies are less invasive making them safer and repeatable. This allows researchers and clinicians to take samples throughout treatment and monitor changes that occur. In my work, I have drastically increased the number of cells that can be isolated from a patient by increasing the blood volume that can be processed through an ex-dwelling system. I achieved these high flow rates by introducing the CTCKey™, an inertial microfluidic device, to pre-enrich CTCs in whole blood before being flown through the previously used ^{HB}GO device where the CTCs are captured on the chips surface. Complementary to increasing the number of cells that can be captured, I also isolated CTCs from HCC patients and correlated the data to patient outcomes. The data indicates that CTCs can be informative in predicting patient outcomes. Although these data are informative, certain information is missed in bulk samples. To overcome this limitation, single cells need to be isolated. I developed a protocol to incorporate the DEPArray, a single cell isolation method, into our current lab processing. Together, these methods will improve the data that can be obtained from liquid biopsies which will in turn direct treatment decisions and improve patient outcomes.

5.2 Limitations and Future Directions

Although this work has improved the data that can be obtained from CTCs there are limitations that remain. The current ex-dwelling system has only been tested on canines with human cancer cell lines. The next step is to move into canines with endogenous cancer. To do this an appropriate antibody needs to be identified and biotinylated for use with the current system. Once the antibody is verified with canine cancer cell lines, the system will be tested on canines with endogenous breast cancer before being tested on human patients. The current set up only

isolates EpCAM positive cells; however, previous studies from our lab have used an antibody cocktail to increase the number of cells that are captured and decrease biases in the data caused by only isolating EpCAM positive cells.[131] Since this antibody cocktail was designed for use with the same chemistry as the ^{HB}GO, it can be used directly in this system when human studies are performed.

While the antibody cocktail captures various cell types, it is still antibody dependent. Ideally a cell isolation technology that is ligand dependent would eventually be incorporated into the ex-dwelling system. This is challenging in whole blood because whole blood is densely packed with particles. Filters would quickly be packed with particles and inertial technology does not have the ability to isolate CTCs to the degree necessary in whole blood for current antibody dependent isolation. More studies need to be performed to either incorporate more antibodies into the capture technology or better separate CTCs from other blood components in an antibody dependent manner.

The system developed here has the ability to process much larger blood volumes and isolate more CTCs than other available system but the number of CTCs isolated could be increased by increasing the processing flow rate. Currently the flow rate is limited by the strength of the PDMS to glass bond present in the CTCKey™ device. The flow rate could be increased by changing the material used to construct the CTCKey™ then tested to determine the flow rate where focusing decreases. Based on the optimal flow rate determined, the CTCKey™ may then need to be modified such that the flow rate through each ^{HB}GO remains near 6 mL/ hr to maintain high capture efficiency.

Moving into humans is an exciting step for the ex-dwelling system; however, long-term success requires that it be implemented in a clinical setting. To achieve this goal, the system needs

to have proper engineering controls and be clinically useful. A control scheme needs to be able to shut the system off in the case of critical failure or if it clogs. We have shown this can be achieved with the addition of a simple pressure gauge. Clinical utility will be determined by the type of data that can be obtained from the captured cells. Since other CTC studies conducted on patient cohorts have been found to be significant, it is reasonable to conclude that processing a large blood volume will improve the significance of outcomes and likelihood that the data will be clinically relevant. To implement the system in clinics, the system must be operable in many locations by various personnel. Since we are planning to use fairly standard aphaeretic draw and return sites, the system can be operated by nurses trained in standard aphaeretic procedures.

CTCs isolated from HCC samples were shown to be very informative about disease prognosis, but, unfortunately, most of the results were not significant. When the data was correlated with patient outcomes, the trends indicated that the CTC enumeration data would likely be significant if the patient cohort were larger. By including additional patients, these trends could be confirmed and other trends may emerge. Analysis of the transcriptomic expression data yielded very few differentially expressed genes. The lack of relevance likely has two main causes: background WBCs and low patient numbers, especially for the during and after treatment time points. The WBC background can likely be removed bioinformatically. The Bioinformatics Core at the University of Michigan is working on modifying methods used to remove differential expression of cell cycle genes in single cell analysis.[132] Many genes were insignificant due to the false discovery rate of such large data sets. This insignificance can be overcome by increasing the sample size. After obtaining enough data for significance to be determined, these data should be further analyzed such that it can be used by clinicians to direct treatment decisions in such a way to improve patient outcomes.

Modifying our current patient processing to be compatible with the DEPArray allows us to isolate single cells from patient samples. In the current set-up, only fixed cells can be isolated. While methods were developed to achieve the current project goals, being able to isolate live cells would be ideal. Processing time needs to be reduced for this to be feasible. either by decreasing the time it takes to complete individual steps or by combining steps. Additionally, the DEPArray protocol needs to be modified to effectively isolate live cells.

While there are definitely improvements to be made to incorporate CTC detection and analysis technologies into the clinic, these studies demonstrate that it is possible to focus CTCs in whole blood and obtain data from single cells. This lays the foundation needed to improve both the CTC isolation methods and the downstream analysis technologies that must be developed to ensure that these tests will provide relevant data that can inform treatment decisions.

References

1. Cancer Facts & Figures 2020. *American Cancer Society* (2020). Available at: https://www.cancer.org/content/dam/cancer-org/research/cancer-facts-and-statistics/annual-cancer-facts-and-figures/2020/cancer-facts-and-figures-2020.pdf. (Accessed: 17th November 2020)

2. Mehlen, P. & Puisieux, A. Metastasis: a question of life or death. *Nat. Rev. Cancer* **6**, 449–58 (2006).

3. The Advantages and Limitations of Liquid Biopsies . *LabCE MediaLab* Available at: https://www.labce.com/spg1629022_the_advantages_and_limitations_of_liquid_biopsies.aspx. (Accessed: 4th May 2021)

4. Eisenstein, M. Taking cancer out of circulation. *Nature* **579**, (2020).

5. Alix-Panabiè Res, C. & Pantel, K. Circulating Tumor Cells: Liquid Biopsy of Cancer. (2012). doi:10.1373/clinchem.2012.194258

6. Palmirotta, R. *et al.* Liquid biopsy of cancer: a multimodal diagnostic tool in clinical oncology. *Therapeutic Advances in Medical Oncology* **10**, (2018).

7. Kim, M. Y. *et al.* Tumor Self-Seeding by Circulating Cancer Cells. *Cell* **139**, 1315–1326 (2009).

8. Pantel, K. & Speicher, M. R. The biology of circulating tumor cells. *Oncogene* **35**, 1–9 (2015).

9. Azevedo, A. S., Follain, G., Patthabhiraman, S., Harlepp, S. & Goetz, J. G. Metastasis of circulating tumor cells: Favorable soil or suitable biomechanics, or both? *Cell Adhesion and Migration* **9**, 345–356 (2015).

10. Micalizzi, D. S., Maheswaran, S. & Haber, D. A. A conduit to metastasis: Circulating tumor cell biology. *Genes and Development* **31**, 1827–1840 (2017).

11. Bai, Y. & Zhao, H. Liquid biopsy in tumors: opportunities and challenges. *Ann. Transl. Med.* **6**, S89–S89 (2018).

12. Rossi, E. & Zamarchi, R. Single-cell analysis of circulating tumor cells: How far have we come in the-omics era? *Frontiers in Genetics* **7**, 958 (2019).

13. Hwang, W. L., Pleskow, H. M. & Miyamoto, D. T. Molecular analysis of circulating tumor cells: Biomarkers beyond enumeration. **125**, 122–131 (2018).

14. Mcdermott, D. F. & Atkins, M. B. PD-1 as a potential target in cancer therapy. *Cancer Medicine* **2**, 662–673 (2013).

15. Akinleye, A. & Rasool, Z. Immune checkpoint inhibitors of PD-L1 as cancer therapeutics. *Journal of Hematology and Oncology* **12**, 92 (2019).

16. Targeted Cancer Therapies Fact Sheet - National Cancer Institute. Available at: https://www.cancer.gov/about-cancer/treatment/types/targeted-therapies/targeted-therapies-fact-sheet. (Accessed: 4th May 2021)

17. Joosse, S. A., Gorges, T. M. & Pantel, K. Biology, detection, and clinical implications of circulating tumor cells. *EMBO Mol. Med.* **7**, 1–11 (2014).

18. Felman, A. & Wilson, D. R. How does blood work, and what problems occur? *Medical*

News Today (2017). Available at: https://www.medicalnewstoday.com/articles/196001#structure. (Accessed: 3rd May 2021)

19. Testing for Circulating Tumor Cells (CTC) - Mayo Medical Laboratories. (2013). Available at: http://www.mayomedicallaboratories.com/articles/features/ctc/. (Accessed: 28th April 2017)

20. Miller, M. C., Doyle, G. V. & Terstappen, L. W. M. M. Significance of Circulating Tumor Cells Detected by the CellSearch System in Patients with Metastatic Breast Colorectal and Prostate Cancer. *J. Oncol.* **2010**, 1–8 (2010).

21. Yang, J. D. *et al.* Circulating Tumor Cells Are Associated With Poor Overall Survival in Patients With Cholangiocarcinoma. (2015). doi:10.1002/hep.27944

22. Potdar, P. & Lotey, N. Role of circulating tumor cells in future diagnosis and therapy of cancer. *J. Cancer Metastasis Treat.* **1**, 44 (2015).

23. Martini, V., Timme-Bronsert, S., Fichtner-Feigl, S., Hoeppner, J. & Kulemann, B. Circulating tumor cells in pancreatic cancer: Current perspectives. *Cancers* **11**, (2019).

24. Marsavela, G., Aya-Bonilla, C. A., Warkiani, M. E., Gray, E. S. & Ziman, M. Melanoma circulating tumor cells: Benefits and challenges required for clinical application. *Cancer Letters* **424**, 1–8 (2018).

25. Dorsey, J. F. *et al.* Tracking viable circulating tumor cells (CTCs) in the peripheral blood of non-small cell lung cancer (NSCLC) patients undergoing definitive radiation therapy: Pilot study results. *Cancer* **121**, 139–149 (2015).

26. Nagrath, S. *et al.* Isolation of rare circulating tumour cells in cancer patients by microchip

technology. *Nature* **450**, 1235–1239 (2007).

27. How the CELLSEARCH® CTC Test Works? (2021). Available at: https://www.cellsearchctc.com/about-cellsearch/how-cellsearch-ctc-test-works. (Accessed: 29th January 2021)

28. Ferreira, M. M., Ramani, V. C. & Jeffrey, S. S. Circulating tumor cell technologies. (2016). doi:10.1016/j.molonc.2016.01.007

29. Alix-Panabieres, C. & Pantel, K. Challenges in circulating tumour cell research. *Nat Rev Cancer* **14**, 623–631 (2014).

30. Bankó, P. *et al.* Technologies for circulating tumor cell separation from whole blood. *Journal of Hematology and Oncology* **12**, (2019).

31. Sequist, L. V, Nagrath, S., Toner, M., Haber, D. A. & Lynch, T. J. The CTC-chip: an exciting new tool to detect circulating tumor cells in lung cancer patients. *J. Thorac. Oncol.* **4**, 281–3 (2009).

32. Yoon, H. J. *et al.* Sensitive capture of circulating tumour cells by functionalized graphene oxide nanosheets. *Nat. Nanotechnol.* **8**, 735–881 (2013).

33. Stott, S. L. *et al.* Isolation of circulating tumor cells using a microvortex-generating herringbone-chip. *Proc. Natl. Acad. Sci. U. S. A.* **107**, 18392–18397 (2010).

34. Hvichia, G. E. *et al.* A novel microfluidic platform for size and deformability based separation and the subsequent molecular characterization of viable circulating tumor cells. *Int. J. Cancer* **138**, 2894–2904 (2016).

35. Lin, E. *et al.* High-Throughput Microfluidic Labyrinth for the Label-free Isolation of

Circulating Tumor Cells. *Cell Syst.* **5**, 295-304.e4 (2017).

36. Ozkumur, E. *et al.* Inertial focusing for tumor antigen-dependent and -independent sorting of rare circulating tumor cells. *Sci. Transl. Med.* **5**, 179ra47 (2013).

37. Myung, J. H. & Hong, S. Microfluidic devices to enrich and isolate circulating tumor cells. *Lab Chip* **15**, 4500–4511 (2015).

38. Kozminsky, M., Wang, Y. & Nagrath, S. The incorporation of microfluidics into circulating tumor cell isolation for clinical applications. *Curr. Opin. Chem. Eng.* **11**, 59–66 (2016).

39. Yin, J., Deng, J., Du, C., Zhang, W. & Jiang, X. Microfluidics-based approaches for separation and analysis of circulating tumor cells. *TrAC - Trends in Analytical Chemistry* **117**, 84–100 (2019).

40. Warkiani, M. E. brahim. *et al.* Ultra-fast, label-free isolation of circulating tumor cells from blood using spiral microfluidics. *Nat. Protoc.* **11**, 134–148 (2016).

41. Li, X., Chen, W., Liu, G., Lu, W. & Fu, J. Continuous-flow microfluidic blood cell sorting for unprocessed whole blood using surface- micromachined microfiltration membranes. *Lab Chip* **14**, (2014).

42. Murlidhar, V., Rivera-Báez, L. & Nagrath, S. Affinity Versus Label-Free Isolation of Circulating Tumor Cells: Who Wins? *Small* **12**, 4450–4463 (2016).

43. Wang, Y. *et al.* PD-L1 Expression in Circulating Tumor Cells Increases during Radio(chemo)therapy and Indicates Poor Prognosis in Non-small Cell Lung Cancer. *Sci. Rep.* **9**, (2019).

44. Meye, A. *et al.* Isolation and enrichment of urologic tumor cells in blood samples by a semi-

automated CD45 depletion autoMACS protocol. *Int. J. Oncol.* **21**, 521–530 (2002).

45. Bagnall, J. S. *et al.* Deformability of Tumor Cells versus Blood Cells. *Sci. Rep.* **5**, 1–11 (2015).

46. Hao, S. J., Wan, Y., Xia, Y. Q., Zou, X. & Zheng, S. Y. Size-based separation methods of circulating tumor cells. *Advanced Drug Delivery Reviews* **125**, 3–20 (2018).

47. Vona, G. *et al.* Isolation by size of epithelial tumor cells: A new method for the immunomorphological and molecular characterization of circulating tumor cells. *Am. J. Pathol.* **156**, 57–63 (2000).

48. Tamminga, M. *et al.* Detection of circulating tumor cells in the diagnostic leukapheresis product of non-small-cell lung cancer patients comparing cellsearch® and ISET. *Cancers (Basel).* **12**, (2020).

49. Sarioglu, A. F. *et al.* A microfluidic device for label-free, physical capture of circulating tumor cell clusters. *Nat. Methods* **12**, 685–91 (2015).

50. Carlo, D. Di, Irimia, D., Tompkins, R. G. & Toner, M. *Continuous inertial focusing, ordering, and separation of particles in microchannels*. (2007).

51. Zhou, J. *et al.* Isolation of cells from whole blood using shear-induced diffusion. *Sci. Rep.* **8**, (2018).

52. Kim, T. H., Yoon, H. J., Stella, P. & Nagrath, S. Cascaded spiral microfluidic device for deterministic and high purity continuous separation of circulating tumor cells. *Biomicrofluidics* **8**, 1–13 (2014).

53. Warkiani, M. E. brahim. *et al.* Ultra-fast, label-free isolation of circulating tumor cells from

blood using spiral microfluidics. *Nat. Protoc.* **11**, 134–148 (2016).

54. Özbey, A., Karimzadehkhouei, M., Akgönül, S., Gozuacik, D. & Koşar, A. Inertial Focusing of Microparticles in Curvilinear Microchannels. (2016). doi:10.1038/srep38809

55. Fehm, T. N. *et al.* Diagnostic leukapheresis for CTC analysis in breast cancer patients: CTC frequency, clinical experiences and recommendations for standardized reporting. *Cytom. Part A* **93**, 1213–1219 (2018).

56. Xuan, X., Zhu, J. & Church, C. Particle focusing in microfluidic devices. *Microfluidics and Nanofluidics* **9**, 1–16 (2010).

57. Nivedita, N. & Papautsky, I. Continuous separation of blood cells in spiral microfluidic devices. *Biomicrofluidics* **7**, 1–14 (2013).

58. Di Carlo, D. Inertial microfluidics. *Lab Chip* **9**, 3038–3046 (2009).

59. Amini, H., Lee, W. & Di Carlo, D. Inertial microfluidic physics. *Lab on a Chip* **14**, 2739–2761 (2014).

60. Zhang, J. *et al.* Fundamentals and applications of inertial microfluidics: A review. *Lab Chip* **16**, 10–34 (2016).

61. Ozbey, A. *et al.* Inertial focusing of cancer cell lines in curvilinear microchannels. *Micro Nano Eng.* **2**, 53–63 (2019).

62. Zhou, J. & Papautsky, I. Viscoelastic microfluidics: progress and challanges. *Microsystems Nanoeng.* **6**, (2020).

63. Final Report Summary - CTCTRAP (Circulating Tumor Cells TheRapeutic APheresis: a novel biotechnology enabling personalized therapy for all cancer patients) | Report

Summary | CTCTRAP | FP7 | CORDIS | European Commission. Available at: https://cordis.europa.eu/project/id/305341/reporting. (Accessed: 12th April 2021)

64. Fischer, J. C. *et al.* Diagnostic leukapheresis enables reliable detection of circulating tumor cells of nonmetastatic cancer patients. *Proc. Natl. Acad. Sci. U. S. A.* **110**, 16580–16585 (2013).

65. GILUPI - about. Available at: http://www.gilupi.com/about.html. (Accessed: 22nd April 2018)

66. Theil, G. *et al.* The Use of a New CellCollector to Isolate Circulating Tumor Cells from the Blood of Patients with Different Stages of Prostate Cancer and Clinical Outcomes - A Proof-of-Concept Study. *PLoS One* **11**, e0158354 (2016).

67. Circulating Tumor Cell Kit (Epithelial).

68. Vermesh, O. *et al.* An intravascular magnetic wire for the high-throughput retrieval of circulating tumour cells in vivo. *Nat. Biomed. Eng.* doi:10.1038/s41551-018-0257-3

69. VIATAR - The Cancer Dialysis Company on Vimeo. Available at: https://vimeo.com/272764784. (Accessed: 25th November 2020)

70. Ng, S. P. *et al.* Detection of Circulating Tumor Cells During Radiation Therapy in Patients with Head and Neck Cancer. *Int. J. Radiat. Oncol.* **102**, e177 (2018).

71. Balogh, J. *et al.* Hepatocellular carcinoma: a review. *J. Hepatocell. carcinoma* **3**, 41–53 (2016).

72. Yang, J. D. *et al.* A global view of hepatocellular carcinoma: trends, risk, prevention and management. *Nature Reviews Gastroenterology and Hepatology* **16**, 589–604 (2019).

73. O'Connor, S., Ward, J., Watson, M., Momin, B. & Richardson, L. Hepatocellular Carcinoma --- United States, 2001--2006. *Center for Disease Control and Prevention* (2010). Available at: https://www.cdc.gov/mmwr/preview/mmwrhtml/mm5917a3.htm. (Accessed: 6th January 2017)

74. Loomba, R., Lim, J. K., Patton, H. & El-Serag, H. B. AGA Clinical Practice Update on Screening and Surveillance for Hepatocellular Carcinoma in Patients With Nonalcoholic Fatty Liver Disease: Expert Review. *Gastroenterology* **158**, 1822–1830 (2020).

75. Waller, L. P., Deshpande, V. & Pyrsopoulos, N. Hepatocellular carcinoma: A comprehensive review. *World J. Hepatol.* **7**, 2648–63 (2015).

76. Rawla, P., Sunkara, T., Muralidharan, P. & Raj, J. P. Update in global trends and aetiology of hepatocellular carcinoma. *Wspolczesna Onkologia* **22**, 141–150 (2018).

77. Crissien, A. M. & Frenette, C. Current management of hepatocellular carcinoma. *Gastroenterol. Hepatol. (N. Y).* **10**, 153–61 (2014).

78. Li, N. *et al.* Adjuvant Adenovirus-Mediated Delivery of Herpes Simplex Virus Thymidine Kinase Administration Improves Outcome of Liver Transplantation in Patients with Advanced Hepatocellular Carcinoma. *Clin. Cancer Res.* **13**, 5847–5854 (2007).

79. Cristofanilli, M. *et al.* Circulating Tumor Cells, Disease Progression, and Survival in Metastatic Breast Cancer. *N. Engl. J. Med.* **351**, 781–791 (2004).

80. Stewart, C. A. *et al.* Single-cell analyses reveal increased intratumoral heterogeneity after the onset of therapy resistance in small-cell lung cancer. *Nat. Cancer* **1**, 423–436 (2020).

81. Hu, P., Zhang, W., Xin, H. & Deng, G. Single cell isolation and analysis. *Frontiers in Cell*

and Developmental Biology **4**, 116 (2016).

82. Schulz, K. R., Danna, E. A., Krutzik, P. O. & Nolan, G. P. Single-Cell Phospho-Protein Analysis by Flow Cytometry. *Curr. Protoc. Immunol.* **78**, 8.17.1-8.17.20 (2007).

83. Miltenyi, S., Müller, W., Weichel, W. & Radbruch, A. High gradient magnetic cell separation with MACS. *Cytometry* **11**, 231–238 (1990).

84. Emmert-Buck, M. R. *et al. Laser Capture Microdissection*. (1996).

85. Citri, A., Pang, Z. P., Südhof, T. C., Wernig, M. & Malenka, R. C. Comprehensive qPCR profiling of gene expression in single neuronal cells. *Nat. Protoc.* **7**, 118–127 (2012).

86. Zeb, Q., Wang, C., Shafiq, S. & Liu, L. An overview of single-cell isolation techniques. in *Single-Cell Omics: Volume 1: Technological Advances and Applications* 101–135 (Elsevier, 2019). doi:10.1016/B978-0-12-814919-5.00006-3

87. Owen, S. *et al.* Simultaneous Single Cell Gene Expression and EGFR Mutation Analysis of Circulating Tumor Cells Reveals Distinct Phenotypes in NSCLC. *Adv. Biosyst.* **4**, 2000110 (2020).

88. Multiplex PCR: An overview of multiplex PCR assay, primer design for multiplexing, primer design software for multiplex PCR. Available at: http://www.premierbiosoft.com/tech_notes/multiplex-pcr.html. (Accessed: 4th May 2021)

89. Corporation, F. *Using C1 to Capture Cells from Cell Culture and Perform Preamplification Using TaqMan Assays Protocol (PN 100-6117 J1)*. (2018).

90. Zeinali, M. *et al.* High-Throughput Label-Free Isolation of Heterogeneous Circulating Tumor Cells and CTC Clusters from Non-Small-Cell Lung Cancer Patients. *Cancers*

(Basel). **12**, 127 (2020).

91. Di Trapani, M., Manaresi, N. & Medoro, G. DEPArray^{TM} system: An automatic image-based sorter for isolation of pure circulating tumor cells. *Cytom. Part A* **93**, 1260–1266 (2018).

92. American Cancer Society. *Cancer Facts and Figures 2021*.

93. Budd, G. T. *et al.* Circulating tumor cells versus imaging - Predicting overall survival in metastatic breast cancer. *Clin. Cancer Res.* **12**, 6403–6409 (2006).

94. Kim, T. H. *et al.* Characterizing Circulating Tumor Cells Isolated from Metastatic Breast Cancer Patients Using Graphene Oxide Based Microfluidic Assay. **1800278**, 1–10 (2019).

95. Ding, S., Chen, X. & Shen, K. Single-cell RNA sequencing in breast cancer: Understanding tumor heterogeneity and paving roads to individualized therapy. *Cancer Commun.* **40**, 329–344 (2020).

96. Bidard, F. C. *et al.* Efficacy of Circulating Tumor Cell Count-Driven vs Clinician-Driven First-line Therapy Choice in Hormone Receptor-Positive, ERBB2-Negative Metastatic Breast Cancer: The STIC CTC Randomized Clinical Trial. *JAMA Oncol.* **7**, 34–41 (2020).

97. Wang, D. *et al.* In Vivo Enrichment and Elimination of Circulating Tumor Cells by Using a Black Phosphorus and Antibody Functionalized Intravenous Catheter. *Adv. Sci.* **7**, 2000940 (2020).

98. Kim, T. H. *et al.* A temporary indwelling intravascular aphaeretic system for in vivo enrichment of circulating tumor cells. *Nat. Commun.* **10**, 1478 (2019).

99. Warkiani, M. E. *et al.* Slanted spiral microfluidics for the ultra-fast, label-free isolation of

circulating tumor cells. *Lab Chip* **14**, 128–37 (2014).

100. Serum total protein - Wikipedia. Available at: https://en.wikipedia.org/wiki/Serum_total_protein. (Accessed: 29th December 2020)

101. Smyth, J., Smith, K., Nagrath, S. & Oldham, K. Modeling, Identification, and Flow Control for a Microfluidic Device using a Peristaltic Pump. in *Proceedings of the American Control Conference* **2020-July**, 1360–1366 (Institute of Electrical and Electronics Engineers Inc., 2020).

102. Bray, F. *et al.* Global cancer statistics 2018: GLOBOCAN estimates of incidence and mortality worldwide for 36 cancers in 185 countries. *CA. Cancer J. Clin.* **68**, 394–424 (2018).

103. Hepatitis C - Diagnosis and treatment - Mayo Clinic. Available at: https://www.mayoclinic.org/diseases-conditions/hepatitis-c/diagnosis-treatment/drc-20354284. (Accessed: 2nd February 2021)

104. Tabrizian, P., Jibara, G., Shrager, B., Schwartz, M. & Roayaie, S. Recurrence of Hepatocellular Cancer After Resection. *Ann. Surg.* **261**, 947–955 (2015).

105. Schulze, K. *et al.* Presence of EpCAM-positive circulating tumor cells as biomarker for systemic disease strongly correlates to survival in patients with hepatocellular carcinoma. *Int. J. Cancer* **133**, 2165–2171 (2013).

106. Yamashita, T. *et al.* EpCAM and α-fetoprotein expression defines novel prognostic subtypes of hepatocellular carcinoma. *Cancer Res.* **68**, 1451–1461 (2008).

107. Nagrath, S., Jack, R. M., Sahai, V. & Simeone, D. M. Opportunities and Challenges for

Pancreatic Circulating Tumor Cells. *Gastroenterology* **151**, 412–426 (2016).

108. Rivera-Báez, L. *et al.* Expansion of circulating tumor cells from patients with locally advanced pancreatic cancer enable patient derived xenografts and functional studies for personalized medicine. *Cancers (Basel).* **12**, 1–18 (2020).

109. Wan, S. *et al.* New Labyrinth Microfluidic Device Detects Circulating Tumor Cells Expressing Cancer Stem Cell Marker and Circulating Tumor Microemboli in Hepatocellular Carcinoma. doi:10.1038/s41598-019-54960-y

110. Chu, P. G. & Weiss, L. M. Keratin expression in human tissues and neoplasms. *Histopathology* **40**, 403–439 (2002).

111. Li, J. *et al.* Detection of Circulating Tumor Cells in Hepatocellular Carcinoma Using Antibodies against Asialoglycoprotein Receptor, Carbamoyl Phosphate Synthetase 1 and Pan-Cytokeratin. *PLoS One* **9**, (2014).

112. Li, Y.-M. *et al.* Epithelial-mesenchymal transition markers expressed in circulating tumor cells in hepatocellular carcinoma patients with different stages of disease. *Cell Death Dis.* **4**, e831 (2013).

113. Sun, Y.-F. *et al.* Circulating stem cell-like epithelial cell adhesion molecule-positive tumor cells indicate poor prognosis of hepatocellular carcinoma after curative resection. *Hepatology* **57**, 1458–1468 (2013).

114. Transcriptome Analysis Console (TAC) Software. *Applied Biosystems* (2017). Available at: https://tools.thermofisher.com/content/sfs/brochures/tac_software_datasheet.pdf. (Accessed: 3rd May 2021)

115. R Core Team. R: A Language and Environment for Statistical Computing. (2021).

116. CNTNAP3P2 Gene - GeneCards | CNTNAP3P2 Pseudogene. Available at: https://www.genecards.org/cgi-bin/carddisp.pl?gene=CNTNAP3P2&keywords=cntnap3p2#pathways_interactions. (Accessed: 5th May 2021)

117. Wang, Z. *et al.* MTMR3 is upregulated in patients with breast cancer and regulates proliferation, cell cycle progression and autophagy in breast cancer cells. *Oncol. Rep.* **42**, 1915–1923 (2019).

118. Wang, B. *et al.* Exosomal miR-1910-3p promotes proliferation, metastasis, and autophagy of breast cancer cells by targeting MTMR3 and activating the NF-κB signaling pathway. *Cancer Lett.* **489**, 87–99 (2020).

119. Ryding, S. Multi-color IHC: Principles, Applications & Perspectives. *News Medical Life Sciences* (2019). Available at: https://www.news-medical.net/life-sciences/Multi-color-Immunohistochemistry-(IHC).aspx. (Accessed: 27th April 2021)

120. Schieker, M. *et al.* The use of four-colour immunofluorescence techniques to identify mesenchymal stem cells. *J. Anat.* **204**, 133–139 (2004).

121. Appierto, V. *et al.* How to study and overcome tumor heterogeneity with circulating biomarkers : The breast cancer case. *Semin. Cancer Biol.* **44**, 106–116 (2017).

122. Chen, G., Ning, B. & Shi, T. Single-cell RNA-seq technologies and related computational data analysis. *Frontiers in Genetics* **10**, 317 (2019).

123. Papalexi, E. & Satija, R. Single-cell RNA sequencing to explore immune cell heterogeneity.

Nature Reviews Immunology **18**, 35–45 (2018).

124. Petti, A. A. *et al.* A general approach for detecting expressed mutations in AML cells using single cell RNA-sequencing. *Nat. Commun.* **10**, 1–16 (2019).

125. Paoletti, C. *et al.* Comprehensive Mutation and Copy Number Profiling in Archived Circulating Breast Cancer Tumor Cells Documents Heterogeneous Resistance Mechanisms. *Cancer Res.* **78**, 1110–1122 (2018).

126. DEPArray™ System. (2017). Available at: http://www.siliconbiosystems.com/deparray-system. (Accessed: 2nd May 2018)

127. Vishnoi, M. *et al.* The isolation and characterization of CTC subsets related to breast cancer dormancy. *Sci. Rep.* **5**, 17533 (2015).

128. Palmirotta, R. *et al.* Next-generation sequencing (NGS) analysis on single circulating tumor cells (CTCs) with no need of whole-genome amplification (WGA). *Cancer Genomics and Proteomics* **14**, 173–179 (2017).

129. Mu, Z. *et al.* Detection and Characterization of Circulating Tumor Associated Cells in Metastatic Breast Cancer. *Int. J. Mol. Sci.* **17**, 1665 (2016).

130. Alles, J. *et al.* Cell fixation and preservation for droplet-based single-cell transcriptomics. *BMC Biol.* **15**, 44 (2017).

131. Wang, Y. *et al.* PD-L1 Expression in Circulating Tumor Cells Increases during Radio(chemo)therapy and Indicates Poor Prognosis in Non-small Cell Lung Cancer. *Sci. Rep.* **9**, 1–9 (2019).

132. Barron, M. & Li, J. *Identifying and removing the cell-cycle effect from single-cell RNA-*

Sequencing data.